DYSTROPHIN PROTEIN COMPLEX ASSEMBLY IN LIVING CELLS

by

Romesh Adrian Draviam

BS in Life Sciences, The Pennsylvania State University, 1998

Submitted to the Graduate Faculty of

School of Medicine in partial fulfillment

of the requirements for the degree of

Doctor of Philosophy

University of Pittsburgh

2006

DYSTROPHIN PROTEIN COMPLEX ASSEMBLY IN LIVING CELLS

Romesh Adrian Draviam, Ph.D.

University of Pittsburgh, 2006

The Duchenne and Limb Girdle Muscular Dystrophies (DMD, LGMD) are a heterogeneous group of genetic disorders. Primary mutations in the dystrophin gene result in the absence of the protein in DMD, and mutations in any one of four sarcoglycan (α, β, δ, γ) genes results in a loss of the entire sarcoglycan complex in LGMD. Mutations of the α-sarcoglycan gene are clinically the most frequently observed, and of these cases, one-third have a missense substitution of a cysteine for an arginine at residue 77 (R77C) of the α-sarcoglycan protein. The function of α-sarcoglycan and the implications of the R77C mutation on protein traffic are currently unknown. Here a model system has been developed to study dystrophin protein complex (DPC) assembly in living cells. We report that a minidystrophin gene construct, currently the most promising avenue for adeno-associated virus mediated gene therapy, properly assembles and integrates into the DPC in vivo, utilizing similar mechanisms as wild type dystrophin. We also demonstrate by a variety of assays that in the absence of sarcoglycan complex assembly, α-sarcoglycan is recycled from the plasma membrane. Furthermore, I provide evidence that R77C, the most commonly occurring LGMD mutation, causes a fundamental defect in protein biosynthesis, trapping the mutant protein in the endoplasmic reticulum in vitro and in vivo. Additionally, I show through re-introduction of selected sarcoglycans that the sarcoglycans are able to associate intracellularly to form specific sub-complexes. Central to sarcoglycan complex assembly is the formation of a β-δ-core complex which promotes the deposition of both the core complex and α-sarcoglycan at the plasma membrane, as seen clinically in the microscopic pathology of some cases of LGMD-2C (γ-sarcoglycan deficiency).

Taken together these data show the DPC follows a systematic and sequential assembly process, where proper integration, delivery and deposition of each protein into the complex is dependent on several protein-protein associations that in turn allow appropriate trafficking and assembly at the plasma membrane. The multi-factorial reconstruction of the DPC must therefore be carefully evaluated when treating the muscular dystrophies in humans.

ACKNOWLEDGEMENTS

TABLE OF CONTENTS

LIST OF FIGURES

LIST OF TABLES

INTRODUCTION

I.1 DUCHENNE MUSCULAR DYSTROPHY

I.1.1 History

The history of muscular dystrophy may trace back to the Egyptian dynasties, however the earliest and most comprehensive description of the disorder must be credited to Dr Edward Meryon of St. Thomas's Hospital, London, in 1852 (1). Meryon not only noted that the disease was familial with a predilection for males, but also noted that the disease primarily affected muscle tissue, specifically the sarcolemma of muscle tissue (2). His work, however, was overshadowed by that of Duchenne de Boulogne. Duchenne studied many cases of the disease through the greater part of the 1860's. Duchenne defined the disease as being characterized by: progressive weakness of movement, affecting first the lower limbs and then later the upper limbs; a gradual increase in the size of many affected muscles; an increase in interstitial connective tissue in affected muscles with the production of abundant fibrous and adipose tissue in the later stages (1). In 1955 Dr. Peter Emil Becker teamed up with Dr. Franz Kiener to detail a distinct version of Duchenne muscular dystrophy (DMD), which resulted in milder phenotype (3, 4). We now know that both these dystrophies are due to mutations at the same locus on the X-chromosome (1).

I.1.2 Clinical features

Today, the clinical features of DMD are clearly defined. The onset of the disease is typically in early childhood, delayed intellectual milestones and speech development are common features at

presentation (1), and about 20% of affected boys have an IQ of less than 70 (5). Weakness of the knee and hip extensors results in Gower's maneuver, first detailed by Sir William Gowers in 1879 (6), where a child rather than simply standing, has to move his hands along the ground, and then knees and thighs to bring the trunk into the upright posture. Most patients have enlarged calves (pseudohypertrophy), and are ultimately wheelchair bound in their early teens. Pneumonia compounded by cardiac involvement is the most frequent cause of death around the second decade of life (5).

Becker muscular dystrophy (BMD) although symptomatically similar to DMD has a later onset and progression. In BMD patients generally show no symptoms till their teens and may live till their forth or fifth decade (5).

I.1.3 Diagnosis

Generally the diagnosis of DMD is confirmed by measuring creatine kinase levels, reflective of damaged muscle fibers. In DMD serum creatine kinase levels are elevated at birth and may be tested in neonates for early diagnosis (7). This may be further confirmed by histological evaluation. DMD muscle displays several characteristic features, which include central nucleation, variations in fiber size, the classic phenotype of hyaline or hyper contracted fibers, fiber necrosis, invasion by macrophages, and replacement by fat and connective tissue (5). Immunohistochemistry is also commonly used to test patient biopsies for a deficiency in a specific protein that is mutated depending on the form of muscular dystrophy (8)(Figure I-1).
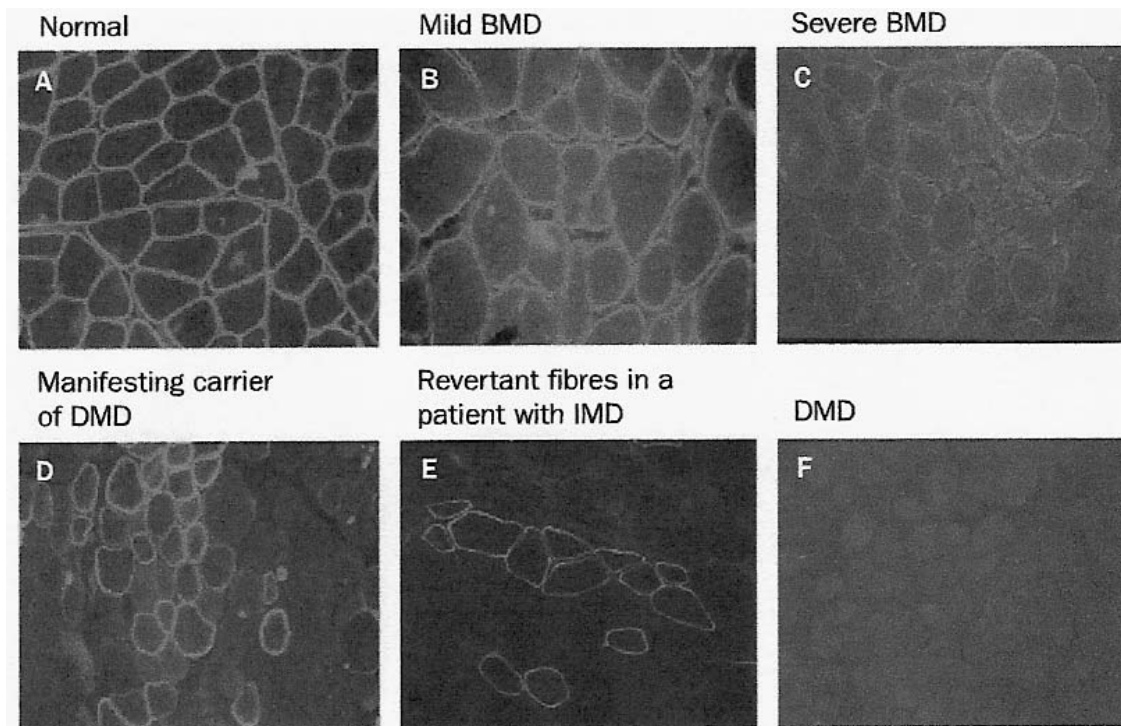
Figure I-1. Examples of immunocytochemical findings in normal muscle (A); patients with BMD (B and C), in a manifesting carrier of DMD (D) and in a patient with an intermediate between DMD and BMD phenotype (IMD; E). In normal muscle, dystrophin is localised at the periphery of each muscle fibre;in patients with DMD (F) the protein expression is absent from muscle tissue. In patients with BMD there is low protein expression in the muscles that is commonly discontinuous. In the manifesting carrier of DMD (D) a "mosaic" expression of dystrophin in different fibres is seen. An apparently similar pattern characterises patients with IMD (E), who show relatively abundant revertant fibres. Figure taken from ref. 14.

I.1.4 Genetic basis

In the early 1980's DMD, which affects roughly 1 in 3500 male births a year (9), was determined to be an X-linked recessive disease linked to the Xp21 chromosome (10). Subsequently Koenig and colleagues first cloned the 14 kb cDNA which was mutated or deleted in 53 of 104 patients tested (11). Furthermore, this transcript was 90% homologous in mice and humans (12). In 1987, Hoffman et al. reported the production of antibodies against the DMD gene protein product. The gene produced a protein approximately 427 kDa, which was termed Dystrophin (13).

I.1.5 Dystrophin

The most abundant dystrophin protein isoform represents about 0.002% of total muscle protein (13) and consists of 3685 amino acids, which form a large rod shaped protein. Dystrophin is composed of four major domains: The N-terminal domain with homology to α-actinin contains between 232 and 240 amino acids (depending on the isoform). The central rod domain is formed by a succession of 25 triple helical repeats similar to spectrin, and contains about 3000 residues. A cysteine-rich domain contains 280 amino acids, and the C-terminal domain of the protein comprises 420 residues (1, 14, 15). Immunohistochemical studies showed that dystrophin is localized to the inner leaflet of the plasma membrane, and is thought to form a intracellular lattice that is absent in patients suffering from DMD (16-19) (Figure I-1). BMD patients often retain residual levels of truncated forms of dystrophin at the plasma membrane which in turn protect against some aspects of the disease phenotype (Figure I-1). Functionally, it links the intracellular actin cytoskeleton to the integral membrane glycoproteins (20). Dystrophin exists as a number of isoforms on different specialized membranes (1), and therefore, potentially may have multiple functional roles.

I.2 LIMB GIRDLE MUSCULAR DYSTROPHY

I.2.1 History

Concurrent with a growing understanding of Duchenne muscular dystrophy, another similar pathology was also commonly seen. The clinical manifestation was similar to that of DMD/BMD, however the mode of inheritance was autosomal recessive rather than X-linked recessive (21). The first published case study was reported by Buss in 1887 (22). He described a German family consisting of healthy consanguineous parents, who bore one boy and one girl

suffering from muscular dystrophy with symptoms similar to those of DMD (22, 23). This form of muscular dystrophy was termed Duchenne-like autosomal recessive muscular dystrophy, or severe childhood autosomal recessive muscular dystrophy (SCARMD) (21, 24-26). Additional reports began to emerge slowly over the following half a century, and descriptions of SCARMD patients were published in Switzerland in 1928 (27) and in Japan in 1944 (28). However, the definitive report of SCARMD was not presented until 1958, by Kloepfer and Talley (21). The authors reported an American family pedigree of Spanish descent which included at least four consanguineous marriages. Importantly, in all of these marriages male and/or female children suffered from Duchenne-like muscular dystrophy (21, 23). Following this report many other SCARMD cases were published world wide (29-31), including additional cases by Myoshi's group in Japan (32, 33). At this time SCARMD was also referred to as LGMD, as the progressive disorders mainly affected the pelvic and shoulder girdle muscles.

I.2.2 Clinical variation from DMD

In the past, clinical differentiation of DMD/BMD from LGMD was difficult, unless the different mode of inheritance was clear in the family history (23). However the pattern of muscle involvement, age of onset and mode of inheritance is also used to subdivide the muscular dystrophies (34). Along with the muscle groups that are classically affected in LGMD, the onset is later than that of DMD. LGMD onset is generally in the second or third decade of life and has a slower progression than DMD (34). Within the LGMDs however there is significant variability in phenotype, which reflects the complicated molecular mechanisms that underlie the pathology. Amongst the LGMDs multiple genetically distinct subtypes have been determined (35-38). Progress in defining these different types of LGMD has in turn resulted in a dramatic increase in our understanding of the molecular basis for these diseases (39).

I.2.3 The Sarcoglycans

In the early 1990s DMD was being readily diagnosed using "dystrophin diagnostics," SCARMD/LGMD however did not have a molecular marker that was identified with the disease. Around this time biochemical isolation of dystrophin confirmed that dystrophin co-purifies as part of a macromolecular complex that includes a number of transmembrane glycoproteins (20, 40-42). Because of the nearly simultaneous and independent description by multiple groups, most of the dystrophin associated proteins (DAP's) were given different names (23). However, in 1994, Yoshida et al. fractionated the DAPs into three distinct groups, which are now referred to as the dystroglycan complex, sarcoglycan complex, and syntrophin complex (43). The term sarcoglycan complex was chosen because the majority of the sarcoglycan subunits are glycosylated and found exclusively in skeletal and cardiac muscles by immunoblot and northern blot analysis (43-45). Versions of LGMD or SCARMD are therefore, also referred to as sarcoglycanopathies.

The sarcoglycan complex is composed of four major integral membrane glycoproteins in striated muscle. These are the α, β, δ, and γ sarcoglycans (35-38) (Figure I-2). The sarcoglycans are all N-glycosylated with a large cysteine cluster containing extra cellular domains, and relatively short intracellular domains (46) (Figure I-2). The tight association of the transmembrane sarcoglycans suggests they may function as a single unit in striated muscle (43, 47). Furthermore Yoshida et al. demonstrated that the molar ratio of the sarcoglycan subunits in the sarcoglycan complex is 1:1:1:1, supporting the autosomal recessive mode of inheritance (23, 43, 48).

Based on immunohistochemical studies of SCARMD patients, Mizuno et al. hypothesized that SCARMD is primarily caused by a mutation in any one gene of the sarcoglycan

complex. Furthermore, it was believed that if any one sarcoglycan gene is mutated, the respective protein would be lost or truncated, and as a consequence the entire sarcoglycan complex would not assemble correctly at the sarcolemma (49, 50).
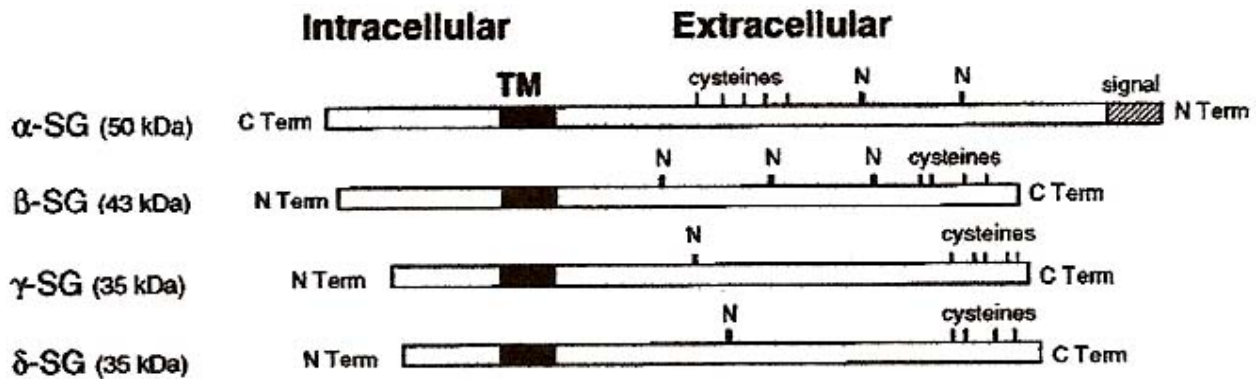
Figure I-2. Human sarcoglycan expression constructs. A schematic of the sarcoglycan expression constructs is shown. Transmembrane domains (TM), cysteine clusters (cysteines), consensus sites for asparagines linked glycosylation (N), and the signal sequence (signal) are indicated. Expected molecular masses are in parentheses. Figure was adapted from ref. 46.

I.2.3A α-Sarcoglycan

α-sarcoglycan, also referred to as Adhain, A2, or 50-kD DAG, was first isolated and cloned by Roberds et al. in 1993 from rabbit skeletal muscle. The 50-kDa dystrophin-associated glycoprotein was found specifically deficient in the skeletal muscle of patients with SCARMD (51). These studies predicted a protein consisting of 387 amino acids, including a 17 amino acid signal sequence, one trans-membrane domain, two potential sites for N-linked glycosylation and a cytoplasmic carboxyl-terminus (51) (Figure I-2). α-sarcoglycan and its non-muscle homologue ε-sarcoglycan have a cadherin-like domain, and calcium binding pockets, which are present close to the signal sequence. These cadherin domains have been implicated in protein-protein interactions and therefore, are presumed to interact with other glycoproteins in the context of α-sarcoglycan (52, 53). The gene was mapped to 17q12-21.33 (38), gene locus 17q21 (54). The α-

sarcoglycan gene is composed of 1,410 nucleotides, and has an open reading frame of 1,161 nucleotides. This produces a core protein of about 40.4 kDa without the signal sequence (53).

Mutations in the α-sarcoglycan gene result in a form of LGMD, termed LGMD 2D. Although the prevalence of the sarcoglycanopathies varies among LGMD patients in different populations, mutations within the α-sarcoglycan gene cause the most commonly reported sarcoglycanopathy (38, 55, 56). To date a large number of different mutations have been described in the human α-sarcoglycan gene, and result in a highly variable disease phenotype, however, the most common mutation is at a CpG hotspot (57-61). The mutation is a missense mutation at position 229 CGC > TGC in exon 3 of the SGCA gene, substituting a cysteine for an arginine in codon 77, and is therefore, referred to as the R77C mutation (57, 59, 62). Recent studies have reported an enrichment of the R77C mutation in Finnish patients, probably due to a founder effect (62). There have been no studies to date, however, examining the effect of this mutation on the traffic or localization of the α-sarcoglycan protein.

It is not surprising that α-sarcoglycan stands out among the sarcoglycan subunits. It is the only sarcoglycan subunit that is not cross-linked into the complex (43, 47), and unlike the other subunits it is the only sarcoglycan with an intracellular C-terminus (46, 51) (Figure I-2). Also, it is the only sarcoglycan with an extracellular cysteine cluster close to the membrane-spanning domain as opposed to the C-terminus (53). Additionally, it is unique in that α- sarcoglycan is reported to have Ecto-ATPase activity (63, 64). Betto and his colleagues showed in 1999 that α-sarcoglycan is a sarcolemmal ecto-ATPase and may control the extracellular concentration of ATP, and thus modulate the activity of various other cell surface receptors (63). The function of α-sarcoglycan however remains unknown.

I.2.3B β-Sarcoglycan

β-sarcoglycan also referred to as A3b, is one of two 43 kDa proteins within the DPC (43). The β- sarcoglycan gene is 35 kb long and is mapped to 4q12 (35, 65). The gene consists of 1,225 nucleotides with an open reading frame of 954 nucleotides. This gene segment encodes a protein with 318 amino acids and a predicted molecular mass of 34.8 kDa (53). Unlike α-sarcoglycan, β-sarcoglycan is a type II transmembrane protein, with an N-terminal cytoplasmic domain, containing a large hydrophobic region (Figure I-2). β-sarcoglycan is for the most part restricted to striated muscle, however, there have been reports of β-sarcoglycan mRNA in brain tissue, although there are no signs of the protein product in these tissues (41, 66).

Mutations within the β-sarcoglycan gene most often result in a complete loss of the protein and all the other members in the sarcoglycan complex (35), and result in LGMD 2E. Additionally, missense mutations that affect the membrane-proximal portion of β-sarcoglycan seem to correlate with a more severe dystrophic progression (41, 67).

I.2.3C γ-Sarcoglycan

Gamma-sarcoglycan is also referred to as 35-kD DAG or A4. Noguchi et al. first cloned this gene from skeletal muscle in 1995, and mapped it to chromosome 13q12 (37). The γ-sarcoglycan gene has an open reading frame of 873 nucleotides, which encodes a protein with 291 amino acid residues, having a predicted molecular mass of 35 kDa (Figure I-2). The extracellular C-terminal domain, and the intracellular N-terminal domain comprise 231 and 35 amino acid residues respectively (53).

Mutations within the γ-sarcoglycan gene result in LGMD 2C. γ-sarcoglycan is expressed most highly in striated muscles, however there have been reports of γ-sarcoglycan mRNA in other tissue types as well (68). It has also been demonstrated that γ-sarcoglycan along with δ-

9

sarcoglycan interacts with Filamin 2 (69), that in turn interacts with the actin cytoskeleton, and thus may provide a link between the sarcoglycan transmembrane complex and the intracellular actin network, aside from actin links to dystrophin.

I.2.3D δ-sarcoglycan

The fourth sarcoglycan subunit in muscle tissue, and the last to be identified is δ-Sarcoglycan (36). In 1996, Nigro et al. identified the 439 kb gene and localized it to 5q33 (70). The δ-sarcoglycan cDNA has an open reading frame of 870 nucleotides. This encodes a protein comprising 290 amino acids with a molecular mass of about 35 kDa (Figure I-2). The extracellular C-terminal domain, and the intracellular N-terminal domain comprise 231 and 34 amino acids respectively (53), similar to γ-sarcoglycan. Additionally, as previously stated, δ-sarcoglycan also interacts with Filamin 2 (69). However, unlike γ-sarcoglycan (an acidic protein), δ-sarcoglycan is a basic protein (53).

Mutations within the δ-sarcoglycan gene result in LGMD 2F, however δ-sarcoglycan mutations are relatively rare (36, 55).

I.2.4 Variations in molecular pathology

Although the LGMD's can now be broadly classified both clinically and on a molecular level, it is important to remember that unlike DMD, there is a tremendous amount of variation in both phenotype severity and molecular pathology from patient to patient. This was demonstrated in a study I conducted in 2001 (8). I examined the muscle biopsies of multiple patients suffering from various forms of LGMDs and DMDs, and found that in patients where a single sarcoglycan was mutated and lost, there are variations in the expression of the remaining sarcoglycans.

In patients suffering from a primary α-sarcoglycanopathy (LGMD 2D), some patients had no sarcoglycans detectable at the sarcolemma. In other patients, residual amounts of sarcoglycans

were retained at or close to the plasma membrane, and appeared to require α-sarcoglycan to maintain the presence of the complex at the plasma membrane, rather than export out of the endoplasmic reticulum (8) (Figure I-3). This data correlated well with observations by other groups observations in LGMD 2D patients (71-73). In some patients residual sarcoglycans at the sarcolemma correlated with phenotypic severity (59), though in other patients a severe phenotype was displayed despite the preservation of sarcoglycans at the sarcolemma. Therefore, no direct correlation between the presence of sarcoglycans and disease phenotype could drawn.

A similar variation in molecular pathology is also seen in γ-sarcoglycanopathy (LGMD 2C) patients. Again, while all patients had a complete absence of γ-sarcoglycan, expression of the remaining sarcoglycans ranged from completely absent to almost normal (Figure I-4). The retention of α-, β-, and δ-sarcoglycans in LGMD 2C has also been reported by a number of other groups (71, 74, 75). Interestingly, individual sarcoglycans are rarely retained in LGMD 2C. If residual sarcoglycans are detected at the sarcolemma they are most commonly δ-, β- and α-sarcoglycan in order of abundance (Figure I-4). It is unknown if certain sarcoglycan sub-complexes are able to translocate and get deposited at the plasma membrane more readily than others.

sarcoglycan variation is rarely seen in patients suffering from β-sarcoglycanopathy (LGMD 2E) or δ-sarcoglycanopathy (LGMD 2F). This was also found in our study (8). These two myopathies appear more severe both clinically and at the molecular level, as no residual sarcoglycan's are observed at the sarcolemma. Biochemical and cross-linking studies have been conducted that show a strong association between β- and δ- sarcoglycan (47, 76, 77), which is hypothesized to be central to the assembly of the sarcoglycan complex as a whole. Therefore, it is not surprising that these sarcoglycanopathies ablate sarcoglycan assembly altogether.

11
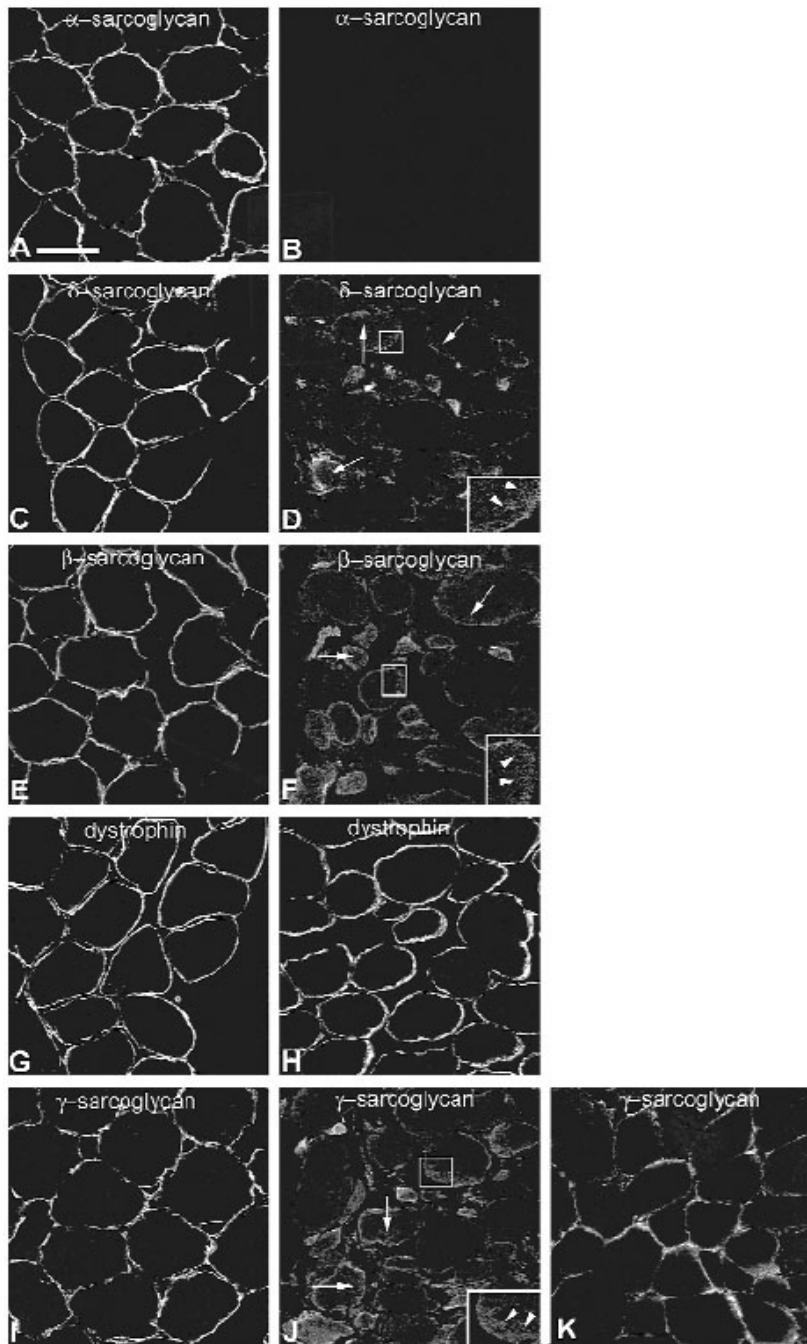
Figure I-3. Immunohistochemical analysis of DGC proteins in a-sarcoglycan–deficient human muscle compared with normal muscle. Control muscle biopsies show normal expression of α-, δ-, β-, and γ-sarcoglycan (A, C, E, and I) and dystrophin (G). Myopathic muscles show an absence of a-sarcoglycan (B), and reductions in δ- and β-sarcoglycan (D, F), accompanied by slight intracellular labeling (arrows and insets [contrast adjusted to amplify intracellular labeling]). Dystrophin expression remains well-preserved (H). Variations are seen between patients in g-sarcoglycan expression, where lower plasma membrane staining results in higher intracellular labeling (J, arrowsand inset [contrast adjusted to amplify intracellular labeling]), and lower intracellular labeling results in higher plasma membrane expression (K). Bar= 50μm. Figure taken from ref. 8.
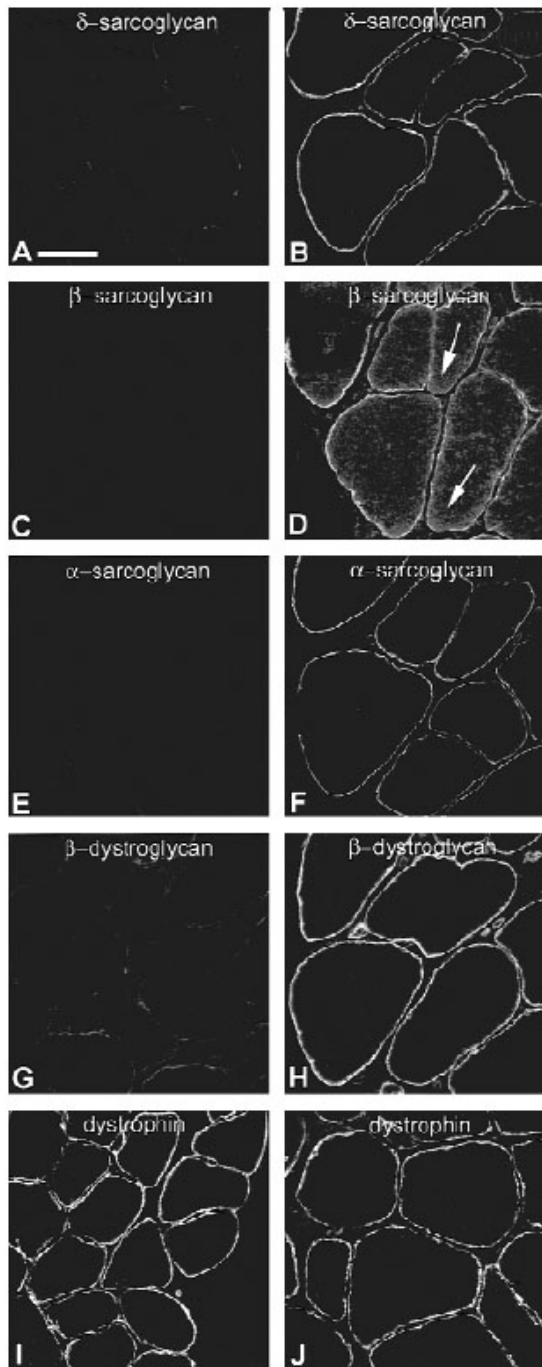
Figure I-4. Immunohistochemical analysis of DGC proteins in g-sarcoglycan–deficient human muscle. Variations are seen in δ-, β-, and γ-sarcoglycans and β-dystroglycan, as some patients showed dramatic reductions in expression (A, C, E, and G), whereas others showed close to normal expression (B, D, F, and H). Dystrophin is well-preserved in this myopathy (J) when compared with the control (I). In D, the arrows indicate intracellular localization of b-sarcoglycan (contrast adjusted to amplify intracellular staining). (Bar = 50 µm.). Figure taken from ref. 8.

I.2.5 Sarcoglycan complex assembly

In 1998, Holt and Campbell used Chinese hamster ovary (CHO) cells to show biochemically that the sarcoglycans are glycosylated and assemble into a tight complex at the plasma membrane (46). When expressed individually, expressed sarcoglycans were glycosylated; but were localized to intracellular pools. Strikingly, mutant sarcoglycan constructs engineered to recapitulate known human mutations were found to abrogate sarcoglycan complex assembly and targeting to the plasma membrane (46). This suggests that the molecular defect in LGMD phenotypes resulted from the aberrant assembly and trafficking of the sarcoglycan complex to the sarcolemma. Noguchi and his colleagues in 2000 used immunoprecipitation methods on cultured myocytes at fixed time points to suggest that the sarcoglycans form a complex in the endoplasmic reticulum distinct from the dystroglycan complex (78). These data corroborate our studies in 2001 (8), indicating that knowledge of assembly and trafficking of the sarcoglycan complex is of fundamental importance in the consideration of treatment. The COS-1 heterologous cell system was used in 2004 by Shi et al. to demonstrate that the assembly pathway occurs as a discrete stepwise process. They used a combination of chemical cross linking and immuno fluorescence to speculate on possible assembly intermediates (77).

Although preliminary studies indicate that sarcoglycan complex formation is a prerequisite for the export of the individual sarcoglycans as well as the complex as a whole to the cell surface, no studies have been performed to evaluate the assembly processes and trafficking patterns of the sarcoglycans in real time. In addition, there is no information available on the specific trafficking mechanisms the sarcoglycans may utilize en route to the plasma membrane both during development and subsequent maintenance of the muscle fiber. It is unclear whether the sarcoglycans associate with adaptor proteins like many other transmembrane proteins at the

trans golgi network, or whether the complex is transported via clathrin coated vesicle, or, alternatively, whether they have some other muscle specific transport process that mediates their regulation.

I.3 DYSTROPHIN PROTEIN COMPLEX

I.3.1 Components of DPC

The picture of the DPC is continually expanding as new proteins are being discovered that interact with the known members of the complex. Below is a summary of the DPC as applicable to this dissertation.

Dystrophin is thought to be linked to the plasma membrane by its cysteine-rich carboxyl terminus. This linkage involves a large oligomeric complex of proteins, including the dystroglycans and sarcoglycans (20, 42, 79) (Figure I-5). The dystroglycans and sarcoglycans include a cluster of five transmembrane proteins: β-dystroglycan (43 kDa protein), α- sarcoglycan (adhalin, or 50 kDa dystrophin-associated glycoprotein (DAG)), β- sarcoglycan (43 kDa DAG), δ-sarcoglycan (35 kDa DAG), and γ-sarcoglycan (35 kDa DAG) (Figure I-5)). The ε-sarcoglycan is of non-muscle origin and exists in the brain. On the external face of the plasma membrane, this molecular complex is bound to a large 156 kDa glycoprotein (α-dystroglycan), via β-dystroglycan. α-dystroglycan binds to merosin (laminin-2 or α2, or m-laminin) found within the basal lamina (80-83). Muscle integrins also likely bind to the basal lamina, thus further anchoring the plasma membrane to the extracellular matrix (84). Other proteins that specifically associate with dystrophin include the syntrophins. the cytoplasmic 59 kDa triplet of α, β1, and β2 syntrophin, which closely associates with the carboxyl terminus of dystrophin (85-87) (Figure I-5). In addition, a variety of novel DAP members are constantly emerging that append to the

functional significance of this complex. These DAP components act in concert to stabilize the sarcolemma during repeated cycles of contraction and relaxation which transmit force generated in the muscle sarcomeres to the extracellular matrix.
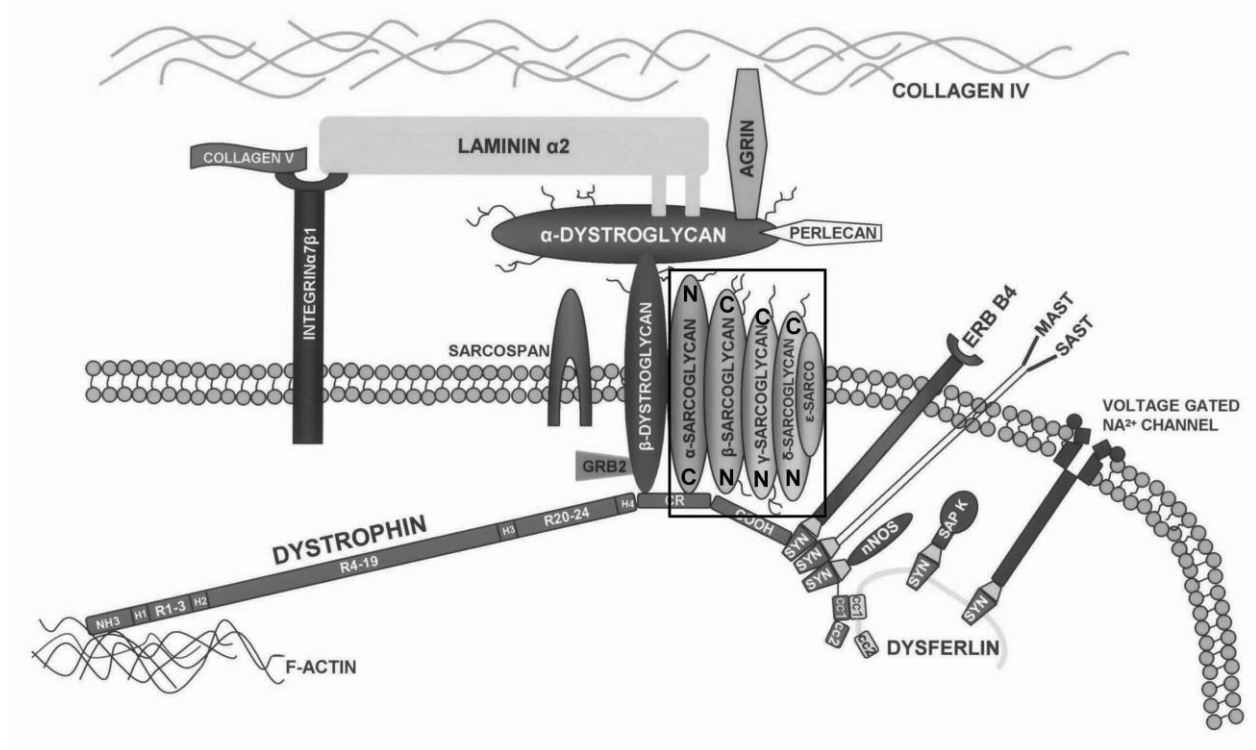
Figure I-5. Schematic representation of the DPC in striated muscle. The sarcoglycan complex which in striated muscle is composed of α, β, δ, and γ sarcoglycans is boxed. From ref. 192.

I.3.2 The Dystroglycans

Dystroglycan was among the proteins isolated by Ervasti et al. in 1990 (79). After it was cloned in 1992 (82), it became apparent that Dystroglycan had roles beyond that of muscle. The dystroglycans are expressed in a wide variety of tissues where they generally serve as a transmembrane linkage between the intracellular cytoskeleton and the extracellular matrix (88) (Figure I-5). The dystroglycans are translated from a one highly conserved gene which encodes a single mRNA (89). The dystroglycan protein is then post-translationally cleaved into the α-

and β-dystroglycan subunits. α-dystroglycan is an extracellular peripheral membrane glycoprotein, with *O*-linked carbohydrates, which is noncovalently attached to the membrane-spanning β-dystroglycan (40, 89). Among the best understood interactions of β-dystroglycan is its interaction with dystrophin. The carboxy C-terminal 15 amino acids of β-dystroglycan have been historically shown to interact with the cysteine rich, WW domain of dystrophin (83, 90). Recent reports; however, have identified an additional ZZ domain adjacent to the WW domain of the dystrophin molecule that also mediates it's interaction with β-dystroglycan (91). Therefore it is important to account for these connections to β-dystroglycan when addressing dystrophin based therapeutics.

I.4 GENE THERAPY

It is important to realize that, because the muscular dystrophies are genetic based myopathies, the current standard of care is supportive rather than corrective. For example, mechanical or surgical treatments can prolong the time before the patient becomes wheelchair-bound or provide improved posture for effective breathing, however there are no cures for the primary deficiency (92). For these reasons the majority of therapeutic avenues over the last decade have been focused on replacing the missing gene, with the hope of restoring the other DPC connections and thus ameliorating the deleterious phenotype. One of the major drawbacks with gene therapy however has been the inefficiency of transducing large amounts of tissue with the gene, while maintaining long term expression with minimal toxicity.

I.4.1 AAV mediated gene therapy for muscular dystrophy

Adeno-associated viruses (AAV) were discovered as a contaminant of adenovirus stocks in the late 1960's, and were identified by electron microscopy as a small (approximately 20 nm

diameter) replication-deficient parvovirus (93). The properties of AAV that make it a useful therapeutic vehicle for gene therapy are the following (94): non-pathogenic; capable of persistent infection; present in over 100 variants with diverse cell tropisms; generally elicits mild innate cytokine response; genome readily modified in proviral plasmids; recombinant production and purification methods in place.

In 1996 Xiao et al., were able to introduce recombinant AAV vector (rAAV) carrying a lacZ reporter into the muscle of immunocompetent mice. The mice continued to express the lacZ reporter more than 1.5 years later, with no sign of a cellular immune response (95). Around this time the "safe" sustained expression of transgenes in muscle tissue was also demonstrated by other groups (96). Furthermore, in 2000 Pruchnic et al. demonstrated that because of the small viral size of AAV, it is able to bypass the extracellular barrier of mature muscle (97). In 1999, AAV encoding a δ-sarcoglycan gene was used to treat a cardiomyopathic hamster model of δ-sarcoglycanopathy (98). Importantly, a quantitative assay demonstrated that vector-transduced muscle fibers are stably protected from sarcolemmal disruption and there was no associated inflammation or immunologic response to the vector-encoded protein (98). The following year a study showed that the muscles of these hamsters treated with AAV-δ-sarcoglycan showed more than 97% recovery in muscle strength for both the specific twitch force and the specific tetanic force, when compared to the age-matched control. Vector treatment also prevented pathological muscle hypertrophy and resulted in normal muscle weight and size, while showing a substantial improvement in histopathology (99). That year (2000), Cordier et al. demonstrated the functional rescue of γ-sarcoglycan deficient mouse muscle with AAV encoding γ-sarcoglycan (100).

At this point all the genes that were transduced efficiently into mouse muscle were relatively small (1-2kb). However, researchers needed to confront how this gene therapy technique can be used to treat DMD, which has a much higher incidence than the LGMDs. An intrinsic limitation of this gene delivery system is the relatively small 4.5kb gene carrying capacity (101). Methods such as DNA dimerization (102), and the dual-vector approach (103) were developed to increase the size of genes that could be transferred. However these efforts were still insufficient to accommodate the 14 kb dystrophin gene.

I.4.2 Mini-Dystrophin

In 2000, Wang et al. were able to overcome the problem of packaging the large dystrophin gene by creating a miniature dystrophin gene that was small enough to fit into the AAV vector cassette, and effectively ameliorates muscular dystrophy in the mdx mouse model (104). The C57 mdx mouse, is the most commonly used model for DMD, as it has a mutation in the DMD gene, which causes a loss of the dystrophin protein. Although it does not share some of the clinical features that patients have, such as substantially weakened muscle strength and a shorter life span, most of the histological features in the muscle tissue are the equivalent to that seen in patients (105, 106).

The rationale for the creation of miniature versions of dystrophin stem from the truncated BMD gene, which correlates with a substantially milder phenotype. Many BMD patients have large deletions in the spectrin repeat rod region, and still retain abundant detectable dystrophin at the sarcolemma. In turn, the residual dystrophin partially protects the muscle from dystrophic change (Figure I-1) and the patients live substantially longer (107, 108). Minidystrophin genes have been tested as early as 1996, however these genes were substantially larger (6.3kb)(109)

than the ones created by Xiao's group (3.8kb), and were designed primarily for delivery vehicles aside from AAV, such as adenovirus vector.

The minidystrophin genes created by Wang et al. were constructed mainly by the PCR cloning method using Pfu polymerase (Stratagene) and human dystrophin cDNA as a template. The mini gene has 3849 nucleotides (and is therefore, referred to as Δ3849) containing nucleotides 1-1668 (N terminus, hinge 1, and rods 1 and 2, which corresponds to amino acids (aa) 1-556), nucleotides 8059-10227 (rods 22, 23, 24, hinge 4, and CR domain, corresponding to aa. 2686-3409), and nucleotides11047-11058 (the last 3 aa, 3682-3684) of full length dystrophin (104) (Figure 1-1A). This Δ3849 minidystrophin construct was driven by a CMV promoter.

Despite lacking the entire distal C-terminal domain, down stream of the cytetine rich region which mediates the important connections to β-dystroglycan, Δ3849 was able to restore normal levels of the other DPC members (such as the sarcoglycans) to the sarcolemma (104). Histologically, the muscles also appeared rescued, as the AAV vector treatment led to normal histology in terms of peripheral placement of myofiber nuclei, consistent myofiber size, and lack of fibrosis in the mini-dystrophin positive fibers (104). Additionally, the integrity of the muscle fiber was also preserved in cells expressing the transgenes, as they did not allow the intake of an Evans blue dye, that is only capable of penetrating compromised muscle fibers (104). Therefore, these results demonstrated that the Δ3849 minidystrophin gene can maintain membrane integrity and protect myofibers from mechanical damage.

This construct is currently being tested in larger animal models and is in the early phases of clinical trials (personal communication- Xiao X.), however there have been no studies to date examining the efficacy of this Δ3849 minidystrophin in living cell culture models. Additionally,

it is unknown as to whether Δ3849 is actually integrating into the DPC through primary interactions with β-dystroglycan, similar to full length wild-type dystrophin.

I.5 VISUALIZING PROTEINS IN LIVING CELLS

I.5.1 GFP and relatives

Until the 1990's, a major drawback to studying protein behavior in cells was the inability to visualize the localization of the protein, without treatment that kills the cells. These usually required cell fixation and permeablization of the membrane to allow access of the antibody, which in turn compromised the dynamic nature of cellular behavior. The way we visualize proteins in living cells was revolutionized in 1992 with the cloning of the gene which encoded green fluorescent protein (GFP) (110).

GFP was first discovered and isolated in 1962, by Shimomura et al. from the *Aequorea victoria*, a small jellyfish common in the waters of the north pacific (111). The bioluminescent protein was shown to emit bright green fluorescence under UV light, making it an ideal candidate for a visible marker. However, its true potential was not utilized until Prasher et al. published the gene sequence (110). In 1994, Chalfie et al. demonstrated the potential of GFP to act as a reporter gene in prokaryotic and eukaryotic cells (112). Since then, GFP has been used extensively as a tool in various fields of biology and medicine. It is particularly useful due to its stability and the fact that its chromophore is formed in an autocatalytic cyclization that does not require a cofactor. This has enabled researchers to use GFP in living systems, and has led to widespread use in dynamic and developmental cell studies (113). GFP requires around 2 hours from transcription to form a fluorescent functional protein (114), and importantly, numerous

studies have indicated that fusion of GFP to a protein, or rather the gene encoding that protein, generally does not alter the function or localization of the protein (115).

Through the course of experimentation, wild-type GFP in its native form was determined to be suboptimal for use in cultured cells and living animals. Mostly due to an inability to fold correctly at 37^oC, which in turn weakens the protein's fluorescence (116). For these reasons commercially available forms of the reporter gene, such as enhanced GFP (EGFP- BD Biosciences- Clontech), are generally mutated versions that correct for these issues, and ensure bright stable fluorescence in vertebrate cells.

In 1999 Matz et al. hypothesized that GFP-like proteins are not necessarily linked to bioluminescence, and were able to isolate a family of fluorescent proteins homologous to GFP from reef corals (117). One of the proteins cloned from *Discosoma* sp. was a red variant, at the time called drFP583. Mutagenized versions of this protein have also been optimized over the last 6 years are now known as DsRed (clontech), or DsRed-express (clontech), which do not have many of the dimerization properties associated with the original DsRed constructs.

Recently a number of other GFP variants have also been created, where the properties of GFP are altered upon physiological changes, such as pH, or changes in illumination. This has enabled the GFP reporter to also be used as a biosensor, and has allowed users to manipulate the visible expression of specific populations of the protein. One such variant was created by Patterson and Lippincott-Schwartz in 2002 and is termed photo-activatable GFP (PA-GFP) (118). By introducing 4 mutations in the EGFP gene (one of which, T203H, is crucial to the photoactivatable properties), EGFP is virtually invisible under the 488 nm wavelength (its usual excitation wavelength), however upon a brief irradiation with 413-nm UV light, the fluorescence

excitation at 488nm increases about a 100-fold. This is important for highlighting specific cells or pools of intracellular proteins and then tracking their intracellular dynamics.

Thus, in the last decade our knowledge and use of the fluorescent properties in proteins has grown exponentially and now enables us to understand proteins in dynamic systems relative to components around them in live cells.

I.5.2 EGFP fusion genes in muscular dystrophy

In 2000 Chapdelaine et al. first reported a functional minidystrophin-EGFP fusion gene (119). Here the authors fused the EGFP reporter to a 6 kb variant minidystrophin, and showed its correct localization at the sarcolemma. The goals for this construct however were to study the efficacy of gene therapy, and not the basic biology and efficiency of the minidystrophin protein itself. In addition, a more pertinant question was how $\Delta 3849$ behaves when it is attached to the EGFP reporter, as it is currently the most promising candidate for minidystrophin based gene therapies.

Currently, there are no reports of EGFP fusion genes fused to any of the sarcoglycans, which may serve as important tools in understanding the behavior and function of these proteins in living systems.

I.6 ADVANCES IN LIVE CELL MICROSCOPY TECHNIQUES

In the last decade, the advances in the field of live cell microscopy have had a direct impact on the progress in the field of cell biology. Today looking at multiple proteins in living cells, although expensive and technically demanding, is routine, while a decade ago it was a novelty. To study the behavior of proteins that interact with the plasma membrane, one technique that has recently proved to be especially useful is total internal reflection fluorescence microscopy.

I.6.1 Total internal reflection fluorescence microscopy (TIR-FM)

TIR-FM is a technique that was pioneered by Axelrod in the 1980's to study interactions between cultured cells and their substrate at the coverslip (120). The basis for TIR-FM lies upon the following principle taken from Schneckenburger's review-

> "…When a light beam propagating through a medium of refractive index n_1 (e.g. glass) meets an interface with a second medium of refractive index $n_2 < n_1$ (e.g. the cytoplasm), TIR occurs at all angles of incidence Θ that are greater than a critical angle $\Theta_c = \arcsin(n_2/n_1)$. Despite being totally reflected, the incident beam establishes an evanescent electromagnetic field that penetrates into the second medium and decays exponentially with the distance z from the interface. According to the relation $d = (\lambda/4\pi) (n_1^2 \sin^2\Theta - n_2^2)^{-1/2}$ (where l corresponds to the wavelength of light) penetration depths (d) can be adjusted between about 70 nm and 300 nm. Therefore, fluorophores located within or close to the plasma membrane are detected selectively in living cells. (121)…"

TIR-FM has been utilized in the recent years to study not only cell-substrate interactions but also the delivery and internalization of proteins from the cell surface (122, 123).

This technique is especially applicable to studying the delivery and trafficking of DAPs, as most of them reside at or very close to the plasma membrane, however there have been no studies to date which have implemented TIR-FM to study the delivery of DAPs to the plasma membrane in living cells.

I.7 GOALS OF DISSERTAION

In the last decade our understanding of the genetic basis underlying the muscular dystrophy phenotype has grown exponentially. With the discovery of the genes responsible for DMD, and the LGMDs, have come tremendous advances in the fields of gene therapy. The minidystrophin construct shows the most promise in AAV-mediated gene therapy for DMD, however, while the construct appears to be functioning correctly in static systems, there is no data examining how efficiently the transgene is able to integrate into the DPC on a molecular level, in living cells. Alternatively, while the sarcoglycans are small enough to be delivered without alteration by AAV-mediated gene therapy, we still do not know their precise function, or trafficking pathways *in vivo*. Furthermore, while reoccurring mutations have been identified, there is no data describing how these mutations affect the localization and trafficking of the mutated protein.

In the following thesis, my goal was to develop a model system for studying and visualizing the assembly and trafficking of DAPs in live cells. My first aim was to determine if the Δ3849 minidystrophin construct effectively integrates into the DPC, when delivered as gene therapy. Next, I aimed at implementing this model system to study the behavior and trafficking pathways of α- sarcoglycan, as it is responsible for the large majority of LGMD's. These results should determine if α-sarcoglycan utilizes known trafficking mechanisms. Additionally, I aimed at determining the implications of the most commonly occurring R77C mutation on α-sarcoglycan protein traffic Finally, I plan to resolve if specific sarcoglycan sub-complexes are able to translocate to the plasma membrane, as is often documented in cases of γ-sarcoglycanopathy (LGMD 2C).

The following chapters describe the research conducted and the results obtained that shed light on how the genes involved in the muscular dystrophies behave and assemble in living cells.

CHAPTER 1

Mini-dystrophin efficiently incorporates into the DPC- A model system for studying dystrophin associated proteins in living cells*

ABSTRACT

Dystrophin is a critical muscle cell structural protein which when deficient results in Duchenne muscular dystrophy. Recently miniature versions of the dystrophin gene have been constructed that ameliorate the pathology in mouse models. To characterize mini-dystrophin's incorporation into the DPC in living cells, two fusion proteins were constructed where mini-dystrophin is fused to the N- or C- terminus of an enhanced green fluorescent protein reporter gene. Both fusion proteins correctly localize at the plasma membrane in vitro and in vivo. Live cell microscopy establishes that mini-dystrophin translocates directly to the plasma membrane of differentiating muscle cells, within four hours of expression. Latrunculin A treatment, actin and β-dystroglycan binding domain deletion constructs, and co-immunoprecipitation assays demonstrate that mini-dystrophin is firmly anchored to the sarcolemma primarily through its connections to β-dystroglycan, mimicking effects seen with wild type dystrophin. Furthermore, point mutations made within the putative β-dystroglycan anchoring ZZ domain of minidystrophin result in an ablation of β-dystroglycan binding and a nuclear translocation of the protein. These results demonstrate that mini-dystrophin is efficiently bound and incorporated into the DPC, via β-dystroglycan in living cells, similarly to the full length dystrophin protein.

INTRODUCTION

Duchenne Muscular dystrophy (DMD) is an X linked, debilitating and lethal genetic disease that affects about 1 in 3,500 male births each year (124). One third of the cases arise from de novo mutations (125). Patients are generally wheel chair bound by 6-10 years of age and die in their early twenties (126).

In 1987 the protein product of the largest gene in the human body, dystrophin, was discovered (13). Dystrophin is 14kb gene (cDNA) that encodes a 110 nm long, 427-kDa protein composed of 3685 amino acids (13). The protein resides directly underneath the sarcolemma of skeletal and cardiac muscle, forming a homogeneous network (18). Functionally, dystrophin links the intracellular actin cytoskeleton to the extracellular basement membrane via distinct structural domains. Specifically, at the N-terminal domain dystrophin binds cytoskeletal F-actin. The central rod domain contains 24 triple helix rod repeats and 4 hinges (104), which serve to stabilize the protein. Its C-terminus contains a cysteine rich (CR) region and a distal region. At the CR region it binds the dystroglycans, which are part of the DPC (DPC) (Figure I-5). The dystroglycans comprise a transmembrane β-dystroglycan adjoined to an extracellular α-dystroglycan subunit, which binds Laminin α2, a key component of the extracellular basement membrane, completing the molecular bridge between the inside and the outside of the cell (Figure I-5). In the absence of dystrophin, the integrity of the entire DPC and plasma membrane are compromised, leading to chronic muscle damage and degenerative pathology (8, 104).

Recent studies have revealed that the CR region can be further subdivided into four additional domains that specifically mediate β-dystroglycan binding. The first 37 amino acids of the CR region are identified as the WW domain (127, 128). Following the WW domain are two EF hand like domains (EF1 and EF2) (129), which separate the WW domain from the terminal 47 amino acids of the CR region denoted as the ZZ domain (130). In 2004, in vitro overlay binding assays were used to show that this domain is also involved in forming a stable interaction between dystrophin and β-dystroglycan. In addition, patient case specific mutations of cysteines within this region, correlated with diminished binding activity (91).

The absence of normal dystrophin expression and interactions at the plasma membrane accounts for approximately 60% of the "primary muscular dystrophies" (17). Several attempts have been made to deliver dystrophin back into muscle to reverse the pathology. Adeno-Associated virus (AAV) vectors have proved to be successful in establishing efficient and long term gene expression in muscle tissue in vivo (95, 96, 131). This is largely due to the fact that the vector is small enough to bypass the extracellular barriers (97, 104, 132). However, the virus also has a small packaging limit of 4.5 kb (96, 99, 104, 133), far too small to accommodate the 14 kb dystrophin gene. Wang & colleagues (2000) have overcome this problem by engineering miniature versions of the dystrophin gene that have deletions in major portions of the rod domain, yet still retain their full functionality (104). Importantly, the modified genes are small enough to fit into the AAV vector cassette, and restore long term gene expression and pathologic phenotypes in the mdx mouse (104), a DMD mouse model, lacking dystrophin at the sarcolemma of muscle fibers. Success of these mini transgenes at improving force output and other features of the dystrophic mdx phenotype makes them a promising therapy option in larger mammals (126). As efforts to expand AAV capacity, while increasing specificity and reducing toxicity,

take the spot light, less focus has been placed on whether the minidystrophin protein itself is integrating efficiently into the DPC on a molecular level, and whether it truly mimics the behavior of normal dystrophin.

In the following study I employ a combination of live cell, confocal imaging and biochemical assays to investigate minidystrophin's integration into the DPC in living cells. Live cell microscopy demonstrates that minidystrophin is efficiently translocated to the plasma membrane of muscle cells early in differentiation. Once at the surface, drug treatment, binding domain deletion constructs, co-immunoprecipitation's and site directed mutagenesis demonstrate that minidystrophin is anchored firmly to the sarcolemma, primarily through its connections to β-dystroglycan, similar to wild type dystrophin. Additionally minidystrophin conforms to the sequential assembly of the DPC, properly translocating to the plasma membrane only after β-dystroglycan deposition (8). These results demonstrate that minidystrophin is efficiently incorporated into the DPC through similar binding domains, and mechanisms used by full length dystrophin.

RESULTS

Localization of EGFP-tagged minidystrophin

To examine the localization of the N- and C- terminal 3849 bp minidystrophin-EGFP constructs (Figure 1-1A), they were transiently transfected into C57 skeletal muscle cells and confocal microscopy was used to visualize the fluorescent proteins in differentiated myotubes (3 days into differentiation). Both 3849-EGFP-N1 and C1 correctly localized to the sarcolemma of differentiated myotubes, and co-localized with an antibody directed against the mini-dystrophin protein (Figure 1-1B). Protein size was evaluated by western blot, and antibodies directed

against Rod regions 23 & 24 of minidystrophin, as well as antibodies directed against EGFP were used to probe for the fusion proteins. The minidystrophin antibody successfully detected the 143-kDa 3849 protein, as well as the 170-kDa fusion 3849-EGFP-N1 protein (data not shown). 3849-EGFP-C1 is detected at a slightly lower molecular weight than expected, approximately 167 kDa (data not shown). The EGFP antibody also detected the same fusion proteins, and did not detect untagged 3849 (data not shown). We next confirmed the expression and correct localization of the fusion proteins *in vivo*. 3849-EGFP-N1 and C1 were injected as plasmid DNA into the hind legs of an mdx mouse, which does not endogenously express dystrophin. This therefore, is a good model to test if the fusion proteins are deposited at the sarcolemma similar to established un-tagged models administered as gene therapy (104). One week after injection, muscle was harvested and examined. 3849-EGFP-N1 and C1 correctly localized to the sarcolemma of the mdx mouse skeletal muscle fiber (Figure 1-1C). Taken together these results demonstrate the proper localization of N- and C-terminal minidystrophin-EGFP fusion proteins in vitro and in vivo. Although both constructs seem to deposit similarly at the plasma membrane, 3849-EGFP-N1 produces a protein product of the correct size (slightly larger than the 3849-EGFP-C1), that localizes and functions similarly to the untagged 3849 minidystrophin in myopathic muscle. Additionally, because the 3849 protein does not contain the wild-type C-terminal region, I rationalized that the EGFP protein may act as a pseudo C-terminal cap for the CR region. Furthermore, more cells seemed to stably express 3849-EGFP-N1 at the plasma membrane than 3849-EGFP-C1. We therefore, choose to use the 3849-EGFP-N1 for the rest of our experiments.

A

Human Dystrophin

| N | H1 | R1 | R2 | R3 | H2 | R4 | R5 | R6 | R7 | R8 | R9 | R10 | R11 | R12 | R13 | R14 | R15 | R16 | R17 | R18 | R19 | H3 | R20 | R21 | R22 | R23 | R24 | H4 | CR | CT |

| N | H1 | R1 | R2 | R22 | R23 | R24 | H4 | CR | Egfp | Δ3849 minidystrophin-EGFP-N1

| Egfp | N | H1 | R1 | R2 | R22 | R23 | R24 | H4 | CR | Δ3849 minidystrophin-EGFP-C1

B

	EGFP	Dystrophin	Overlay
3849-EGFP-N1			
3849-EGFP-C1			
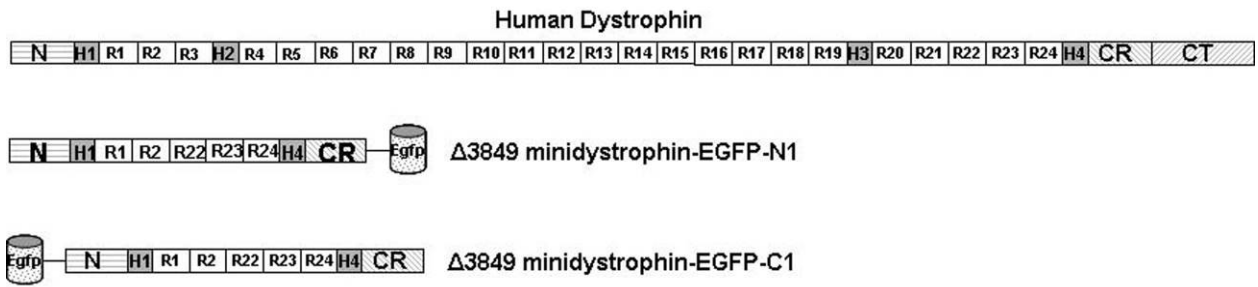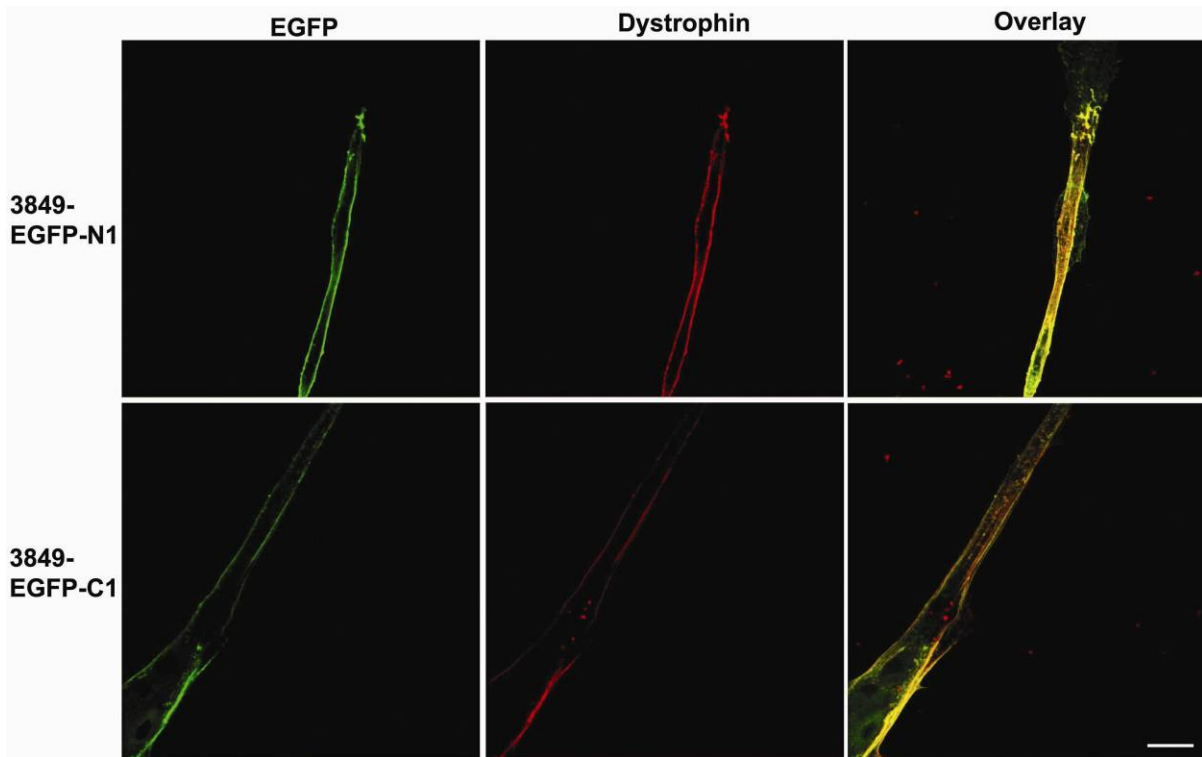
C
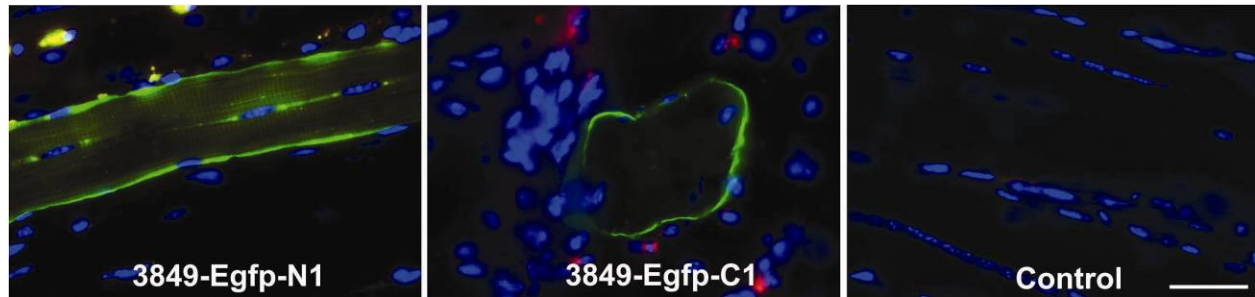
Figure 1-1. Minidystrophin-EGFP function in vitro and in vivo. (A) Schematic representation of full length and 3849bp mini-dystrophin, tagged to the N- and C- terminus of EGFP. (B) 3849-EGFP-N1 and C1 were transfected into C57 muscle cells which were allowed to differentiate for 3 days after transfection. Confocal analysis was then conducted on differentiated myotubes. Mid plane sections are shown for the fusion protein in green and mini-dystrophin staining in red. An 8 plane projection overlay is shown for both constructs. Bar=10μm. (C) 3849-EGFP-N1 and 3849-EGFP-C1 were injected (as plasmid DNA) into a 5 month old mouse TA muscle. Electroporation of the muscle at 100v was administered during the injection for amplification of plasmid entry. Muscle was harvested 2 weeks after injection, and 8 μm frozen sections were cut and analyzed for by wide-field microscopy. The fusion protein is in green, and nuclei are shown in blue. Bar=45μm. From ref. 168.

Dynamics of Minidystrophin-EGFP expression and translocation in live muscle cells

Other groups have used tagged dystrophin and minidystrophin constructs primarily as a tool to report the level of gene transduction, to improve delivery protocols (119), and devise novel methods of delivery (134). The goal of these studies, however, is to answer fundamental biological questions about the protein itself, and how it behaves and assembles into the DPC in living muscle. Our first goal was to study the temporal dynamics and trafficking route of 3849-EGFP-N1 as it translocates to the plasma membrane of differentiating muscle cells. Initially no EGFP is observed in the C57 cells (Figure 1-2A & B). After two hours a slight amount of EGFP expression is observed scattered throughout the cytoplasm, with slightly denser regions at the plasma membrane (Figure 1-2C), shown also in pseudo-color to highlight intensity differences (Figure 1-2D). Four hours after the start of expression, distinct plasma membrane localization is observed (Figure 1-2E & F). After about six hours expression is continuous and dense along the plasma membrane (Figure 1-2G). Importantly, as the gene is produced the intensity at the

plasma membrane increases proportionately much more than the signal in the cytoplasm (Figure 1-2H), demonstrating a translocation to plasma membrane after a transient cytoplasmic expression. These data establish that 3849 minidystrophin-EGFP-N1 translocates directly and efficiently to its desired location in living muscle cells early in differentiation, without mistrafficking.
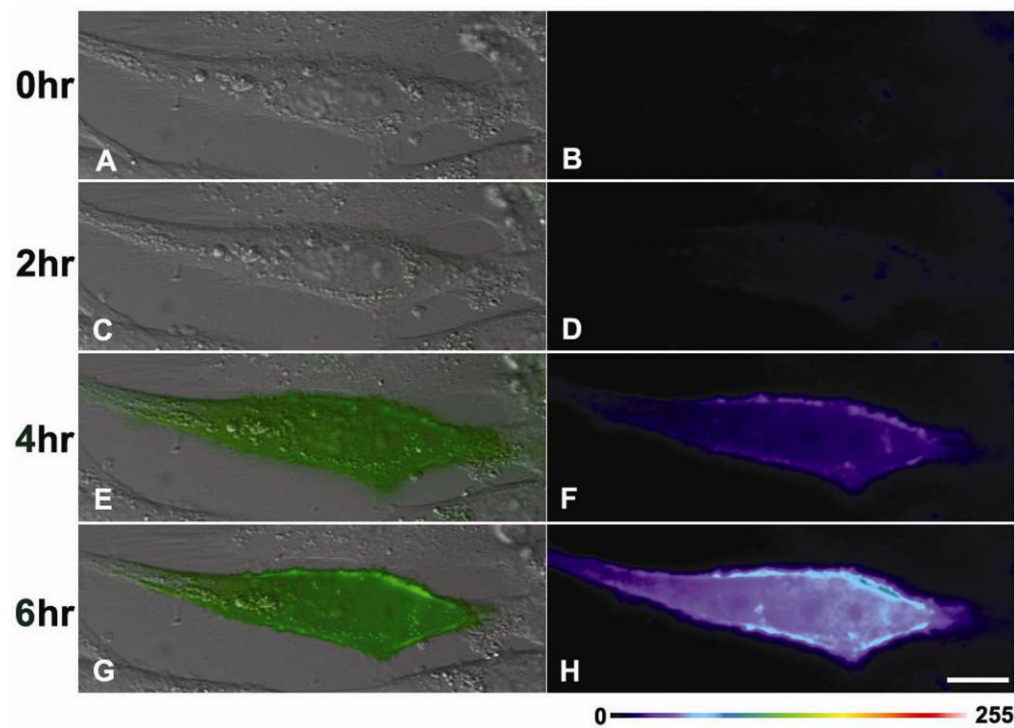
Figure 1-2. Temporal expression of minidystrophin-EGFP in a living C57 muscle cells. 3849-EGFP-N1 was transfected into C57 muscle cells which are imaged about 12 hours after transfection at the start of differentiation. Differential Interference contrast (DIC) and fluorescent images were acquired every 150 seconds, for a period of 24 hours. Mini-dystrophin is shown in green in the left panels (A, C, E, G), along with DIC to show cell morphology. The right panel images (B, D, F, H) are pseudocolored to show fluorescence intensity. A pseudo color chart is provided ranging from 0-255. Bar=10μm. From ref. 168.

Characterizing mini-dystrophin's attachment to the plasma membrane in living cells

The 43 kDa β-dystroglycan isoform is expressed in a wide variety of tissues (data not shown), along with several other isoforms (135) early in differentiation, where it exists as an integral membrane protein and is critical to normal cell development (8, 136-139). We therefore, reasoned that it may also be responsible for the proper deposition of 3849-EGFP-N1. HEK293 cells express β-dystroglycan (Figure 1-3), however, do not express many of the other members of the DPC, such as the sarcoglycans, or normal levels of dystrophin (Figure 1-3). We therefore, chose to use this cell line to identify proteins responsible for anchoring 3849-EGFP-N1 to the plasma membrane. 293 cells were transfected with 3849-EGFP-N1, and imaged by confocal microscopy approximately 18 hours after transfection. 3849-EGFP-N1 correctly localized to the plasma membrane in untreated 293 cells (Figure 1-4A).
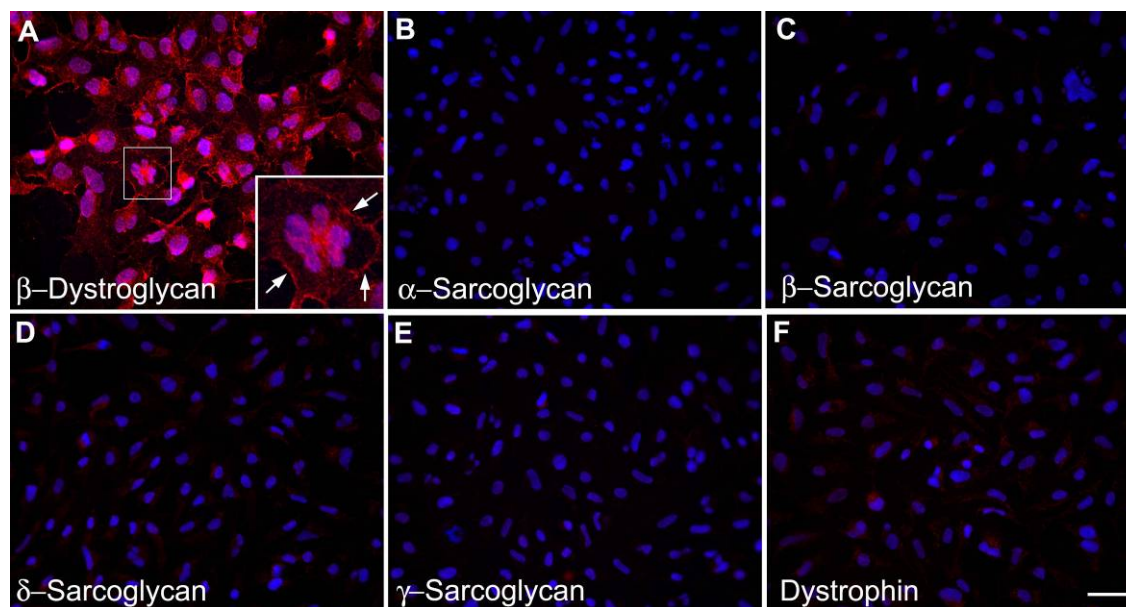
Figure 1-3. . DPC protein expression in 293 cells. 293 cells at about 80% confluency were fixed and stained for DPC proteins β-dystroglycan (A), inset and arrows show membrane localization, α-sarcoglycan (B), β-sarcoglycan (C), δ-sarcoglycan (D), γ-sarcoglycan (E), and dystrophin (F). These proteins are shown in red and nuclei are shown in blue. Bar=35μm. From ref. 168.

35

A

	Untreated	Latrunculin A
3849-EGFP-N1		
Actin		
Overlay		
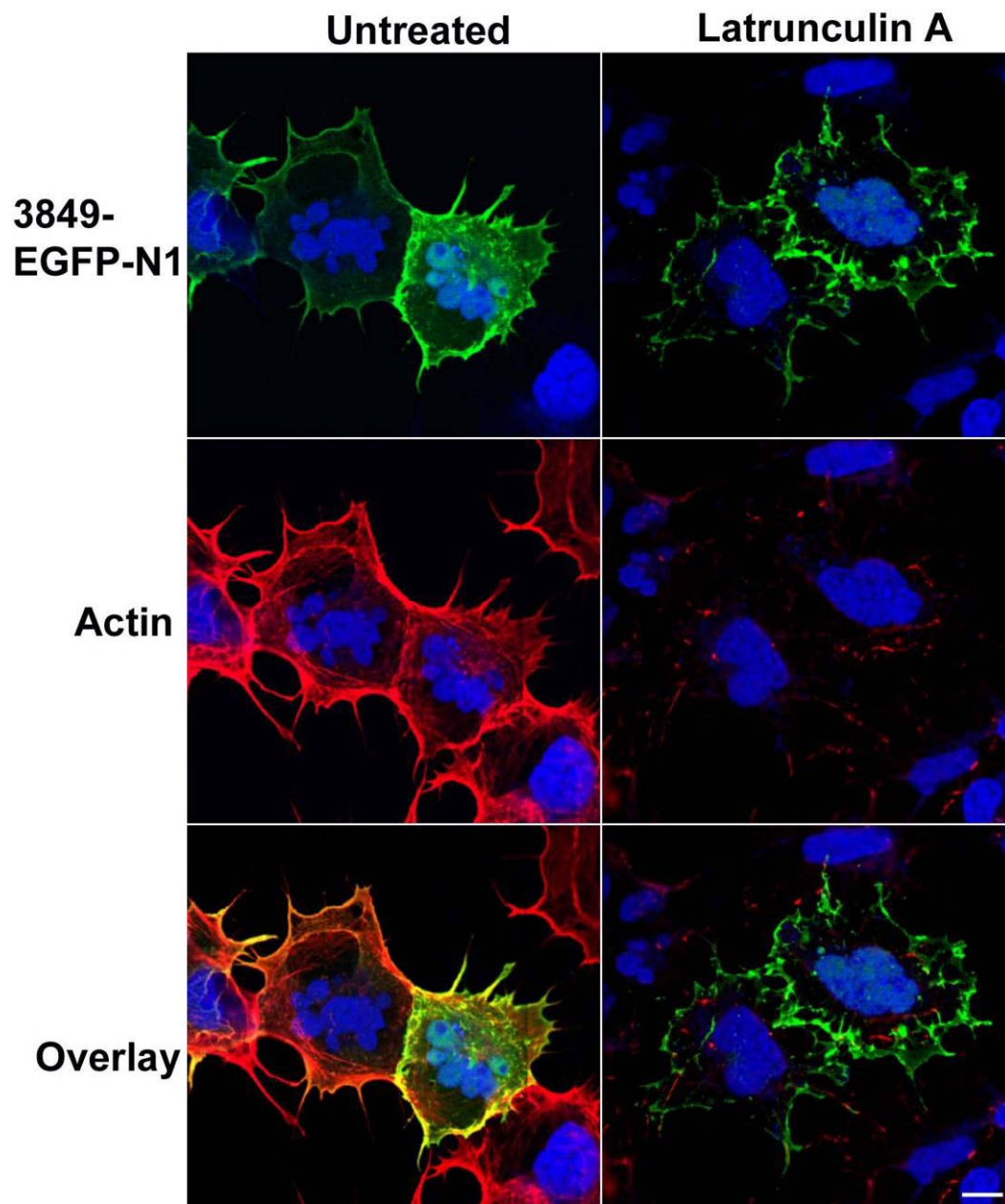
B
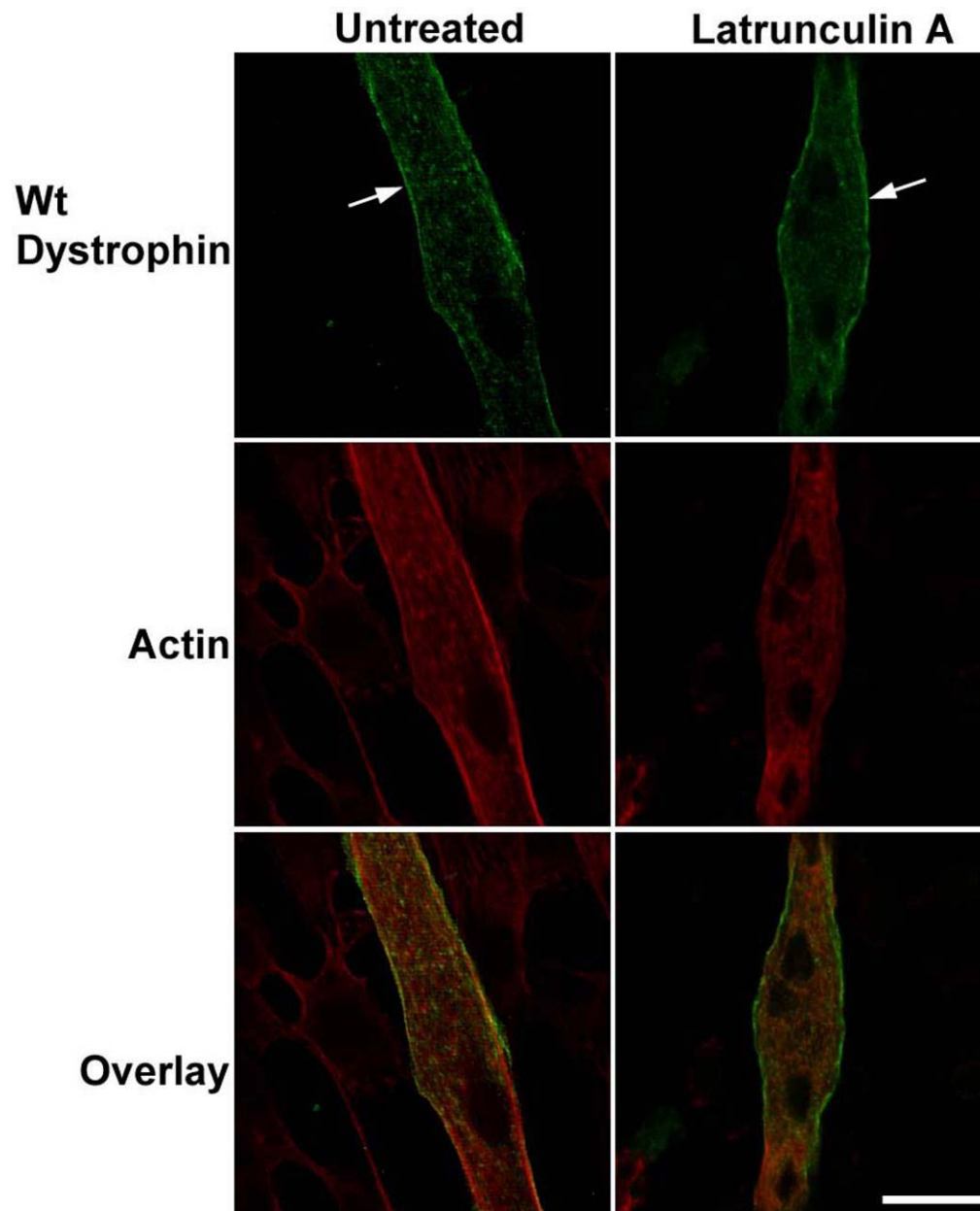
Figure 1-4. Effects of Latrunculin A treatment on 3849-EGFP-N1 and wild type dystrophin localization. (A) 3849-EGFP-N1 was transfected into 293 cells and examined after 18 hours. Cells were then treated with 0.5ug/ml of Latrunculin A for 5 minutes and examined by confocal microscopy. Mini-dystrophin is shown in green, Actin in red, and nuclei in blue. Untreated cells are in the left column and treated cells are in the right. The bottom row is a three color overlay. Bar= 10µm. (B) Endogenous dystrophin in C57 muscle cells treated and imaged the same as above. Untreated cells are in the left column and treated cells are in the right. Wild type dystrophin is shown in green, with arrows to show membrane staining. Actin is shown in red, and an overlay is provided in the bottom row. Bar= 30µm. From ref. 168.

The actin cytoskeleton in many cells functions as a structural framework that holds many proteins in place, including members of the DPC, especially β-dystroglycan and dystrophin itself (8, 140). Because the minidystrophin 3849 contains both the crucial N-terminal F-actin binding domain and the CR β-dystroglycan binding region, it is important to determine if the actin binding domain of minidystrophin is responsible for its interaction with the sarcolemma, as have been described previously in mutant dystrophin molecules lacking C-terminal domains yet retaining the ability to localize to the myofiber membrane (141), or whether the attachment of 3849-EGFP-N1 to the sarcolemma is via firm protein interactions to DPC proteins, independent of an intact actin cytoskeleton. To test this, 293 cells transfected with 3849-EGFP-N1 were treated with 0.5μg/ml of latrunculin A, which disrupts the actin cytoskeleton (142), 3849-EGFP-N1 remains firmly anchored to the plasma membrane of 293 cells (Figure 1-4A), even as the cell undergoes tremendous changes in morphology. Actin staining demonstrates a clustered actin bundle with no fibrous network existing as a cytoskeleton (Figure 1-4A). 3849-EGFP-N1 displacement from the plasma membrane was then quantified. The mean average fluorescence intensity at the plasma membrane in untreated cells is 22.43, and the mean fluorescence at the plasma membrane after latrunculin A treatment is 18.18 (n=10). This demonstrates that, although there is a slight decrease in 3849-EGFP-N1 at the plasma membrane after Latrunculin A treatment, an intact actin cytoskeleton is not significantly responsible for anchoring the majority of 3849-EGFP-N1 to the plasma membrane in non-muscle HEK 293 cells.

To investigate the effects of latrunculin A on wild type dystrophin plasma membrane deposition, C57 muscle cells were allowed to differentiate into myotubes, which expressed dystrophin at the plasma membrane (Figure 1-4B, *arrows*). After myotubes were treated with

0.5μg/ml of latrunculin A, the majority of dystrophin remained anchored to the plasma membrane (Figure 1-4B), as observed by confocal microscopy, recapitulating the results observed with 3849-EGFP-N1.

To further test the hypothesis that the actin binding domain is not the primary mechanism for mini-dystrophin attachment to the plasma membrane, I used two additional miniature dystrophin constructs. Both constructs were engineered from Becker versions of full length dystrophin (141), lacking a major portion of the rod domain, that is also deleted in our minidystrophin construct. Becker versions of full length dystrophin, localize to the plasma membrane in human muscle and result in a milder form of muscular dystrophy in humans (143, 144), additionally, these truncated proteins contain all the components present in minidystrophin making it comparable to our 3849-EGFP-N1 construct (Figure 1-1A). The Becker N-half construct contains the crucial actin binding domain in the N-terminus, rods 1, 2, 3, 20 and 21 but lacks the CR β-dystroglycan binding region (Figure 1-1A). The Becker C-half construct on the other hand contains rods 22, 23, 24 and the CR β-dystroglycan binding region, but does not contain an actin binding domain (Figure 1-1A). When these constructs were expressed in a C2C12 muscle cell line, only the C-half construct, containing the CR region, is detectable and properly localizes to the plasma membrane (Figure 1-5), whereas the N-terminus construct containing the actin binding domain, shows little to no staining, which is consistent with previous studies utilizing a similar construct, reporting a rapid degradation with virtually no protein expression (141). Corroborating results were recapitulated in HEK 293 cells, where once again the actin binding domain alone is insufficient for proper anchoring at the plasma membrane (Figure 1-5), whereas the CR containing region is sufficient. These results suggest

that the majority of minidystrophin anchoring at the sarcolemma is not regulated via the actin binding domain, but rather the CR containing region.
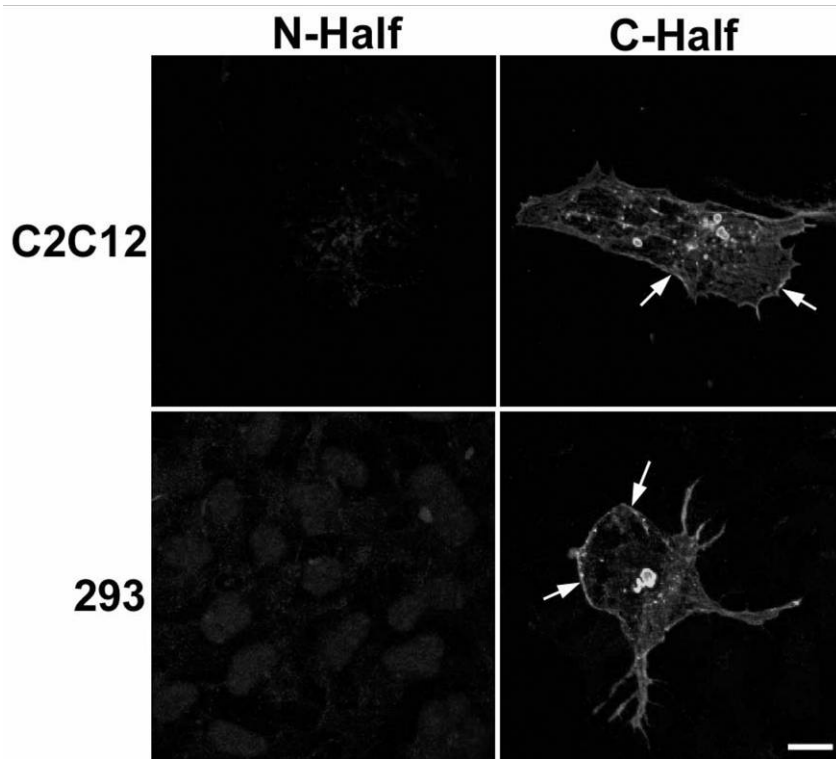
Figure 1-5. Expression of N- and C- half Becker constructs in muscle and non-muscle cells. N-half Becker construct contains the actin binding domain, and C-half Becker construct contains CR region and no actin binding domain, Both constructs were transfected into muscle C2C12 and non-muscle 293 cells. The left panel shows no expression of the N-half construct, where as the right panel shows proper localization of the C-half construct at the plasma membrane. Bar=10um. From ref. 168.

In normal myotube development DPC proteins are thought to follow a sequential assembly process whereby the proper deposition of one protein is dependent on its binding partner, expressed earlier in the development sequence (8), in this case dystrophin deposition is dependent on β-dystroglycan expression (8). To investigate if minidystrophin is likewise dependent on β-dystroglycan deposition, C2C12 muscle cells were transfected with 3849-EGFP-N1, and co-labeled for β-dystroglycan both before and after differentiation. When muscle cells

were not allowed to differentiate, β-dystroglycan was expressed only slightly (Figure 1-6B) and mostly intracellularly (Figure 1-6A), which in turn correlates with increased intracellular 3849-EGFP-N1 expression (Figure 1-6A & C). Interestingly, as the muscle cells are allowed to differentiate, β-dystroglycan is up regulated (Figure 1-6B), and begins to translocate to the plasma membrane (Figure 1-6A), which also correlates with 3849-EGFP-N1 translocation (Figure 1-6A & C). In fact, 3849-EGFP-N1 co-localizes nearly exclusively with β-dystroglycan plasma membrane expression (Figure 1-6A). This observation is more defined 2 days after differentiation, where almost all the 3849-EGFP-N1, and β-dystroglycan co-localize at the plasma membrane, with a significant decrease in the intracellular signal of both proteins (Figure 1-6A & C). No endogenous dystrophin is expressed this early in differentiation (Figure 1-7).

Although these results suggest a minidystrophin- β-dystroglycan association, they do not show a protein-protein interaction. We therefore, utilized a co-immunoprecipitation assay to confirm an interaction between 3849-EGFP-N1 and β-dystroglycan. β-dystroglycan was immunoprecipitated from 293 cells (Figure 1-8- lane 4) transfected with 3849-EGFP-N1 (Figure 1-8- lane 2). B-dystroglycan was immunoprecipitated using a monoclonal antibody. 3849-EGFP-N1 co-immunoprecipitated along with β-dystroglycan (Figure 1-8- lane 4), but not with beads alone (containing no β-dystroglycan antibody) (Figure 1-8- lane 6). Pellets were analyzed by western blot using polyclonal antibodies against EGFP, and β-dystroglycan. Similar results are seen for wild type dystrophin which also has β-dystroglycan bound to it when immunoprecipitated (Figure 1-8- lane 7). We therefore, conclude that minidystrophin is bound to the sarcolemma via its interactions with β-dystroglycan.

A
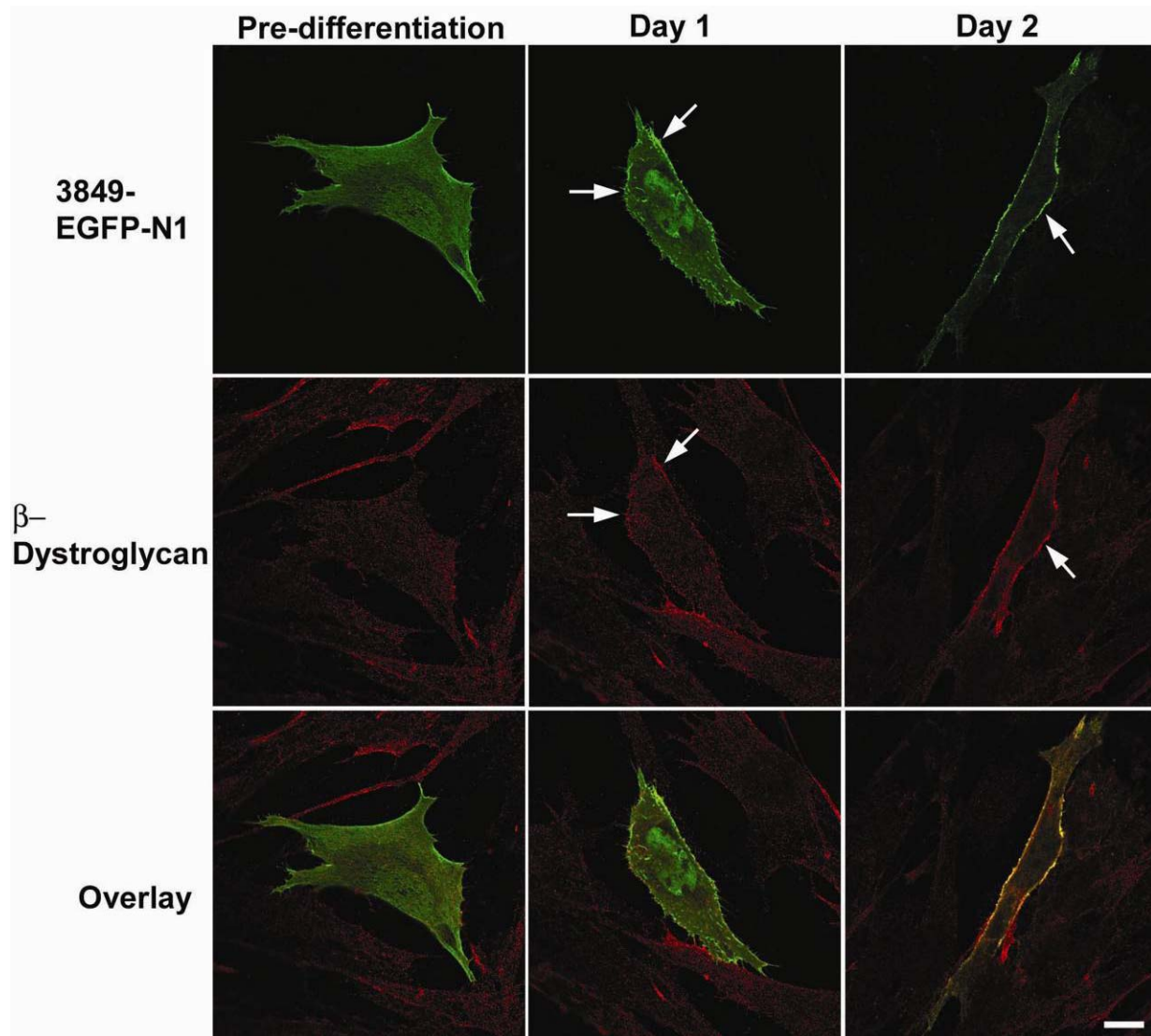
B
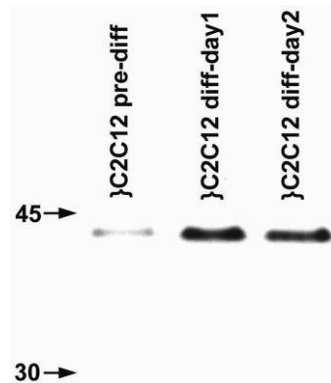
C
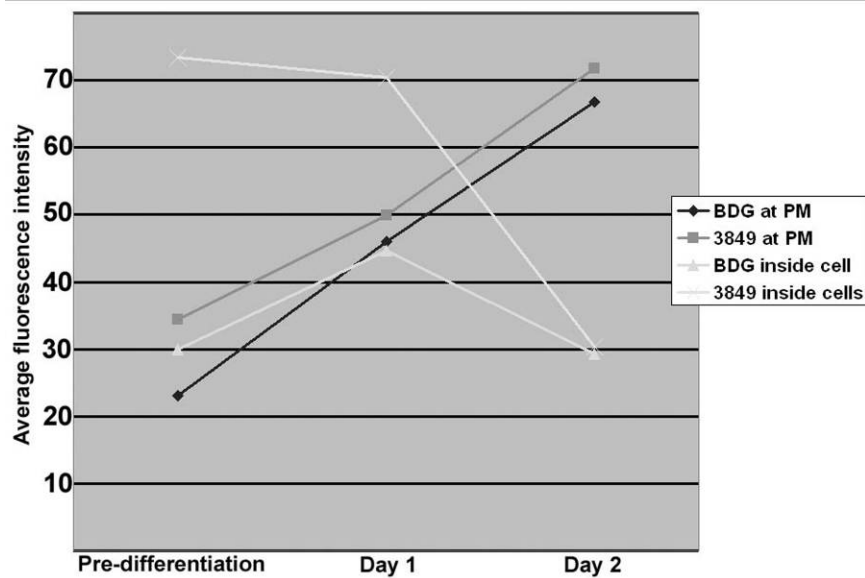
Figure 1-6. Co-translocation of 3849-EGFP-N1 and β-dystroglycan to the membrane of C2C12 muscle cells during early differentiation. (A) in the left column are C2C12 cells transfected with 3849-EGFP-N1 (green), and not allowed to differentiate. β-dystroglycan is stained in red and an overlay is provided in the lowest row. Arrows show co-translocation and co-localization of 3849 and β-dystroglycan to the membrane, 24 hours (middle column) and 48 hours (right column) after cells were allowed to differentiate. Bar= 10um. (B) Western blot of 43kDa β-dystroglycan expression with C2C12 muscle cell differentiation. (C) Mean fluorescence of 3849-EGFP-N1 and β-dystroglycan (BDG) at the membrane and inside the cell were calculated at each of the three time points (n=8), and then plotted as a line graph. From ref. 168.
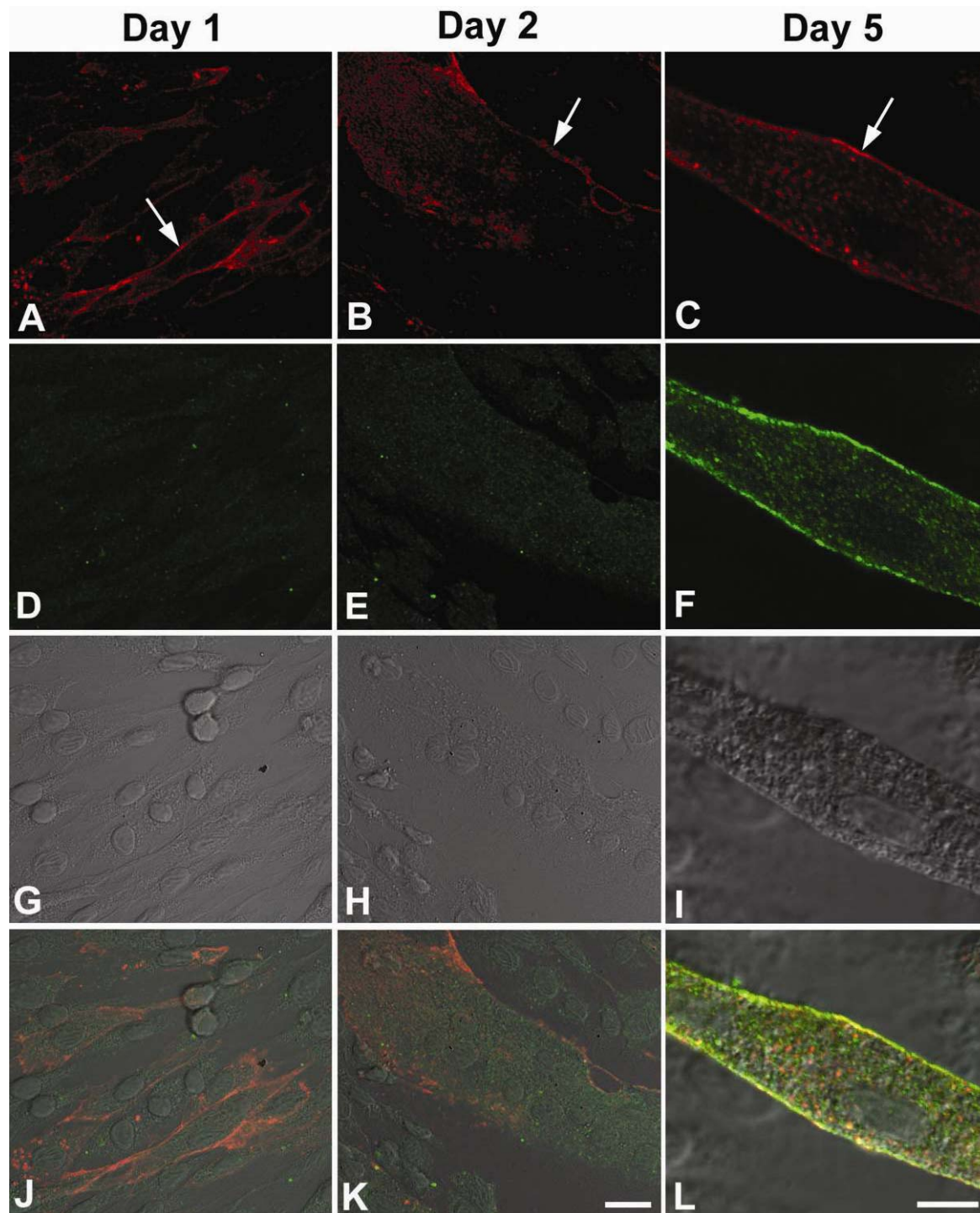
Figure 1-7. Temporal expression of wild-type dystrophin and β-dystroglycan in differentiating C57 muscle cells. C57 myoblasts were allowed to differentiate for five days. Endogenous dystrophin and β-dystroglycan were stained using antibodies directed against β-dystroglycan (A, B, C), and the rod terminus of dystrophin (D, E, F). Arrows show membrane localization of β-dystroglycan prior to dystrophin deposition, except at day 5 when dystrophin is expressed and co-localizes with β-dystroglycan. Cell morphology is shown through DIC (G, H, I), and an overlay is provided (J, K, L). Bar= 25um (A, B, D, E, G, H, J, K), and Bar= 15um (C, F, I, L). From ref. 168.
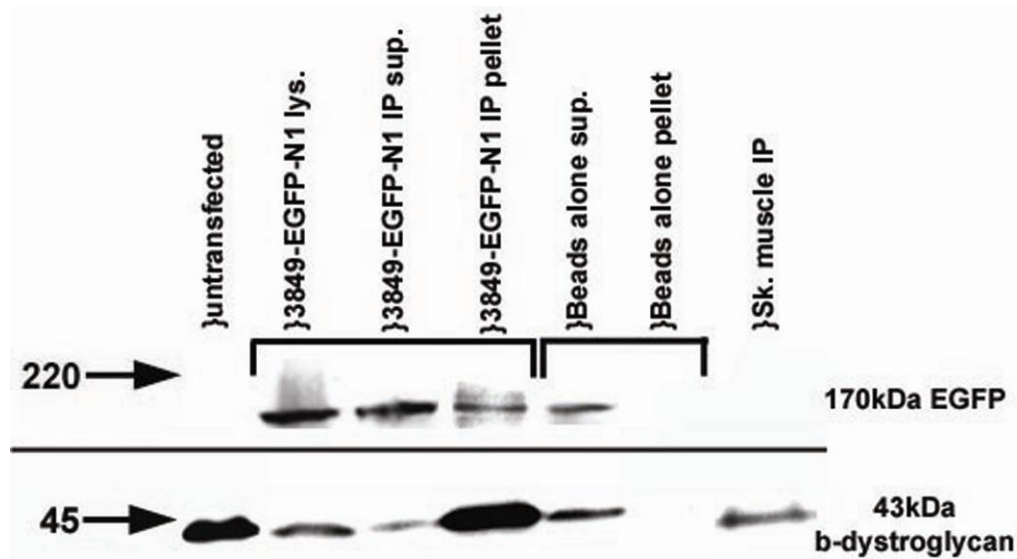
Figure 1-8. Co-immunoprecipitation of 3849-EGFP-N1 with β-dystroglycan. Lane one- 43kDa β-dystroglycan expression in normal 293 cells with no endogenous protein at 170kDa detected with an EGFP antibody. Lane 2- β-dystroglycan and 3849-EGFP-N1 in 293 cell lysates transfected with 3849-EGFP-N1. Lane 3- Reduced β-dystroglycan and 3849-EGFP-N1 in the supernatants of β-dystroglycan immunoprecipitates. Lane 4- Enriched β-dystroglycan in β-dystroglycan immunoprecipitate pellets, accompanied by a co-immunoprecipitation of the 3849-EGFP-N1 protein. Lane 5- When Protein G beads alone (with no antibody) are incubated with the 3849-EGFP-N1 cell lysates, there is no depletion of β-dystroglycan. Lane 6- Protein G beads alone do not immunoprecipitate either β-dystroglycan or co-immunoprecipitate 3849-EGFP-N1. Lane 7- Co-immunoprecipitation of β-dystroglycan with wild type dystrophin from rat skeletal muscle. A monoclonal β-dystroglycan antibody was used for the immunoprecipitations in lanes 1-6, followed by a polyclonal EGFP (top panel) antibody along with a polyclonal β-dystroglycan (bottom panel) antibody for the western blotting. In Lane 7 a polyclonal dystrophin antibody was used for the immunoprecipitation, followed by a monoclonal β-dystroglycan antibody for the western blotting. From ref. 168.

Effects of CR region point mutagenesis on minidystrophin protein traffic

Conserved within the 3849 minidystrophin gene is the complete CR region, which contains multiple putative β-dystroglycan binding sites. Previously *in vitro* assays have been used to correlate patient point mutations with effects on protein binding (91). To test β-dystroglycan binding to 3849-EGFP-N1, and visualize the effects of mutagenesis of the β-dystroglycan binding domain on protein traffic, I generated several constructs with point mutations within the CR region. Table 1-1 describes the mutations made to 3849-EGFP-N1. Mutations are also shown schematically against the minidystrophin molecule (Figure 1-9A). The majority of point

mutations reside within the ZZ domain, and consist of documented cysteine to tyrosine mutations, as well as corresponding cysteine to serine mutations (91).

To confirm that proteins of the right size were being produced from the mutant genes, cell lysates were probed with a dystrophin antibody to detect the fusion protein. All mutant genes produced a protein approximately 170KDa, the same size as the wild type 3849-EGFP-N1 protein (data not shown).

To visualize the effects of the mutagenesis on protein localization, the constructs were transfected and expressed proteins were imaged in 293 cells. As expected, the C433Y mutation within the rod region had no noticeable effect on protein localization (Figure 1-9B). A cysteine to tyrosine mutation within the WW domain at C952Y also had no visible effect on plasma membrane localization (Figure 1-9B), despite reports that this region is critical for proper dystrophin deposition (145). Likewise a C990R mutation within the EF-1 hand domain, observed in one patient (145), did not show an effect on the localization of the protein (Figure 1-9B). Remarkably, all mutations made within the ZZ domain resulted in nuclear localization of the EGFP fusion protein (Figure 1-9B- *C1183F, C1207Y, C1207S, C1210Y, C1210S*). No significant difference in protein localization is noted between cysteine to tyrosine mutants and cysteine to serine mutants, despite *in vitro* data showing differences in β-dystroglycan binding using overlay assays, with similar mutations (91). ZZ domain mutants were also tested in C57 muscle cells, where they also showed nuclear localization (data not shown), corroborating evidence from the 293 cell lines.

Next I investigated if any of these ZZ domain mutant minidystrophin-EGFP proteins actually binds β-dystroglycan. A co-immunoprecipitation was performed following the same procedure used for the un-mutated 3849-EGFP-N1 (Figure 1-8). Our results show that none of

these ZZ domain mutant minidystrophin-EGFP proteins are able to properly bind β-dystroglycan (Figure 1-9C). These data reveal that mutations made within the ZZ domain ablate binding to β-dystroglycan, accompanied by a mislocalization of the minidystrophin protein and translocation into the nucleus. This region is therefore, crucial to the proper plasma membrane deposition and anchoring of the minidystrophin molecule.

Taken together these results confirm the hypothesis that 3849-EGFP-N1 minidystrophin properly integrates and is anchored to the DPC at the plasma membrane of living cells, primarily through its interactions with β-dystroglycan.

Mutation	Protein Domain	Protein localization	Patient correlation & reference
aa. C433Y	Rod domain	No effect- plasma membrane loc.	None
aa. C952Y	WW domain	No effect- plasma membrane loc.	None
aa. C990R	EF-1 hand domain	No effect- plasma membrane loc.	Patient mut., 41
aa. C1183F	ZZ domain	Nucleus	Patient mut., 40
aa. C1207Y	ZZ domain	Nucleus	None
aa. C1207S	ZZ domain	Nucleus	None
aa. C1210Y	ZZ domain	Nucleus	Patient mut., 39, 15
aa. C1210S	ZZ domain	Nucleus	Patient mut., 39, 15

Table 1-1. Minidystrophin mutation table. Point mutations were made by site directed Quik Change mutagenesis at various locations in the minidystrophin gene. Some of these mutations correlated to actual patient mutations, as referenced. Each mutation is correlated to protein behavior. From ref. 168.

A
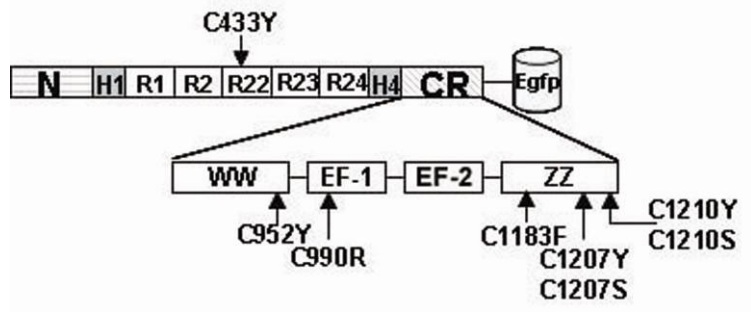
B
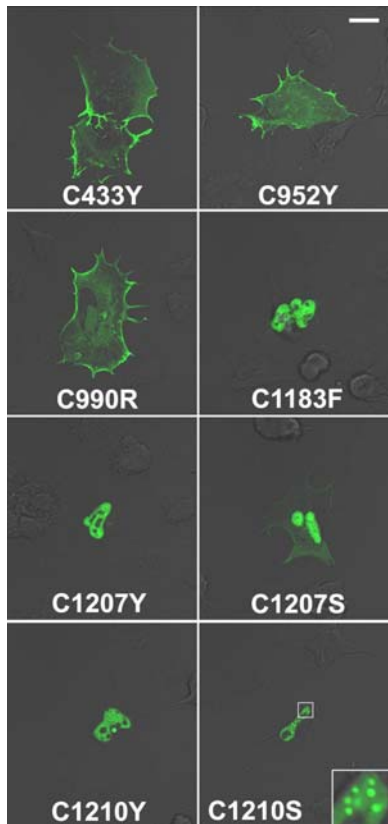
C
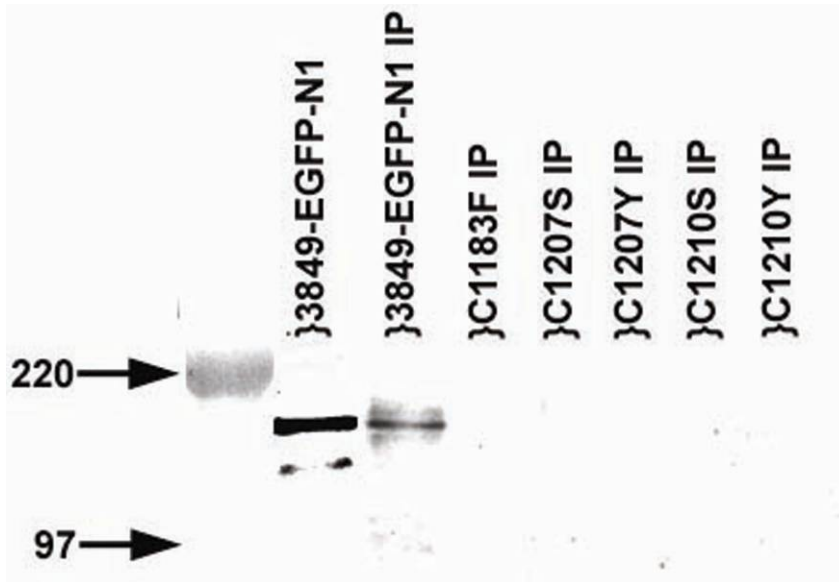
Figure 1-9. Effects of point mutagenesis on 3849-EGFP-N1 protein traffic in 293 cells. (A) Schematic of point mutations made within the mini-dystrophin molecule. Mutation C433Y is a cysteine to tyrosine in the rod region. C952Y is a cysteine to tyrosine mutation in the WW domain, C990R is a cysteine to arginine mutation in the EF-1 hand domain. C1183F is a cysteine to phenylalanine mutation in the ZZ domain. C1207Y and C1210Y are cysteine to tyrosine mutations within the ZZ domain. C1207S and C1210S are cysteine to serine mutations in the ZZ domain. (B) All mutants along with the normal 3849-EGFP-N1 were transfected separately into 293 cells. After 24 hours the cells were imaged using confocal microscopy. The fusion protein is shown in green, cell morphology is shown in DIC. Bar= 35μm. (C) co-immunoprecipitations were conducted on ZZ domain mutant constructs using a monoclonal β-dystroglycan antibody. Pellets were then probed by western blot using a polyclonal EGFP antibody. Lane 1- 3849-EGFP-N1 in 293 cells transfected with the transgene. Lane 2- co-immunoprecipitation of non mutated construct. Lanes 3-7- ZZ domain mutants. From ref. 168.

DISCUSSION

During the last decade several of the significant scientific barriers preventing gene therapy for muscular dystrophy have been bypassed. Miniature versions of dystrophin, which are readily packaged in AAV have proven to be the most effective candidates for AAV vector mediated gene therapy in mdx mice (104, 146-148). However, questions remain as to how effective minidystrophin is at integrating with the DPC at the sarcolemma on a molecular level (149, 150). In this study I report that a 3849 bp minidystrophin-EGFP fusion gene translocates rapidly and

efficiently to the sarcolemma of living C57 muscle cells early in differentiation. Once at the surface minidystrophin is firmly anchored to the plasma membrane via DPC interactions (namely β-dystroglycan). In addition, both documented and novel point mutations made within the ZZ domain, responsible for β-dystroglycan binding, cause a translocation of the fusion protein to the nucleus and an ablation of β-dystroglycan binding. These results are the first to characterize the molecular behavior of therapeutic fusion proteins in living systems, and therefore, provide a novel addition to the biology of gene replacement as well as the biology of the dystrophin protein itself.

It was previously shown that EGFP can be fused to the N-terminus of full length and a 6 kb minidystrophin without perturbation of function (119). However, given the 4.5 kb packaging limit of AAV, I sought to create even smaller functional minidystrophin-EGFP fusion proteins, using a 3849 bp minidystrophin (104). 3849-EGFP-N1 produces a protein that is the correct size and localized to the plasma membrane of muscle cells *in vitro* and *in vivo* more often than did 3849-EGFP-C1. Additionally, because the 3849 construct has a deleted C-terminus, and ends with the CR, I rationalized that placement of the EGFP tag at the C-terminal end may structurally act as a pseudo C-terminal cap for the CR, which may perhaps rationalize why more cells stably expressed 3849-EGFP-N1 at the plasma membrane. We therefore, choose to use the 3849-EGFP-N1 construct for our remaining studies in living cells.

Live cell microscopy allowed us to visualize minidystrophin-EGFP translocating directly to the cell surface approximately 4 hours after expression in newly differentiating primary muscle cells. This demonstrates that minidystrophin will traffic and integrate at the plasma membrane in the absence of many of the muscle specific DPC proteins, produced later in differentiation (137). Studies have shown β-dystroglycan is present at this early time point

(137), and therefore, it may be necessary for integration of minidystrophin. The expression of β-dystroglycan before dystrophin has also been documented in our laboratory, in C57 muscle cells at day 1 and day 2 of differentiation (Figure 1-7A & B). In these cells, dystrophin is not expressed until approximately day 5 (Figure 1-7F). Given that the majority of minidystrophin is found at the plasma membrane, it is also highly likely that the domains necessary for transport and anchoring are present despite the truncation of dystrophin.

To dissect the molecular mechanism of minidystrophin anchoring to the plasma membrane, I first asked if the actin binding domain in 3849 bp minidystrophin is responsible and sufficient for plasma membrane attachment? Latrunculin A selectively inhibited actin polymerization and disrupted the actin cytoskeleton in 293 cells, as evident from phalloiden staining, however, minidystophin remained at the plasma membrane, even when Latrunculin A was administered in excess, suggesting a more crucial β-dystroglycan anchoring interaction, as is the case for wild-type dystrophin, which showed similar effects from latrunculin A treatment, and profound effects on plasma membrane localization in vivo when the COOH-terminal region was deleted (151, 152). Previous studies have also reported that dystrophin and phalloidin compete for binding to actin filaments (153), furthermore, dystrophin might actually stabilize actin filaments against depolymerization (154). Our next series of experiments was therefore, aimed at demonstrating that the actin binding domain is insufficient for plasma membrane localization in 293 cells, where as the COOH-region, containing the CR region of minidystrophin is sufficient. For these experiments I used the N- and C- terminal domains of Becker dystrophin construct which are structurally very similar to 3849 minidystrophin and have been previously characterized (141). Deletion of the N-term actin binding domain did not have a considerable effect on minidystrophin plasma membrane localization in 293 cells, as previously

reported in COS-1 cells and mdx muscle (141). Deletion of the CR region (in the actin binding domain N-half construct); however, had a profound effect, resulting in no significant protein expression at the plasma membrane, correlating with data from human patients (17, 155, 156). Previous studies using this Becker N-half construct have also reported that very small amounts of the protein when over expressed, may be detected in select fibers at a low intensity (141); however, our studies in 293 cells show no labeling comparable to the C-half Becker construct at the plasma membrane.

We and other groups have previously shown that β-dystroglycan expression is necessary for normal tissue differentiation in human patients, and precedes dystrophin expression (8, 137, 139, 157). Furthermore, full length constructs lacking the β-dystroglycan-binding CR, containing only the C-terminal region, while being able to translocate to the membrane, do not restore β-dystroglycan levels (152). Therefore, to bolster the hypothesis that β-dystroglycan is involved in the anchoring of 3849-EGFP-N1 containing only the CR region and not the C-term region of wt dystrophin, both proteins were shown to co-translocate to the plasma membrane in differentiating muscle cells, but not in undifferentiated cells, where β-dystroglycan is not as yet expressed. Additionally, 3849-EGFP-N1 co-immunoprecipitates with β-dystroglycan, as is the case for wild type dystrophin. Taken together, these results imply that 3849-EGFP-N1 requires binding to β-dystroglycan for proper translocation and anchoring to the plasma membrane. These results differ from a study with full length dystrophin, where it has been reported that dystroglycan is not required for the proper localization of dystrophin (158), however, 3849-EGFP-N1 does not contain the C-terminal region that may assist in plasma membrane localization of full length dystrophin in cases where the Dystroglycan connections are missing (152). Therefore, in the case of minidystrophin, containing only the CR region, the β-

dystroglycan interaction may be more crucial for proper localization and anchoring at the plasma membrane.

To confirm this hypothesis, mutations were made within the ZZ β-dystroglycan binding domain which should prevent binding and subsequently plasma membrane localization. When the last cysteine within the ZZ domain at position 1210 was mutated to a serine and a tyrosine, a mutation which causes mental retardation in humans (159) and completely diminished β-dystroglycan binding in vitro (91), a nuclear translocation of minidystrophin occurred with punctuate spots seen within the nucleus, reminiscent of patterns seen in proteins with nuclear localization signals (NLS) (160, 161). This pattern was also observed when the cysteine at position 1207 is switched to a tyrosine or a serine.   Importantly, the former mutation is reported to have no effect on β-dystroglycan binding in overlay assays in vitro (91). In living cells, however, both mutations showed nuclear translocation of the fusion protein, that no longer binds β-dystroglycan. A similar pattern was also seen when the cysteine at position 1183 (at the beginning of the ZZ domain) was mutated to phenylalanine. This is a documented patient mutation, which results in possible DMD symptoms (145). Importantly, a documented patient point mutation, outside of the ZZ domain, in the EF1 hand region (C990R) did not alter the normal plasma membrane localization of the protein or its trafficking. Finally, mutating a cysteine within the WW domain, which is also thought to be involved in proper dystrophin deposition (145), had no effect on minidystrophin localization. These results imply that the ZZ domain not only plays a critical role in the minidytrophin/ β-dystroglycan interaction, but also if mutated may lead to nuclear deposition perhaps by generating a NLS, or by changing the conformational properties of the molecule and thus affecting binding partners that lead to nuclear localization.

Together, these experiments represent the first molecular study of therapeutic transgenes for Duchenne muscular dystrophy in living cells, which is paramount in the development of safe and effective gene therapy protocols in humans.

CHAPTER 2

Implementation of a model system- α-sarcoglycan is recycled from the plasma membrane

in the absence of sarcoglycan complex assembly*

ABSTRACT

The sarcoglycan complex consists of four subunits in skeletal muscle (α, β, γ, and δ-sarcoglycan). Mutations in α-sarcoglycan (α-sarcoglycan) result in the most common form of limb girdle muscular dystrophy. However, the function of α-sarcoglycan remains unknown. In this report, I attempt to clarify its function by delineating the trafficking pathway of α-sarcoglycan in live cells. We present evidence, utilizing total internal reflection microscopy, fluorescence recovery after photobleaching and photoactivation of GFP constructs, that pools of α-sarcoglycan are able to translocate to the plasma membrane in the absence of the remaining sarcoglycans. Internalization assays and drug treatment experiments demonstrate that α-sarcoglycan recycles from the plasma membrane and accumulates in recycling endosomes. We also establish that α-sarcoglycan utilizes well described clathrin mediated mechanisms and microtubules to traffic within the cell. Finally, I show that the most commonly re-occurring limb girdle muscular dystrophy (R77C) mutation, within α-sarcoglycan, causes a fundamental defect in protein biosynthesis, trapping the mutant protein in the endoplasmic reticulum. These results demonstrate that α- sarcoglycan requires assembly into the sarcoglycan complex for stability at the plasma membrane rather than export out of the endoplasmic reticulum. Furthermore, this

data suggests that α-sarcoglycan utilizes known trafficking machinery to control deposition at the plasma membrane through recycling.

INTRODUCTION

In 1992 a 50K dystrophin associated glycoprotein, termed adhalin (α- sarcoglycan) was reported deficient in patients with severe childhood autosomal recessive muscular dystrophy (SCARMD) (162). The time of onset, clinical pathology and rapid progression of SCARMD are similar to the more common Duchenne muscular dystrophy (DMD). Both myopathies are characterized by severe muscle cell necrosis leading to patient death in the second decade. In 1994 the α-sarcoglycan gene was cloned and mapped to chromosome 17q12-q21.33 (38). Soon after, the protein was discovered to be part of a transmembrane protein complex, composed of four sarcoglycan subunits (α, β, δ, γ) (43), which in turn is a component of the DPC.

Dystrophin is a member of the spectrin superfamily and is a long rod shaped protein that resides directly underneath the plasma membrane of skeletal and cardiac muscle (13). Functionally, dystrophin links the intracellular actin cytoskeleton to the extracellular basement membrane via a large oligomeric protein complex (Figure I-5). In the absence of dystrophin, the integrity of the entire DPC is compromised, leading to chronic muscle damage and degenerative pathology (8). Additionally, mutations in any one of the genes that encode the various sarcoglycans (α, β, δ, or γ) is thought to result in the absence of the entire sarcoglycan complex at the plasma membrane (39, 163, 164) (Figure I-5).

Mutations of the sarcoglycans are responsible for a subset of muscular dystrophies termed the limb girdle muscular dystrophies (LGMD 2D also known as SCARMD, 2E, 2F, and 2C respectively) (36, 37, 54, 65). Mutations identified in the α-sarcoglycan gene are clinically the most frequently found (38, 55, 56) and of these cases, one-third of the patients with an α-sarcoglycan mutation, have a missense substitution of a cysteine for an arginine in codon 77 (R77C) of the α-sarcoglycan protein (57, 59, 62).

In 1998 it was proposed that LGMDs are caused by aberrant sarcoglycan complex assembly and trafficking to the plasma membrane (46). Since then, this hypothesis has been supported by multiple other studies which also suggest that sarcoglycan assembly actually occurs in the endoplasmic reticulum (77, 78), and this aforementioned assembly is a prerequisite for successful delivery to the plasma membrane. On the other hand, immunocytochemistry has shown α-sarcoglycan to be detectable at the plasma membrane in patients with mutations in γ-sarcoglycan (8, 75, 165-167), and in α-sarcoglycan deficient patient biopsies, there is still some delivery of other sarcoglycans to the plasma membrane albeit at a low level (8, 71-73). This suggests that α-sarcoglycan may utilize complex assembly primarily for stability at the plasma membrane, rather than trafficking to the plasma membrane. This hypothesis is supported by biochemical studies showing that α-sarcoglycan is not cross-linked to the rest of the sarcoglycan complex (47), and has an intracellular C-terminus (46), unlike the others. To attempt to address this hypothesis I used a variety of molecular and imaging tools to define the intracellular trafficking and deposition of α-sarcoglycan. Our results provide strong evidence that α-sarcoglycan is transported to the plasma membrane, in the absence of the other sarcoglycans. α-sarcoglycan is also constitutively recycled from the plasma membrane and accumulates in recycling endosomes. Additionally α-sarcoglycan containing vesicles utilize clathrin coats to

traffic intracellularly along microtubules.   In contrast, the common R77C α-sarcoglycan mutant is localized and trapped in the endoplasmic reticulum.

RESULTS

Addition of an EGFP tag does not alter the function of α-sarcoglycan

To visualize the dynamics of α-sarcoglycan (α-sarcoglycan) protein trafficking in living cells, an EGFP fluorescent tag was attached to the intracellular C-terminus of α-sarcoglycan (Figure 2-1A). When the α-sarcoglycan-EGFP fusion gene was expressed in HEK 293 cells, it produced a protein of the correct size, which is recognized by both α-sarcoglycan and EGFP antibodies (Figure 2-1B). To examine the intracellular localization of α-sarcoglycan-EGFP, the fusion gene was again expressed and visualized in 293 cells, that do not express any endogenous sarcoglycans (64, 168). The expression profile of α-sarcoglycan-EGFP was compared to that of the untagged α-sarcoglycan. Both proteins showed similar localization patterns (Figure 2-1C), focused in three major compartments; trapped in the perinuclear/endoplasmic reticulum region, at the plasma membrane (Figure 2-1C- inset), and in vesicular/endosomal intracellular compartments (Figure 2-1C). α-sarcoglycan-EGFP also co-localized with an antibody against the protein (Figure 2-1C). This expression profile was also observed in C57 muscle cells early in differentiation, where there is no endogenous sarcoglycan expression (137). In myoblasts α-sarcoglycan-EGFP is present in motile vesicular structures, which appear to traffic on defined tracks (Figure 2-1D, arrowheads), consistent with motor driven vesicular motion. Confocal microscopy demonstrated that α-sarcoglycan-EGFP is also present on membrane projections (Figure 2-1D), and accumulated in intracellular endosomal compartments in muscle (Figure 2-1D, arrow).

A

EGFP-N1 α–Sarcoglycan (1163nt., 387aa., 50KDa)
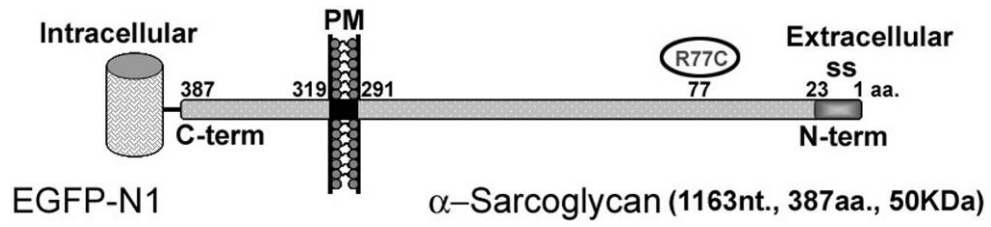
B
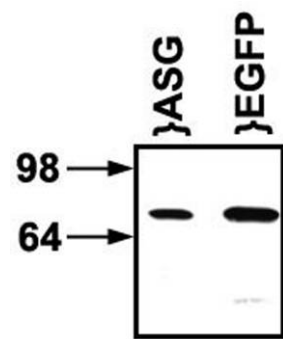
C
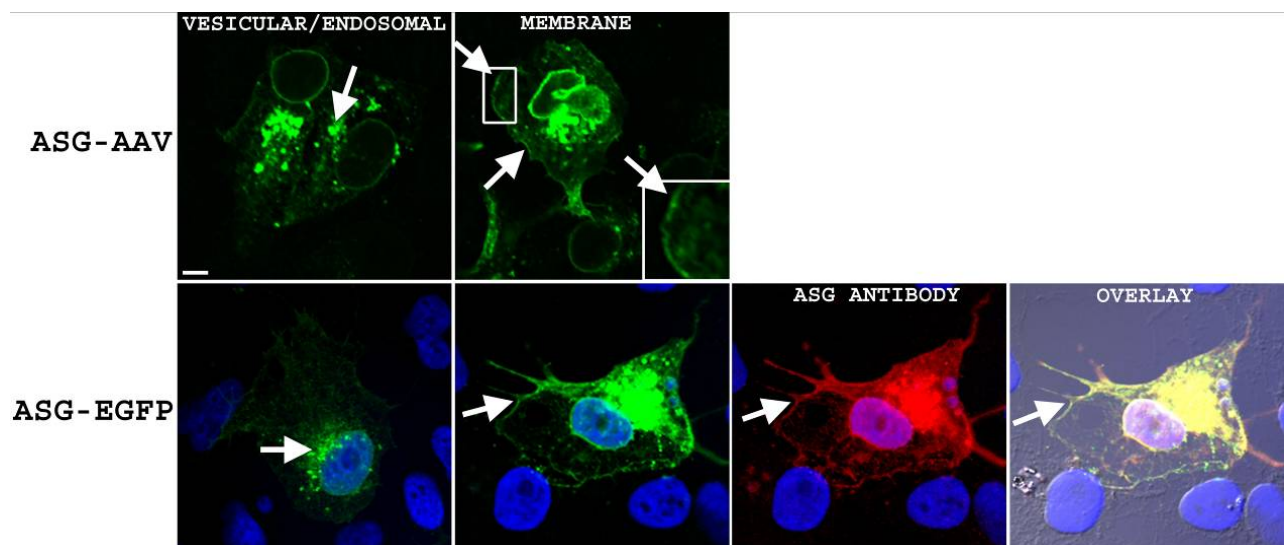
D
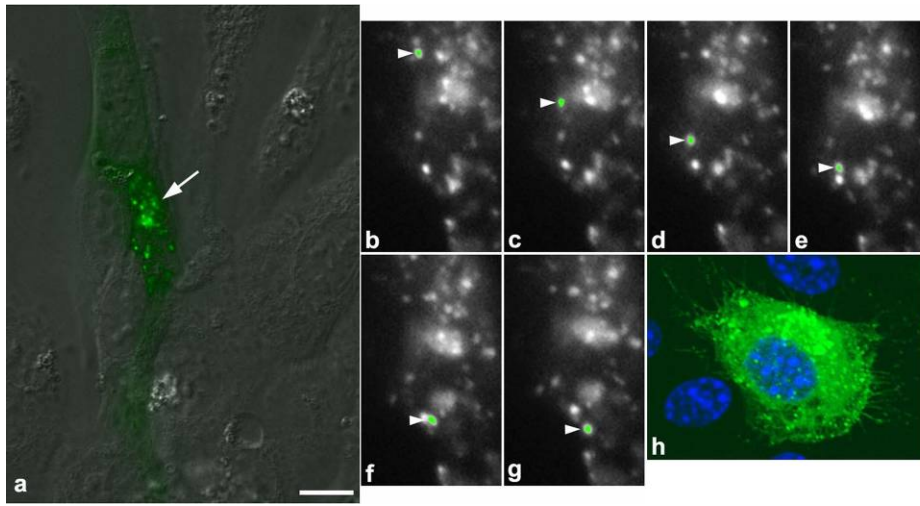
E
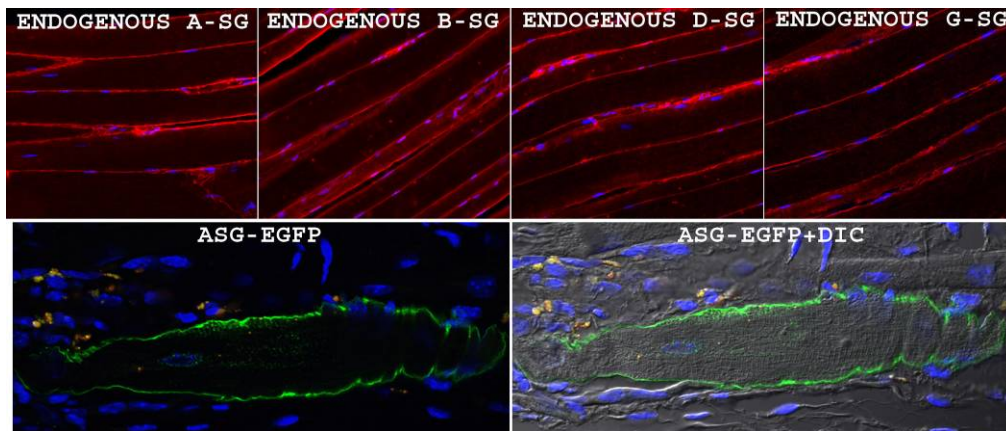
Figure 2-1. Addition of an EGFP tag does not alter the characteristics α-sarcoglycan in muscle and non-muscle cells. (A) Schematic representation of α-sarcoglycan-EGFP, where EGFP is attached to the intracellular C-terminus of α-sarcoglycan. (B) Western blot analysis of α-sarcoglycan-EGFP protein expression in 293 cells using antibodies against α-sarcoglycan and EGFP separately. (C) The localization patterns of untagged α-sarcoglycan and α-sarcoglycan-EGFP (green) were compared by confocal microscopy in fixed 293 cells. Arrows show endosomal and membrane expression as stated. Membrane expression is also shown in the inset. Cells transfected with α-sarcoglycan-EGFP were also stained with an antibody against α-sarcoglycan in red. Nuclei are shown in blue. Bar= approx. 5um. (D) C57 primary muscle cells were transfected with α-sarcoglycan-EGFP (green), whose expression was examined in live cells using time lapse imaging. Arrow shows endosomal accumulations, as were seen in non-muscle cells. In sub-panel a α-sarcoglycan-EGFP is overlaid with differential interference contrast (DIC) to show cell morphology. Arrow heads in sub-panels b-g show a motile α-sarcoglycan-EGFP transport vesicle (artificially highlighted). Lamellar projections of α-sarcoglycan-EGFP on the plasma membrane are shown in the overexposed cell in h. Nuclei are shown in blue. Bar= approx. 10um. (E) α-sarcoglycan-EGFP was injected into a C57 adult mouse. Muscle was examined 1 week after injection for localization of α-sarcoglycan-EGFP. The mouse properly expresses all endogenous sarcoglycans (red) at the sarcolemma of the muscle fibers (red). Additionally α-sarcoglycan-EGFP (green) is properly and stably deposited at the sarcolemma in the presence of the other sarcoglycan members. Nuclei are shown in blue, and muscle fiber morphology is shown in DIC. From ref. 192.

α-sarcoglycan-EGFP was also found to localize correctly at the plasma membrane of muscle *in vivo*. α-sarcoglycan-EGFP plasmid DNA was injected into the hind-leg of a C57 mouse. 14 days later, the animals were sacrificed and muscles were prepared for confocal microscopy. The muscle expressed all the sarcoglycans including α-sarcoglycan-EGFP at the plasma membrane (Figure 2-1E). These data demonstrate that α-sarcoglycan-EGFP, and the endogenous α-sarcoglycan function similarly in muscle and non muscle cells. Furthermore, α-sarcoglycan-EGFP is stable at the plasma membrane in vivo when the other sarcoglycan members are present.

α-sarcoglycan-EGFP translocates to the plasma membrane when expressed alone

Live cell microscopy and genetic manipulation techniques were used to determine whether α-sarcoglycan translocates to the plasma membrane. Initial studies investigated the spatio-temporal expression sequence of α-sarcoglycan-EGFP in living 293 cells. α-sarcoglycan-EGFP was transiently transfected and visualized from initial expression to deposition. The protein initially concentrated in the endoplasmic reticulum-Golgi (Figure 2-2A- Time 5 hours after transfection). After approximately 7.5 hours, α-sarcoglycan-EGFP translocates through the Golgi stacks to vesicular structures around the trans Golgi (Figure 2-2A- Time 7.5hr). These vesicle aggregates then distribute throughout the cell and translocate toward the cell periphery (Figure 2-2A- Time 13hr). At this time intracellular accumulations shift from the perinuclear to endosome like structures (Figure 2-2A- Time 13hr). This shift is more pronounced at 15hrs after transfection (Figure 2-2A- Time 15hr). Additionally at this time point, many more fluorescent aggregates are concentrated at the peripheral area of the cell (Figure 2-2A-Time 15hr). This

sequence demonstrates that following α-sarcoglycan-EGFP synthesis, the vesicular protein aggregates move from a more central location toward the periphery of the cell.

A
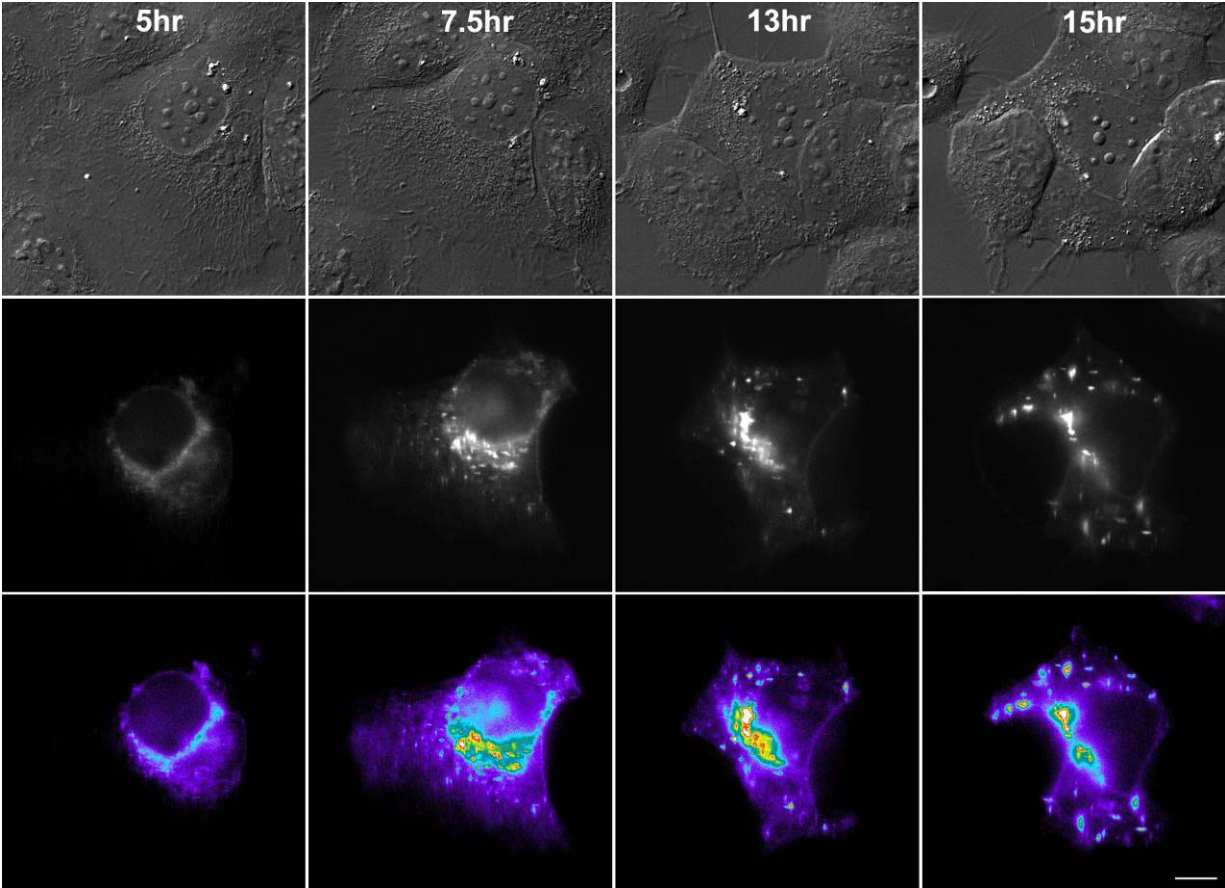
B
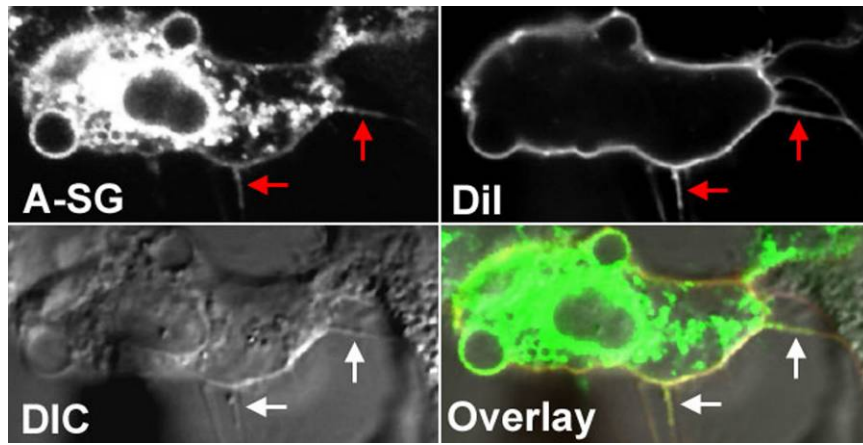
C
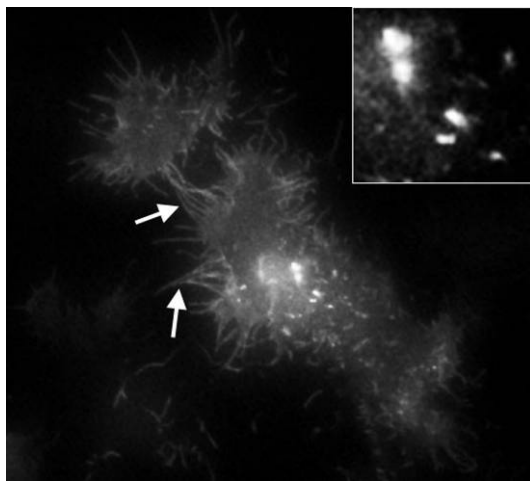
D
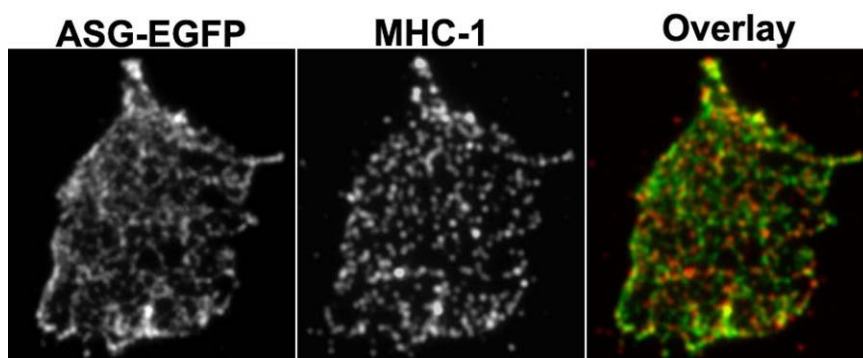
E
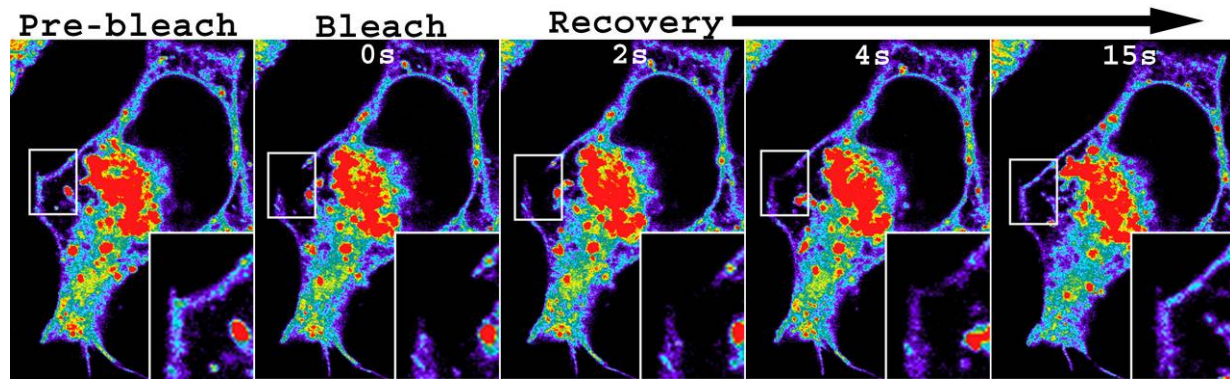
F
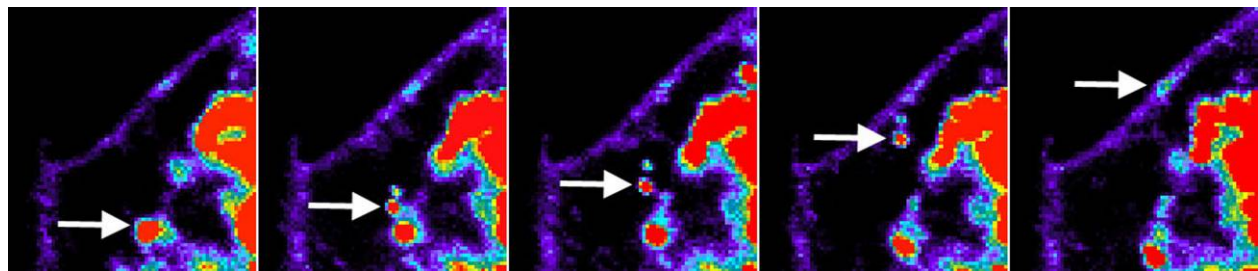
G
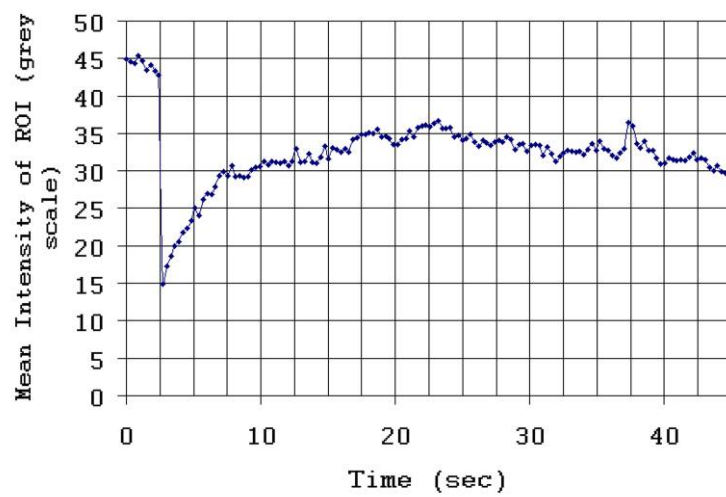
Figure 2-2. Pools of α-sarcoglycan-EGFP translocate to the plasma membrane and are being dynamically replenished, in the absence of the remaining sarcoglycans. (A) α-sarcoglycan-EGFP was transfected into HEK 293 cells which were imaged about 5 hours after transfection. DIC and fluorescent images were acquired every 2.5 minutes for a period of 24 hours. DIC images are shown in the top panels at the indicated time intervals after transfection, and the corresponding α-sarcoglycan-EGFP fluorescent images and pseudo colored images (to show fluorescence intensity) are shown in the bottom panels. Bar= approx. 10um. (B) 293 cells transfected with α-sarcoglycan-EGFP were subsequently loaded with a DiI lipid probe. Cells were fixed and imaged by confocal microscopy. The co-localization on lamellar membrane projections is shown with the arrows, and cell morphology is shown in DIC. (C) α-sarcoglycan-EGFP expression was examined in 293 cells using TIR-FM (left). Arrows show α-sarcoglycan-EGFP concentrated on lamellar membrane projections, and the boxed region magnified in the inset shows motile α-sarcoglycan-EGFP particles being delivered to the cell surface. (D) The panel shows membrane remains on the coverslips, positive for α-sarcoglycan-EGFP (green), and co-labeled for the plasma membrane protein MHC-1 (red). Co-localization is in yellow in the overlay (E) a fluorescence recovery after photobleaching (FRAP) assay was conducted by confocal on 293 cells transfected with α-sarcoglycan-EGFP. Again fluorescent images were pseudo colored, and insets are magnified segments of boxed membrane regions, where bleach and recovery occurred. Bar= approx. 5um. (F) Images are magnified segments of boxed bleached regions in E. Arrows show an intracellular vesicle delivering a fluorescent particle to the bleached area of the membrane. (G) FRAP data was quantified, where mean fluorescence recovery within the bleached region of interest is show over time. From ref. 192.
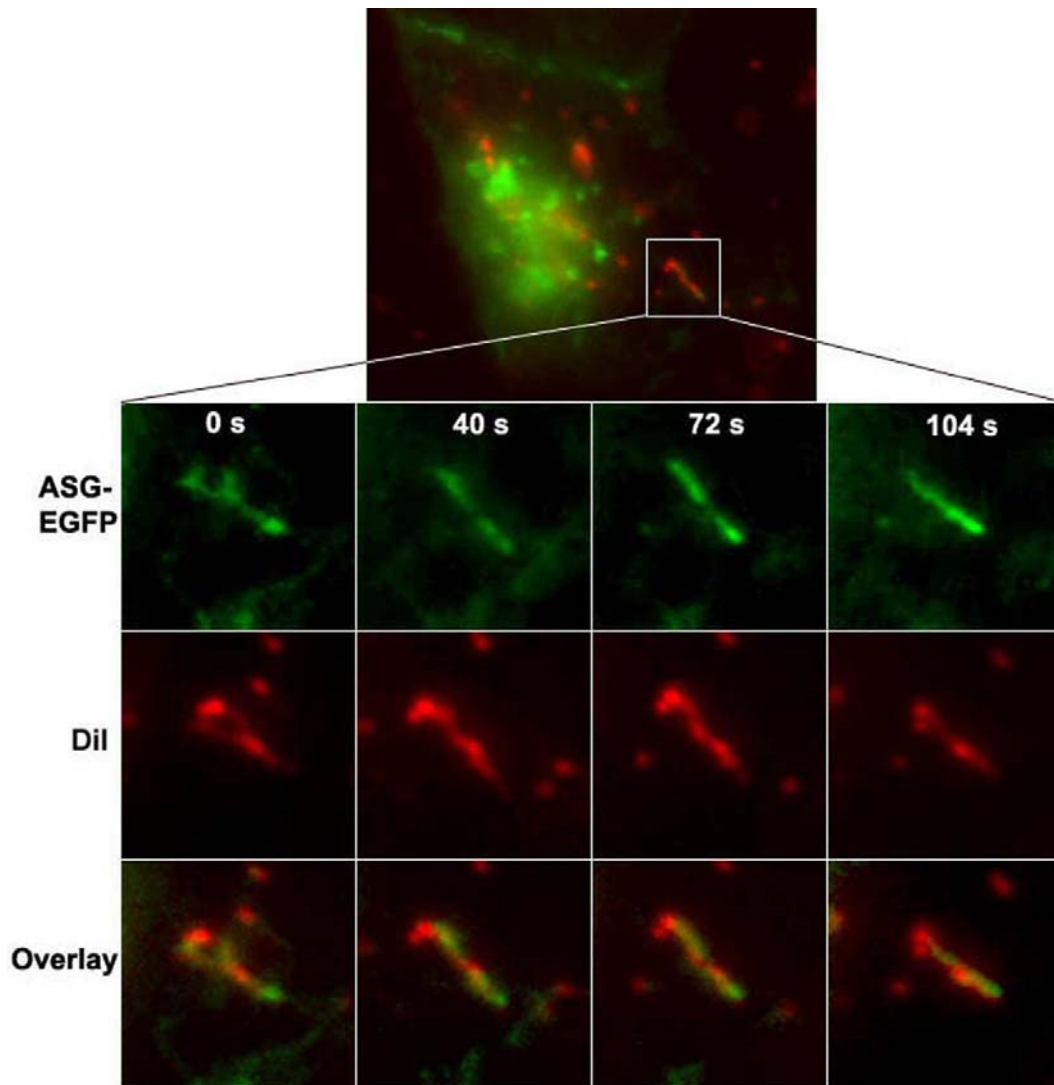
Figure 2-3. α-sarcoglycan-EGFP is present on lipid membranes in live cells. 293 cells transfected with α-sarcoglycan-EGFP (green) were subsequently loaded with a DiI lipid probe (red). Cells were imaged for both colors approximately every 6.5 seconds. The synchronous co-localization on motile membrane projections is shown in the bottom panels. From ref. 192.

To test whether α-sarcoglycan-EGFP is present at the plasma membrane. 293 cells were transfected with α-sarcoglycan-EGFP, labeled with DiI (a lipid dye) and examined by confocal and live cell microscopy. α-sarcoglycan-EGFP co-localized with DiI on the lamellar projections of the cell (Figure 2-2B-arrows) and moved in synchrony with DiI when imaged over time (imaged every 6.5 seconds for about 2 minutes) (Figure 2-3). α-sarcoglycan-EGFP delivery to

the plasma membrane is confirmed by total internal reflection microscopy (TIR-FM), which detects fluorescence at or close to (150-200nm) the coverslip (169) (Figure 2-2C). TIR-FM of the basal membrane of the cell confirms that α-sarcoglycan-EGFP is present on the lamellar projections of the plasma membrane (Figure 2-2C- arrows). Additionally, discrete α-sarcoglycan-EGFP positive trafficking vesicles are also present (Figure 2-2C-inset). When cells expressing α-sarcoglycan-EGFP were pressure washed from the coverslip, leaving only fragments of the plasma membrane on the coverslip, remains were positive for the α-sarcoglycan-EGFP protein (Figure 2-2D), which co-localized with the complexed form of MHC-1 present on the plasma membrane surface (Figure 2-2D).

If α-sarcoglycan-EGFP at the plasma membrane is turning over, fluorescence of the plasma membrane should recover after localized photobleaching. Fluorescence recovery after photobleaching (FRAP) was conducted on a small region of the plasma membrane (Figure 2-2E-bleach). α-sarcoglycan-EGFP fluorescence in this region rapidly recovered within 15 seconds of the bleach (Figure 2-2E-recovery). Additionally, fluorescent particles were observed moving from intracellular accumulations to the localized bleached area of the plasma membrane (Figure 2-2F). Quantification of the bleached region demonstrates that the recovery of α-sarcoglycan-EGFP is dynamic and rapid (Figure 2-2G). Together, this data demonstrates that α-sarcoglycan-EGFP is rapidly and constitutively replenished at the plasma membrane at least partially by intracellular vesicular structures. Once at the plasma membrane it appears evenly distributed across the membrane.

A

B
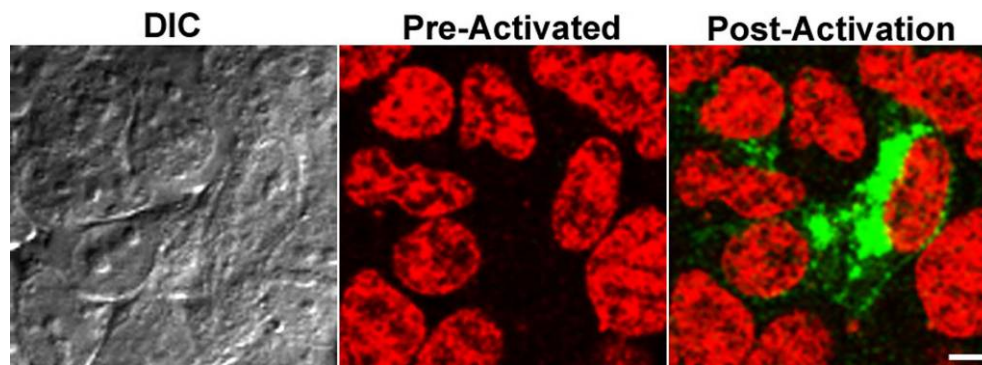
C
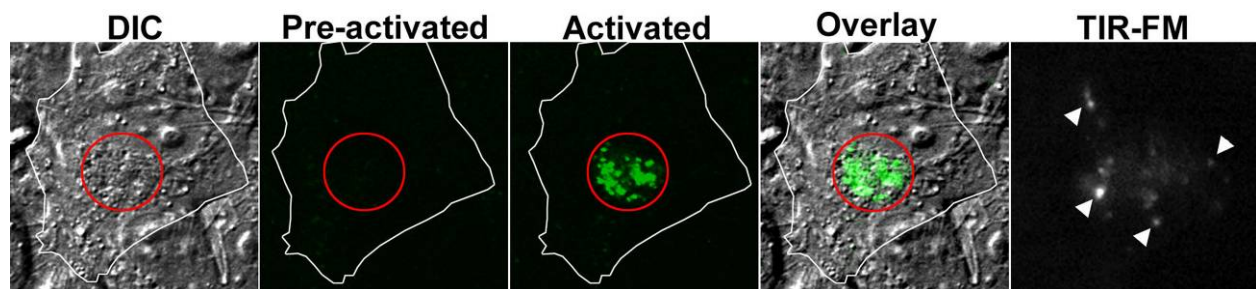
Figure 2-4. Intracellular photoactivated α-sarcoglycan-EGFP is delivered to the cell surface. (A) schematic representation of mutations made in the EGFP portion of α-sarcoglycan-EGFP to make the fusion gene photoactivatable. The V163A mutation, which is crossed out, represents a previously reported mutation which I did not find necessary to make our construct photoactivatable. (B) A whole field of 293 cells transfected with α-sarcoglycan-EGFP were briefly photoactivated with a 405nm laser. Cell morphology is shown in DIC, nuclei are shown in red, and activated PA-α-sarcoglycan-EGFP is shown in green. Bar= approx. 8μm. (C) localized intracellular regions of 293 cells transfected with PA-α-sarcoglycan-EGFP were activated with a 405nm laser. Activated PA-α-sarcoglycan-EGFP is shown in green within the red region of interest. The cell is outlined in white, and cell morphology can be seen with DIC. 15 minutes after activation, activated cells were examined with TIR-FM, arrow heads show widespread intracellular activated PA-α-sarcoglycan-EGFP particles being delivered to the cell surface. From ref. 192.

67

Using Photoactivatable GFP tagged to α-sarcoglycan allows us to study the selective progression of α-sarcoglycan from intracellular compartments to the plasma membrane. Our strategy for mutagenesis was similar to that of Patterson and Lippincott-Schwartz in 2002; however I demonstrate that three mutations (T204H, F64L and S65T) were sufficient to make α-sarcoglycan-EGFP photoactivatable (Figure 2-4A). This construct will be referred to as PA-α-sarcoglycan-EGFP. The mutation at codon 163 (V163A) (118) is redundant for photoactivation (Figure 2-4B). Confocal microscopy was used to specifically activate intracellular pools of PA-α-sarcoglycan-EGFP (Figure 2-4C). These cells were then imaged using TIR-FM, which demonstrated that photoactivated pools of PA-α-sarcoglycan-EGFP are in fact delivered to the plasma membrane (Figure 2-4C). This data further supports our hypothesis that intracellular pools of α-sarcoglycan are delivered to the plasma membrane in the absence of the other sarcoglycan complex members.

α-sarcoglycan-EGFP is recycled from the plasma membrane and accumulates in recycling endosomes

To define intracellular structures and vesicles in which α-sarcoglycan-EGFP is found, confocal microscopy was used to study 293 and HeLa cells labeled with compartment specific antibodies following transfection of α-sarcoglycan-EGFP. α-sarcoglycan-EGFP does not co-localize with Giantin, a Golgi marker, nor does it co-localize with AP-1, an adaptor protein associated with Golgi exit and vesicular formation (170) (Figure 2-5A). Furthermore, α-sarcoglycan-EGFP does not co-localize with LAMP-1, a lysosomal marker (Figure 2-5A). On the other hand, α-sarcoglycan-EGFP does co-localize with Clathrin (171) (Figure 2-5A) and very clearly colocalizes with the transferrin receptor (Tfn-R), which is known to recycle to and from the

plasma membrane and accumulate in recycling endosomes (172-175) (Figure 2-5A). Co-localization of α-sarcoglycan-EGFP is also clearly seen in Hela cells (Figure 2-5B).

A
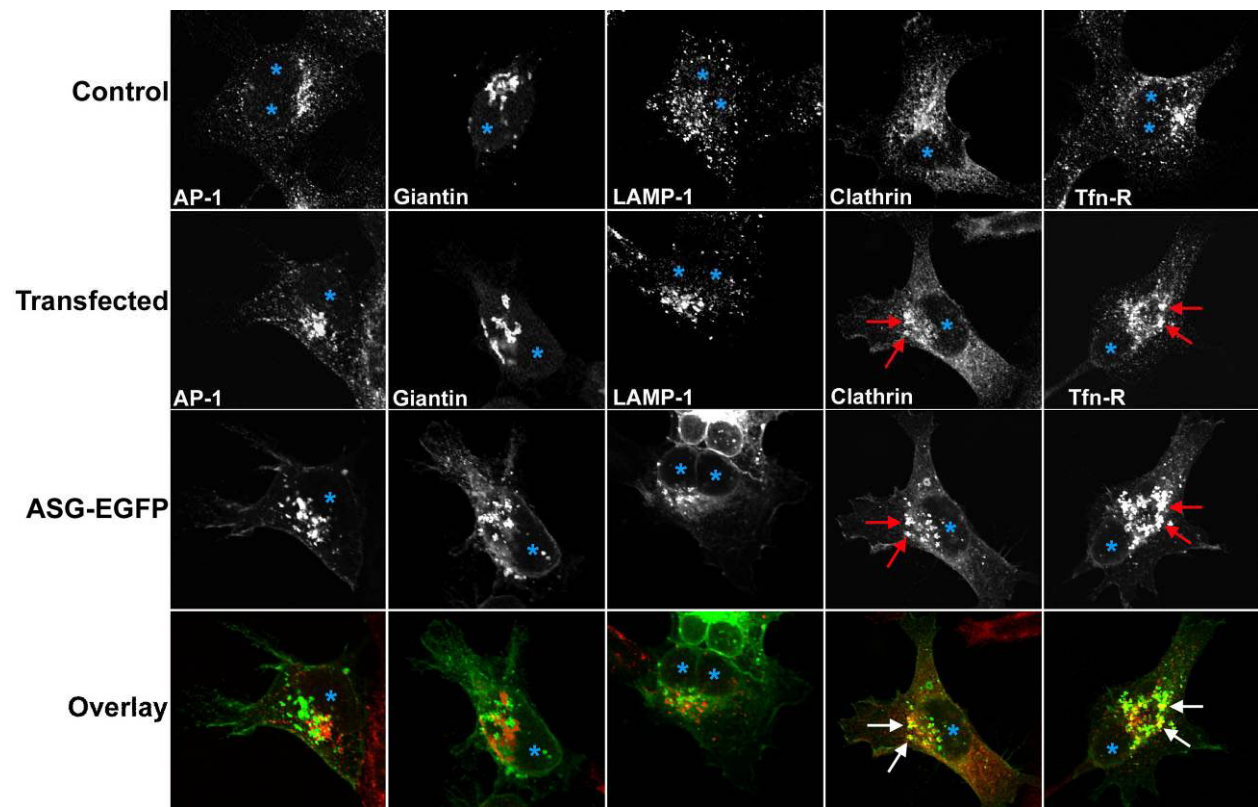
B
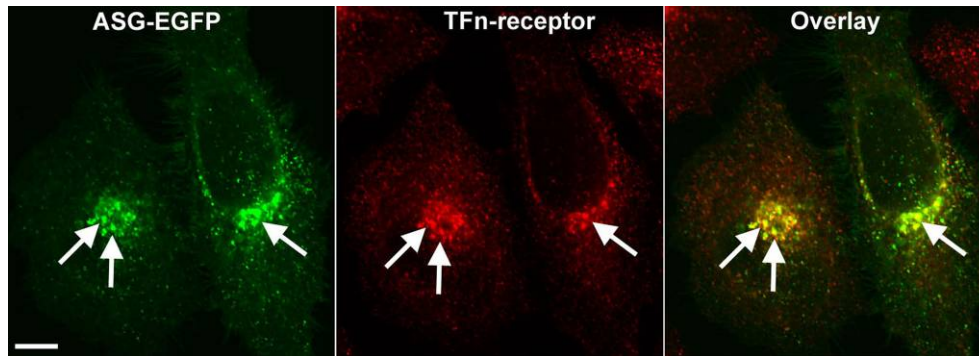
Figure 2-5. α-sarcoglycan-EGFP accumulates in recycling endosomes. (A) α-sarcoglycan-EGFP was transfected into 293 cells, which were then fixed with 2% paraformaldehyde, and stained with various markers. Control untransfected cells are shown in the top row, and α-sarcoglycan-EGFP is shown in the 3rd row from the top. AP-1, giaintin, LAMP-1, clathrin, and the transferrin receptor (Tfn-R) distributions in these transfected cells are shown in the 2nd row from the top. The bottom row shows co-localization of the two respective proteins, with positive co-localization particles denoted with an arrow in yellow. Nuclei are shown with a blue *. (B) Hela cells were transfected with α-sarcoglycan-EGFP (green). Cells were then fixed and stained with an antibody against the Tfn-R (red). Colocalization is shown in the right panel in yellow, and is denoted with arrows. From ref. 192.

To examine if α-sarcoglycan-EGFP is recycled from the plasma membrane in a similar fashion as Tfn and Tfn-R, I performed a Tfn uptake assay. Hela cells, transfected with α-sarcoglycan-EGFP, were surface labeled with fluorescently labeled Tfn (Tfn-568) at $4^{\circ}C$. Cells were then warmed to $37^{\circ}C$, and imaged by TIR-FM. α-sarcoglycan-EGFP and Tfn-568 co-localized at the plasma membrane, and were internalized together, over a minute (Figure 2-6A). Over longer periods (approximately 15-20 minutes), confocal microscopy demonstrated that α-sarcoglycan-EGFP and Tfn-568 co-localized and accumulated in internal endosomal structures, considered to be recycling endosomes (Figure 2-6B) (176). The internalization of α-sarcoglycan from the plasma membrane was definitively confirmed by labeling α-sarcoglycan-EGFP at the cell surface with an antibody that binds to an extracellular portion of α-sarcoglycan (amino acids 217-289), followed by confocal microscopy. The α-sarcoglycan antibody was localized to intracellular structures that co-localized with α-sarcoglycan-EGFP (Figure 2-6C). To determine

if α-sarcoglycan-EGFP from the surface is recycled from recycling endosomes, protein synthesis was blocked with cycloheximide for 2 hours. After 2 hours α-sarcoglycan-EGFP remains detectable at the plasma membrane (Figure 2-6D). This finding supports a model where at least a portion of α-sarcoglycan-EGFP is internalized from the plasma membrane, accumulates in recycling endosomes, and recycles back to the plasma membrane.

A

B

C

D
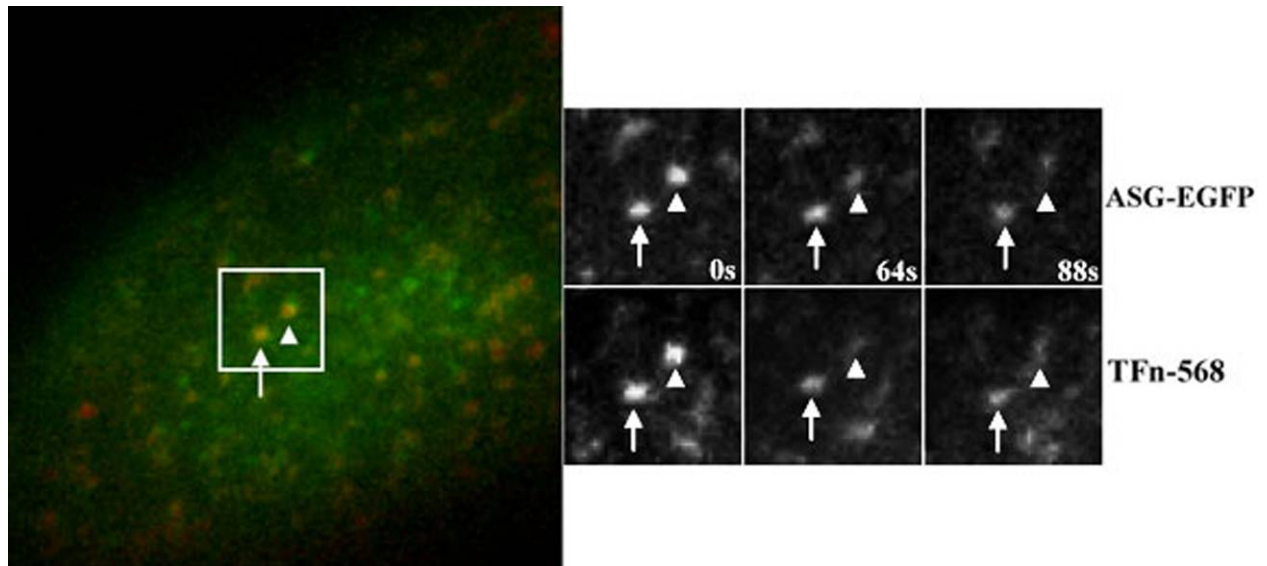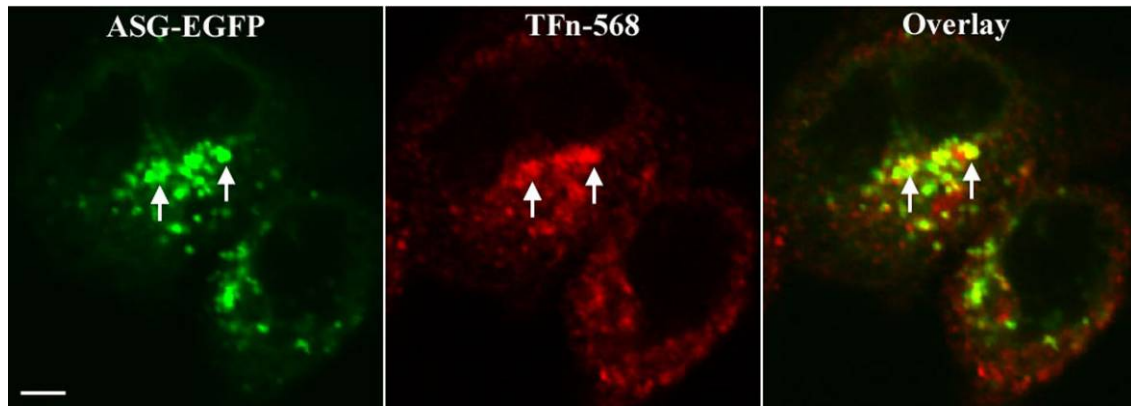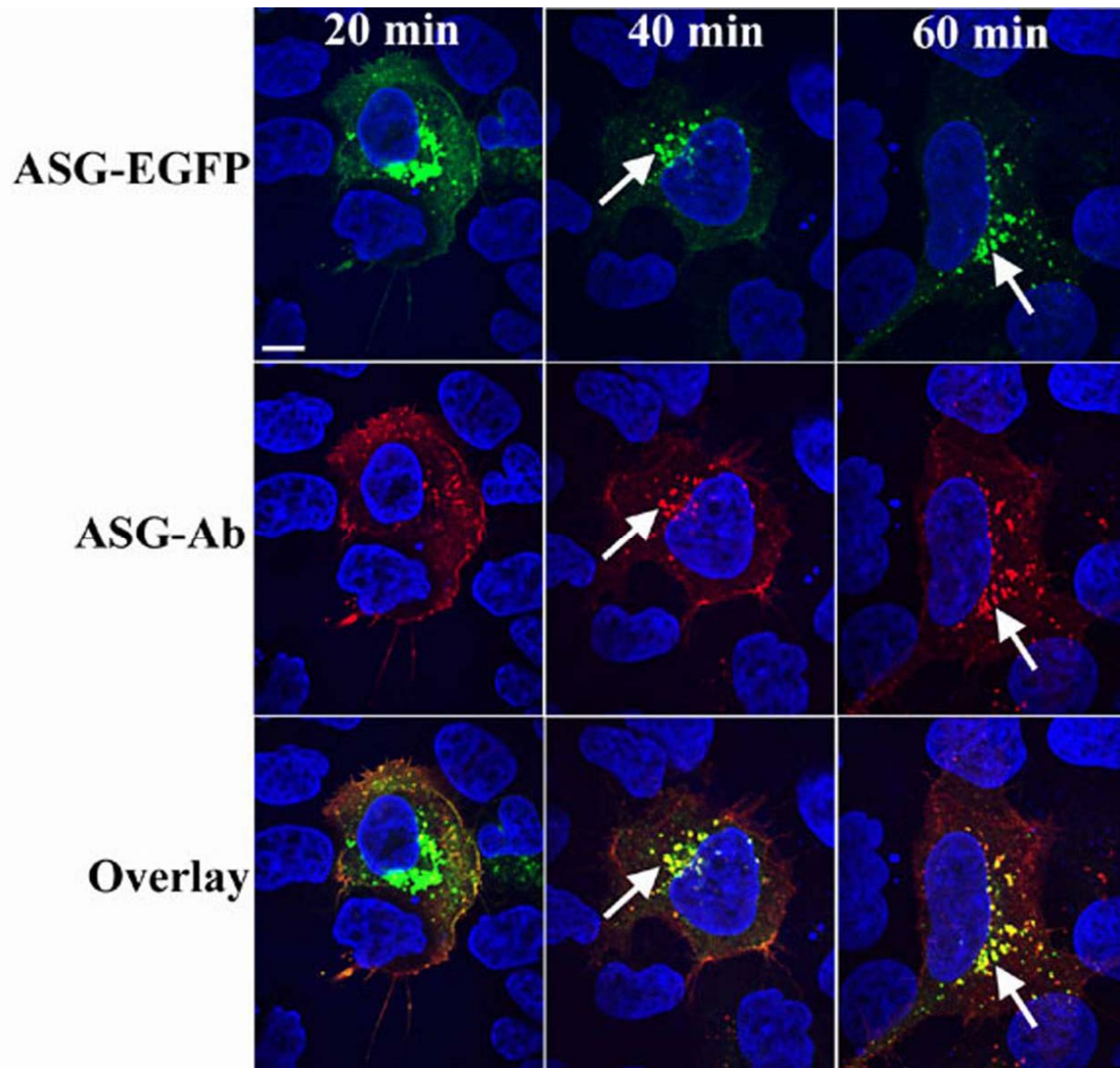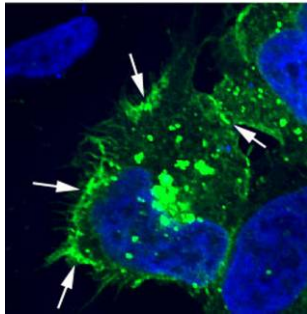
Figure 2-6.   α-sarcoglycan-EGFP is internalized from the cell surface and is redelivered to the plasma membrane. (A) Hela cells were transfected with α-sarcoglycan-EGFP. 24 hrs after transfection, cells were surface labeled with transferrin conjugated to Alexa 568 (Tfn-568) at 4°C for 1hr. Cells were then imaged live by TIR-FM while being heated to 37°C to induce ligand internalization. Boxed region shows co-localization of α-sarcoglycan-EGFP and Tfn-568. Arrows show stationary co-localized particles, while the arrow head shows a co-localized α-sarcoglycan-EGFP+Tfn-568 particle which is being endocytosed. (B) Cells were fixed 20 minutes after being shifted to 37°C and imaged by confocal microscopy. α-sarcoglycan-EGFP is shown in green, and internalized Tfn-568 is shown in red. Co-localization of the two proteins is shown in yellow in the overlay panel. Co-localization is denoted by the arrows. Bar= approx. 5um. (C) 293 cells transfected with α-sarcoglycan-EGFP (green) were then surface labeled for 1hr at 4°C with an α-sarcoglycan antibody (red), recognizing the extracellular domain of the protein. Cells were then allowed to internalize the antibody at 37°C, fixed at 20, 40, and 60 minute time points, and examined by confocal microscopy. Co-localization of the internalized antibody with α-sarcoglycan-EGFP is denoted by the arrows. Bar= approx. 10um   (D) 293 cells expressing α-sarcoglycan-EGFP (green) for 24hrs were treated with cycloheximide for 2hrs, to inhibit de novo protein synthesis. α-sarcoglycan-EGFP which continued to be delivered to the plasma membrane is shown with the arrows. From ref. 192.

α-sarcoglycan-EGFP is transported via clathrin coated vesicles in a microtubule dependent fashion

Clathrin-coated vesicles (CCV's) transport proteins between membrane-bound compartments (170, 171, 177). They are also responsible for the internalization of Tfn-R from the cell surface (178). To examine if α-sarcoglycan-EGFP utilizes this regulated mechanism of transport, co-localization of α-sarcoglycan-EGFP and clathrin was examined. First I assessed whether the α-sarcoglycan-EGFP vesicles, are in fact clathrin coated in living cells. α-sarcoglycan-EGFP and a clathrin light chain-DsRed (CLC-DsRed) construct were transfected into 293 cells and imaged live using confocal microscopy. α-sarcoglycan-EGFP and CLC-DsRed co-localize (Figure 2-

7A- arrow), and move together as vesicles intracellularly (Figure 2-7A- arrowhead). To study the co-localization of these two proteins at the cell surface, I used TIR-FM. This technique demonstrated that clathrin coated vesicles containing α-sarcoglycan-EGFP are formed on the cell surface, over a minute (Figure 2-7B). This correlates well with the rate at which Tfn and α-sarcoglycan-EGFP are taken up from the cell membrane (Figure 2-6A).

α-sarcoglycan-EGFP and CLC-DsRed positive vesicles are motile (Figure 2-7B- circled vesicles). To test if the motility of α-sarcoglycan-EGFP vesicles is microtubule dependent (179, 180), as is also the case for Tfr-R (176), transfected cells were treated with nocodazol, an established microtubule disrupting agent (181), and imaged. Treatment halted vesicular motion, however α-sarcoglycan-EGFP and CLC-DsRed remained colocalized (Figure 2-7B). Quantification of vesicular motion showed the pronounced vesicular motion changing before and after nocodazole treatment (Figure 2-7C). The mean velocity of both α-sarcoglycan-EGFP and CLC-DsRed particles decrease approximately 71% and 62% respectively after treatment (Figure 2-7D). There is also a decrease of approximately 75% and 62% in the mean distance the α-sarcoglycan-EGFP and CLC-DsRed travel (Figure 2-7E) after nocodozole treatment. Taken together these data demonstrate that at least a portion of α-sarcoglycan-EGFP vesicles are clathrin coated, and their motility is microtubule dependent.

C

D

E
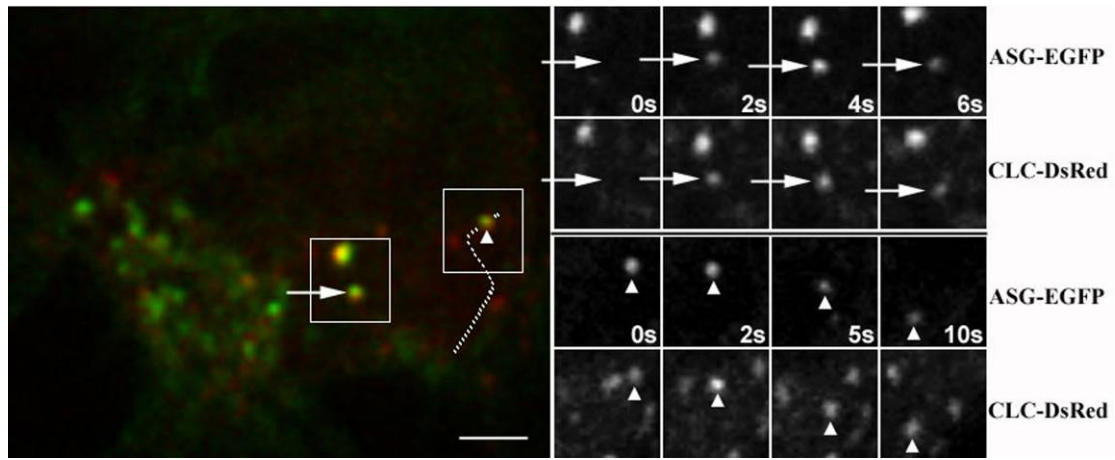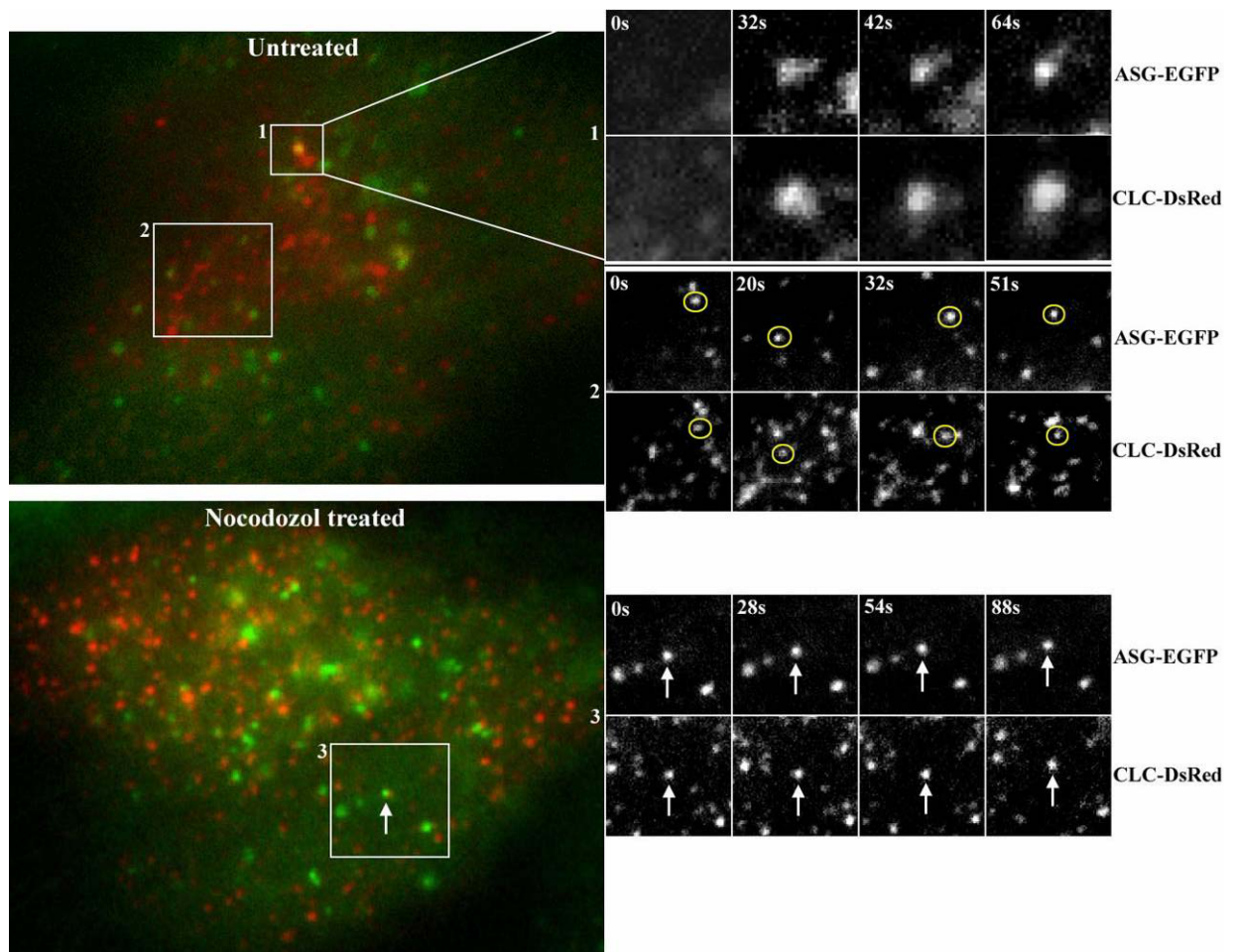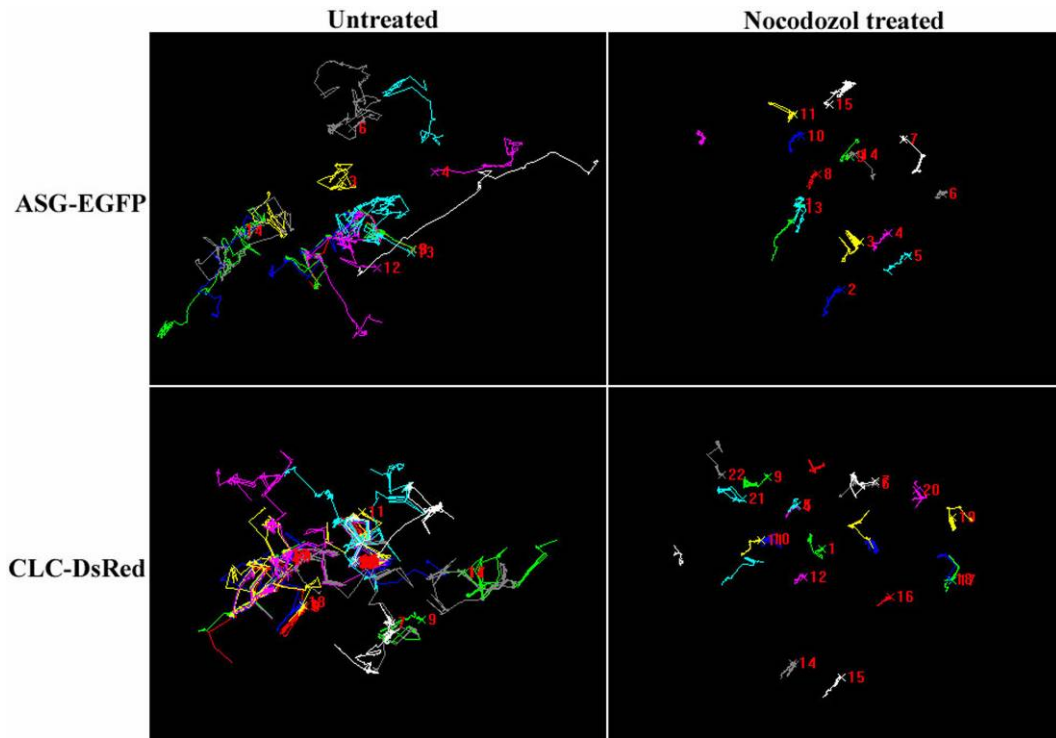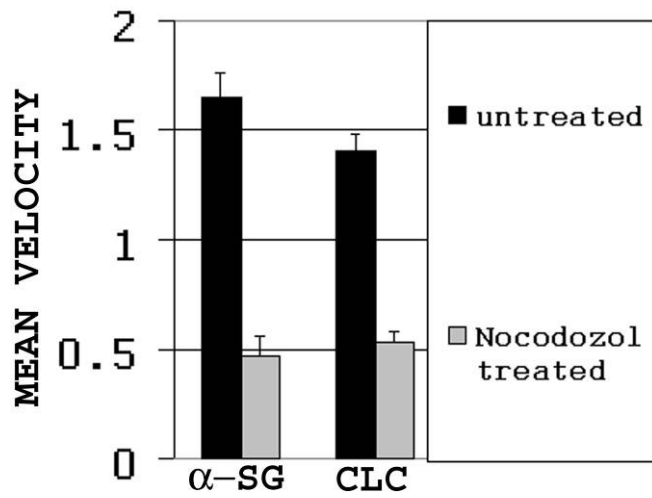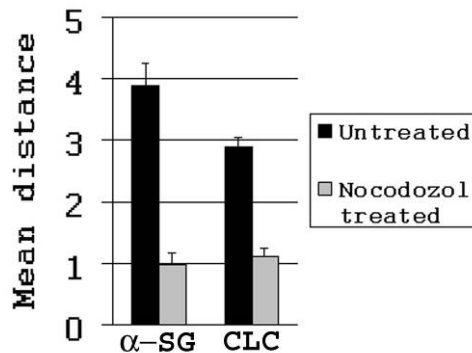
Figure 2-7. α-sarcoglycan-EGFP is transported in clathrin coated vesicles, and motility is microtubule dependent. (A) 293 cells co-transfected with α-sarcoglycan-EGFP and Clathrin light chain-DsRed (CLC-DsRed), were imaged (streamed) by spinning disk confocal microscopy. Co-localized stationary particles which form clathrin coated pits are denoted by the arrow in the boxed region. Motile co-localized particles are denoted by the arrow heads, and follow a path denoted by the dashed line. (B) These cells were also examined by TIR-FM. The boxed region-1 shows a stationary co-localized α-sarcoglycan-EGFP and CLC-DsRed positive particle, forming a clathrin coated vesicle at or very close to the cell surface. The boxed region-2 shows motile co-localized particles at the cell surface, which are circled. This motion is halted by the addition of nocodazole in the lower set of panels. In the boxed region-3 co-localized particles (arrow), and most particles in the field remain stationary through the duration of the imaging sequence. (C) Numerous α-sarcoglycan-EGFP and CLC-DsRed particles are tracked, before and after treatment with nocodazole. Each line is a track of a single particle that varies in time from several seconds to a few minutes. (D) Quantification of mean velocity of tracked α-sarcoglycan-EGFP and CLC-DsRed particles before and after nocodazole treatment. (E) Quantification of mean distance traveled per frame of α-sarcoglycan-EGFP and CLC-DsRed particles before and after nocodazole treatment. From ref. 192.

The R77C mutation in α-sarcoglycan-EGFP traps the protein in the endoplasmic reticulum

In order to gain insight into how the commonly reoccurring R77C α-sarcoglycan mutation affects protein traffic, the mutation was recapitulated by site directed mutagenesis in our α-sarcoglycan-EGFP construct. The localization of the construct was then analyzed by confocal microscopy in 293 cells. The R77C α-sarcoglycan-EGFP mutant is trapped in the endoplasmic reticulum, as demonstrated by its co-localization with calnexin, a marker for the endoplasmic reticulum (Figure 2-8A-inset). R77C α-sarcoglycan-EGFP formed aggresomes in vitro, which are characteristic of misfolded proteins in the endoplasmic reticulum (182-184) (Figure 2-8B).

These aggresomes increase steadily over time, stabilizing after about 34 hours when approximately 56% of the cells had aggresomes (Figure 2-8C). In contrast, cells expressing normal α-sarcoglycan-EGFP only started to form aggresomes after about 24 hours, reaching their peak value of approximately 17% after 47hrs (Figure 2-8C). Importantly, these cells (transfected with R77C-α-sarcoglycan) continued to have a subset of protein which co-localized with the Tfn-R (data not shown), whereas there was no co-localization with the Tfn-R in the R77C cells. TIR-FM demonstrates that no mutant protein is found at the plasma membrane (Figure 2-8D). When the R77C α-sarcoglycan-EGFP mutant was injected into a normal C57 mouse, expressing all the sarcoglycans (data not shown), the mutant protein remains trapped in the endoplasmic reticulum, co-localizing with endoplasmic reticulum markers calnexin, and BiP (Figure 2-8E), beneath the plasma membrane (Figure 2-8E). Furthermore, R77C continues to form aggresomes in vivo, characterized by the surrounding halo of the intermediate filament desmin (Figure 2-8E). Taken together these data demonstrate that the R77C mutation leads to a fundamental defect in α-sarcoglycan protein synthesis which arrests its exit from the endoplasmic reticulum.

A

B

R77C-Aggresomes

C

D

E
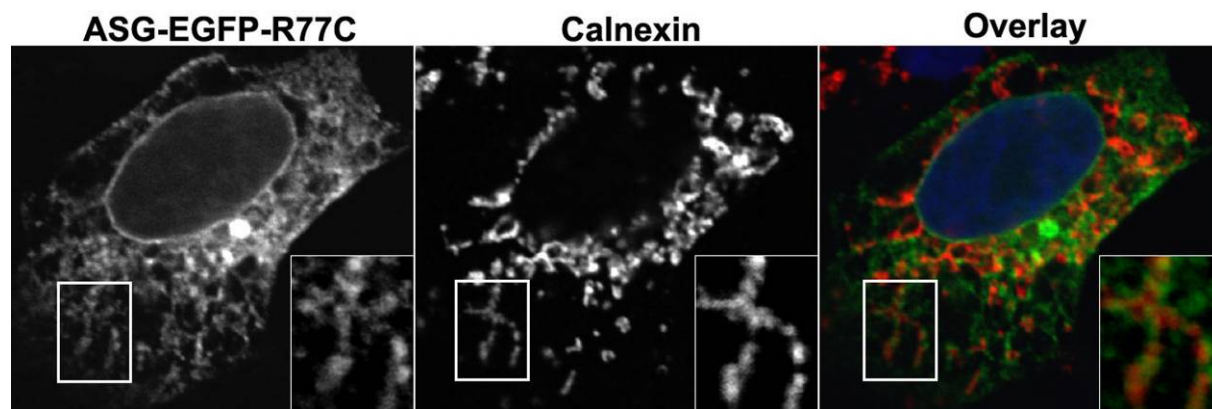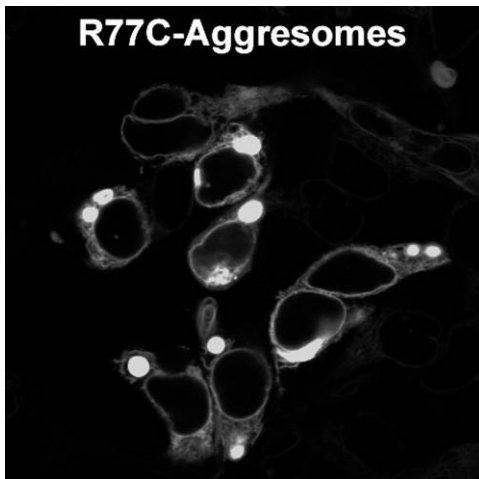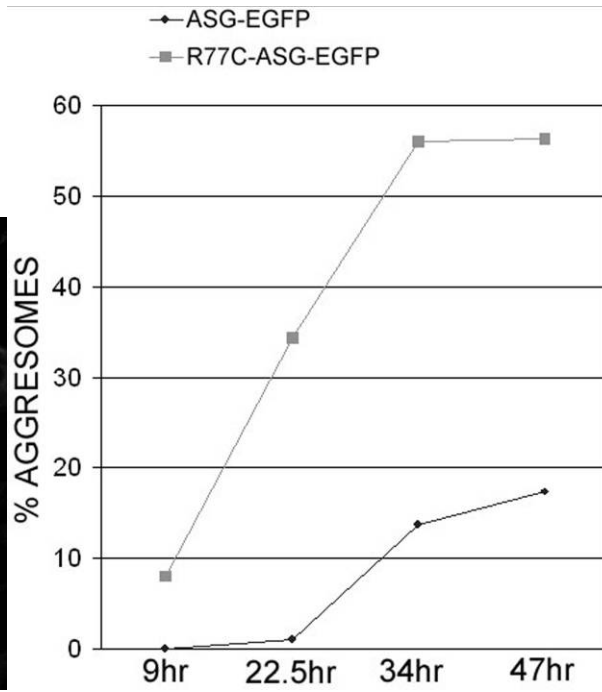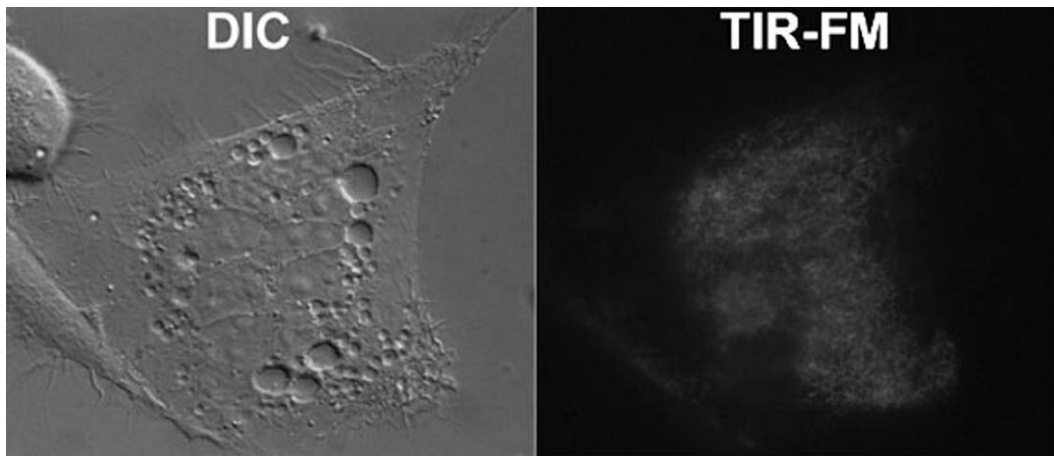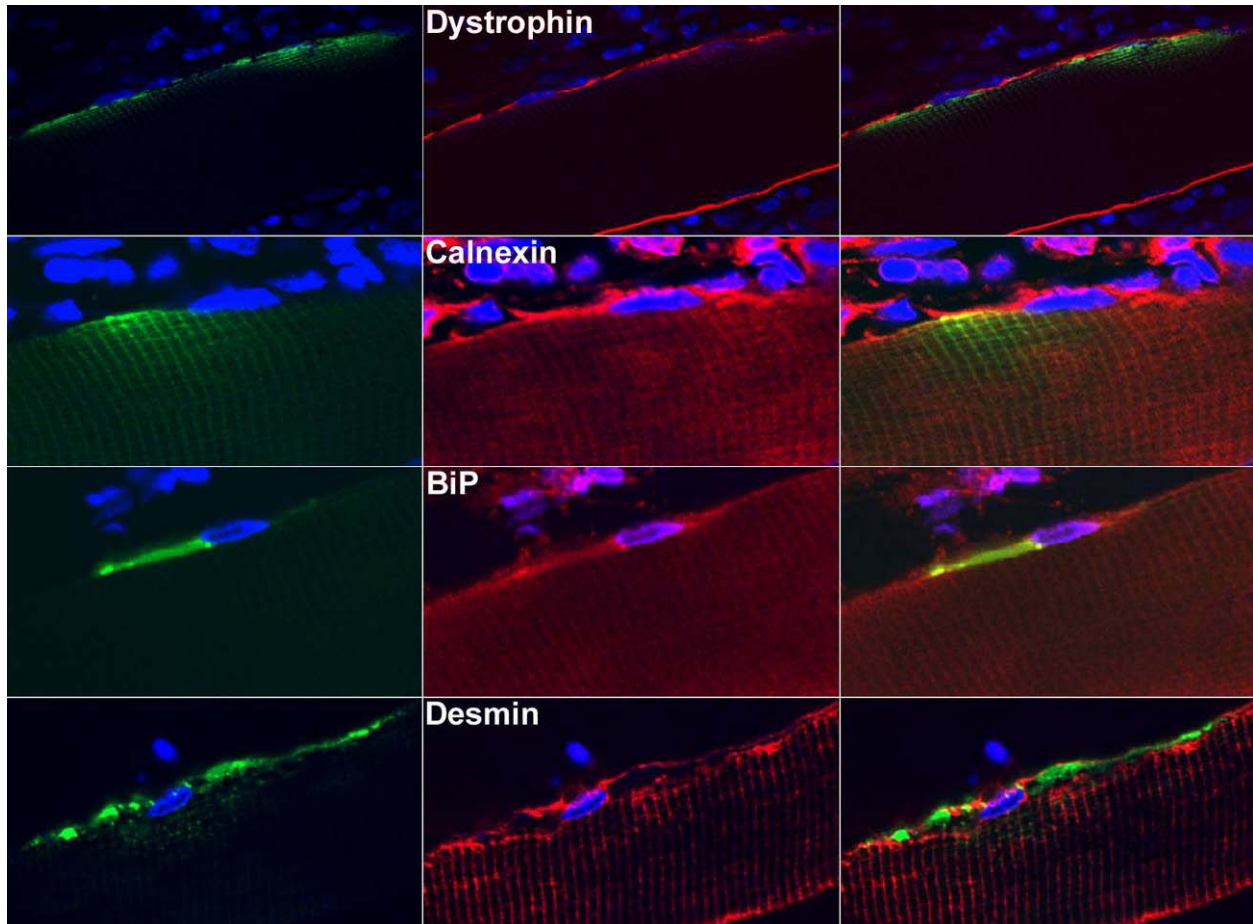
Figure 2-8. R77C α-sarcoglycan-EGFP mutant is trapped in the endoplasmic reticulum. (A) 293 cells transfected with the R77C α-sarcoglycan-EGFP mutant, were fixed and stained with an endoplasmic reticulum antibody-Calnexin. Colocalization is shown in yellow in the overlay image and in the insets. (B) Aggresomes formed by the R77C α-sarcoglycan-EGFP mutant protein in 293 cells by confocal microscopy. (C) 293 cells were transfected in parallel with R77C α-sarcoglycan-EGFP and α-sarcoglycan-EGFP. Cells were fixed at the denoted time intervals after transfection, and >100 cells were counted to give the approximate % of cells containing aggresomes at each time interval. (D)TIR-FM of 293 cells transfected with the R77C α-sarcoglycan-EGFP mutant shows no expression at the membrane, or in membrane lamellar projections. Cell morphology is shown in DIC. (E) R77C α-sarcoglycan-EGFP plasmid DNA was injected into the hind leg of a normal C57 mouse. Muscle was extracted 5 days after the injection, and sections were subjected to immunohistochemistry, using antibodies against dystrophin (red), calnexin (red), BiP (red), and Desmin (red). The R77C α-sarcoglycan-EGFP is seen in green, nuclei are in blue, and the overlay is shown in the right column. Sections were examined by confocal microscopy. From ref. 192.

DISCUSSION

In this study, I delineate the trafficking pathway of α-sarcoglycan in living cells. We demonstrate that α-sarcoglycan-EGFP is not only delivered to the plasma membrane, but also recycles to and from the plasma membrane to recycling endosomes, utilizing known trafficking proteins and mechanisms. Additionally, I demonstrate that this trafficking pathway is dysfunctional in patients presenting the R77C mutation.

When EGFP is attached to the intracellular C-terminus of α-sarcoglycan, the fusion gene retains the ability to correctly localize at the sarcolemma of skeletal muscle in vivo. This confirms previous reports that prolonged stability and robust expression of α-sarcoglycan at the plasma membrane requires the concurrent expression and assembly of all sarcoglycan members. The stability of the assembled sarcoglycan complex at the plasma membrane has also been established in multiple heterologous cell systems (46, 77). Our finding that sub-populations of α-sarcoglycan are able to traffic to the plasma membrane in the absence of the remaining sarcoglycans suggests that the α-sarcoglycan protein is able to interact with intracellular trafficking machinery to be exported to the plasma membrane, although it is not stably retained at high levels at the plasma membrane in the absence of the other sarcoglycans. Whether the interaction with intracellular trafficking machinery is direct or through an accessory protein remains to be resolved. Our data explain the finding that α-sarcoglycan is found at low levels on the plasma membrane of patients lacking the other sarcoglycans (8, 75, 166, 185). The data also supports previous findings suggesting that α-sarcoglycan is one of the last proteins to integrate into the sarcoglycan complex (77, 78). If complex formation was an absolute requirement for export of α-sarcoglycan to the plasma membrane, I should detect no protein at the cell surface.

This is the case for β & δ sarcoglycan, which are trapped in the endoplasmic reticulum (77), and also γ-sarcoglycan which is scattered in vesicles throughout the cell (77). Additionally our FRAP data demonstrates that populations of α-sarcoglycan at the plasma membrane, are dynamic, and are being constitutively and rapidly replenished.

The accumulation of α-sarcoglycan-EGFP in recycling endosomes, and the recycling phenomena of α-sarcoglycan-EGFP that I demonstrate in this report has not been previously described for any member of the DPC. Endocytic recycling of membrane proteins is an important and highly regulated cellular process that contributes to the fine tuning of membrane protein activities due to environmental stimuli (186). Recycling between the plasma membrane and intracellular compartments has been extensively studied in a variety of genetic based diseases (186). α-sarcoglycan may also utilize this trafficking pathway to regulate the expression levels of itself and the assembled sarcoglycan complex as a whole at the plasma membrane. The function of recycling endosomes is poorly understood. They do; however, seem to represent a population of early endosomes that are accessible by endocytic tracers such as transferrin (172, 187). As Mellman described in 2000, recycling endosomes are generally thought to comprise an intracellular pool of components that can be recruited to the plasma membrane in response to specific stimuli. Tfn uptake studies and antibody internalization assays demonstrate that portions of α-sarcoglycan-EGFP are in fact internalized from the plasma membrane and are present in newly endocytosed vesicles that later accumulate in recycling endosomes. Furthermore, by halting de novo protein synthesis with cycloheximide, I demonstrate that some α-sarcoglycan-EGFP on the plasma membrane may actually be recycled back to the surface from recycling endosomes. Recently, recycling endosomes have also been reported to serve as intermediates during transport from the Golgi to the plasma membrane in polarized cells (187). Therefore, the

possibility that some of the α-sarcoglycan-EGFP observed accumulated in recycling endosomes may be trapped in these intermediate compartments en route to the plasma membrane from the Golgi, cannot be ruled out. The recycling endosomes may therefore, serve as an intermediate compartment in the biosynthetic pathway. Based on our results however, the model I favor is one where α-sarcoglycan-EGFP accumulates in recycling endosome's after being internalized from the cell surface due to failure to remain at the plasma membrane in the absence of the other sarcoglycan complex members (Figure 2-9).

Clathrin coated vesicles are responsible for the sorting and trafficking of many transmembrane proteins to and from the plasma membrane (177). Proteins are sorted into clathrin coated vesicles either by interacting with sorting adaptors themselves, or by interacting with other proteins, which in turn interact with sorting adaptors (170). Our data are the first to show that α-sarcoglycan-EGFP is present in motile clathrin coated transport vesicles. These data shed light on one possible mechanism by which α-sarcoglycan-EGFP, and perhaps the sarcoglycan complex as a whole is transported within the cell. Furthermore, our drug treatment experiments using nocodazole demonstrate that the motion of these vesicles is microtubule dependent. This highlights the fact that the clathrin coated α-sarcoglycan-EGFP containing vesicles are in fact moving along tracks to specific destinations, rather than budding constitutively as a default pathway of proteins that accumulate on cellular membranes.

Finally, I show that the most commonly occurring R77C mutation in α-sarcoglycan, causes a re-distribution of the protein in the endoplasmic reticulum, with no membrane expression in vitro and in vivo. There are no traces of the mutant protein in later compartments of the biosynthetic compartments, such as the Golgi or vesicular structures. Additionally, the replacement of the Arginine with a Cysteine does not seem to conform to any known

endoplasmic reticulum retention signals (188). This leads us to believe that the mutation causes a folding defect that in turn has a detrimental effect on sarcoglycan complex assembly, and does not allow the protein to move beyond the endoplasmic reticulum. This hypothesis is further bolstered by the appearance of aggresomes: oligomeric complexes of non-native conformers that arise from non-native interactions among structured, kinetically trapped intermediates in protein folding or assembly (183). Similar aggregated forms of other misfolded or misassembled integral membrane proteins, such as presenilin 1 (189) and peripheral myelin protein PMP22 (190) have been previously reported when expressed in mammalian cells. It remains to be determined as to whether these aggresomes are linked to the R77C α-sarcoglycanopathy disease phenotype, as in the case of amyloid diseases, Alzheimer's disease, Parkinson's disease, Huntington's disease, and alcoholic liver disease (191).

Based on these data, I propose a model in which pools of normal α-sarcoglycan-EGFP are able to proceed through the biosynthetic pathway. Our data favors a model where the protein is translocated to the plasma membrane via clathrin coated transport vesicles. In the absence of proper sarcoglycan complex assembly, the majority of α-sarcoglycan-EGFP is unstable at the plasma membrane and is therefore, internalized, again via a clathrin coated mechanism, where the protein accumulates in recycling endosomes (Figure 2-9). Additionally, in our model, the motion of the coated and uncoated α-sarcoglycan-EGFP vesicles is microtubule dependent, with shedding of the clathrin coat prior to fusion (Figure 2-9). This model supports a functional role for α-sarcoglycan in mediating the transport and maintenance of the sarcoglycan complex to the cell membrane.
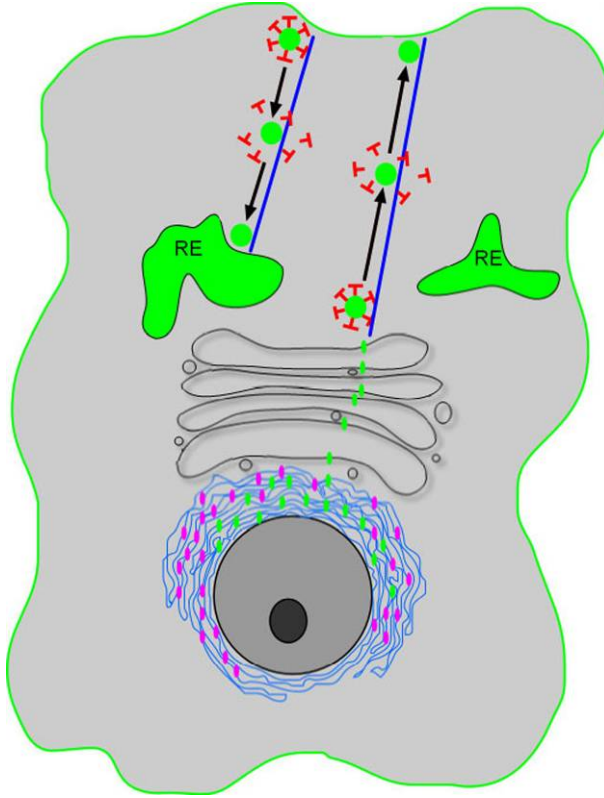
Figure 2-9.   Proposed model of α-sarcoglycan-EGFP trafficking pathway, in the absence of the remaining sarcoglycans.   RE's represent recycling endosomes.   Trafficking model demonstrates that α-sarcoglycan-EGFP (green particles) move through the biosynthetic pathway, past the endoplasmic reticulum and Golgi. Clathrin coated α-sarcoglycan-EGFP containing motile vesicles then transiently move along microtubules toward the cell surface. The clathrin coat is shed after budding, and before fusion. Once at the surface, the protein is then endocytosed due to instability in the absence of the remaining sarcoglycans and accumulates in RE's. R77C mutant is trapped in the endoplasmic reticulum and is shown in pink.

CHAPTER 3

The β-δ-core of sarcoglycan is essential for deposition at the plasma membrane*

ABSTRACT

Mutations of any of the sarcoglycan complex subunits (α, β, δ, and γ) cause limb-girdle muscular dystrophy. Furthermore, individual mutations lead to a reduction or loss of all other members of the complex. In some cases of limb-girdle muscular dystrophies however, residual sarcoglycan expression has been documented. Therefore, in this study I test the hypothesis that formation of specific sarcoglycan subcomplexes is crucial for plasma membrane deposition. Using co-immunoprecipitation assays, I demonstrated that β- and δ-sarcoglycan interact with α-sarcoglycan and these two subunits must be co-expressed for export from the endoplasmic reticulum. Advanced light-microscopic imaging techniques demonstrated that co-expression of β-sarcoglycan and δ-sarcoglycan is also responsible for delivery to and retention of sarcoglycan subcomplexes at the cell surface. These data suggest that formation of the β-δ-core may promote the export and deposition of sarcoglycan subcomplexes at the plasma membrane and therefore, identifies a mechanism for sarcoglycan transport.

INTRODUCTION

Mutations in the sarcoglycans (α, β, δ, or γ) (43) are responsible for the limb-girdle muscular dystrophies (LGMD 2D, 2E, 2F, and 2C, respectively) (35-37, 54, 65). Phenotypically, the onset, clinical features and progression of the LGMDs are often similar to the better known Duchenne muscular dystrophy (DMD) (23). A deficiency of any single member of the sarcoglycan complex results in a concomitant loss of the other members of the complex (35, 39, 163). However, conflicting data have demonstrated that some residual α-, β-, and δ-sarcoglycan protein may be present at the plasma membrane of LGMD 2C (γ-sarcoglycan deficient) patients (8, 71, 74, 75, 166, 167, 185). This observation supports the concept that α-, β-, and δ-sarcoglycan subunits are more tightly associated (56, 164).

In 1997 a strong interaction between the β- and δ-sarcoglycan subunits was demonstrated using in vitro pull-down methods (76). This finding was bolstered by a number of subsequent reports, including cross-linking studies (47), co-immunoprecipitation assays (77) and immunohistochemical analysis, which suggest that the β- and δ-sarcoglycan subunits form a core subcomplex that is central to sarcoglycan complex formation (53). Additionally, Shi et al. reported in 2004 that the co-expression of β- and δ-sarcoglycans in COS-1 cells produces a weak but distinct plasma membrane staining in many cells. The interactions between the β- and δ-sarcoglycan subunits, and α-sarcoglycan are less clearly understood. Although Sakamoto et al. demonstrated binding between β- and δ- sarcoglycan and α- sarcoglycan (76), Shi et al. stated that neither β- nor δ-sarcoglycan subunits co-localized or co-immunoprecipitated with α-sarcoglycan (77).

In this study I test the hypothesis that the co-expression and combination of β- and δ-sarcoglycan are responsible for the delivery and maintenance of the sarcoglycans at the plasma membrane. Using a combination of biochemical, live-cell total internal reflection microscopy, and quantitative immunofluorescence, I demonstrate that β- and δ-sarcoglycan bind to α-sarcoglycan in the endoplasmic reticulum independently of each other. However to move from the endoplasmic reticulum to the plasma membrane, co-expression of β- and δ-sarcoglycan is essential. Furthermore I demonstrate that this translocation is via motile vesicles and once at the cell surface the combination of β- and δ-sarcoglycan leads to increased labeling of the other sarcoglycans.

RESULTS

Sarcoglycans co-localize when expressed in specific combinations

In 2004 Shi et al. demonstrated that β-sarcoglycan interacts with specific sarcoglycans in COS-1 cells. To evaluate the co-localization of specific sarcoglycans in HEK293 cells, different combinations of α-, β- and δ-sarcoglycans were expressed and examined by confocal microscopy. When all four (α-, β-, δ- and γ-sarcoglycan) sarcoglycans are co-expressed in HEK293 cells, the sarcoglycans are localized to the plasma membrane (Figure 3-1), and are believed to exist as a complex as in other heterologous cell systems (46, 77). As I have recently demonstrated (193), α-sarcoglycan–EGFP displays a rather unique expression profile when expressed alone, as it is predominantly present in endosomal structures (Figure 3-2A-arrowhead), identified as recycling endosomes, as well as showing low expression at the plasma membrane (Figure 3-2A-arrow) and in the endoplasmic reticulum (193). In contrast β-sarcoglycan (Figure 3-2B) and δ-sarcoglycan (Figure 3-2C) when expressed alone are

predominantly localized to the perinuclear region and the endoplasmic reticulum (arrowheads), and co-localize with the endoplasmic reticulum marker calnexin (Figure 3-3). No protein is detectable at the plasma membrane. When α-sarcoglycan–EGFP and β-sarcoglycan are co-expressed, there is co-localization of the two proteins on endoplasmic reticulum–like structures (Figure 3-2D, E, F-inset), but no labeling is seen at the plasma membrane (Figure 3-2D, E, F-arrow), and α-sarcoglycan–EGFP does not co-localize with β-sarcoglycan in the endosomal accumulations at a regular exposure (Figure 3-2G). A similar pattern is seen when α-sarcoglycan–EGFP is expressed with δ-sarcoglycan in that co-localization is observed in endoplasmic reticulum–like structures (Figure 3-2H, I, J-inset), with no co-localization of δ-sarcoglycan with α-sarcoglycan-EGFP at the plasma membrane (Figure 3-2H, I, J- arrow), or in endosomal structures at a regular exposure (Figure 3-2K). When β-sarcoglycan and δ-sarcoglycan are expressed together, the proteins co-localize intracellularly in endosomal structures (Figure 3-2L, M, N- arrowhead), and as Shi et al. first reported (77), are also present at the plasma membrane (Figure 3-2L, M, N- arrow). When α-sarcoglycan–EGFP is expressed together with the combination of β-sarcoglycan and δ-sarcoglycan, all three proteins co-localize in intracellular endosomal compartments (Figure 3-2O, P, Q, R- arrowhead) and on the plasma membrane (Figure 3-2O, P, Q, R- arrow). This recapitulates results observed in LGMD-2C γ-sarcoglycan–deficient patients, where α-, β-, and δ-sarcoglycan expression is sometimes detected at the plasma membrane (8, 71, 74, 75). This suggests that formation of the β-, δ-sarcoglycan core is required for progression through the biosynthetic pathway. Furthermore, although α-sarcoglycan–EGFP is exported out of the endoplasmic reticulum alone, it co-localizes with β- and δ-sarcoglycan, both at the plasma membrane and in endosomal compartments, only when β- and δ-sarcoglycan are expressed together.

HEK cells co-transfected with
α–, β–, δ–, and γ–SG
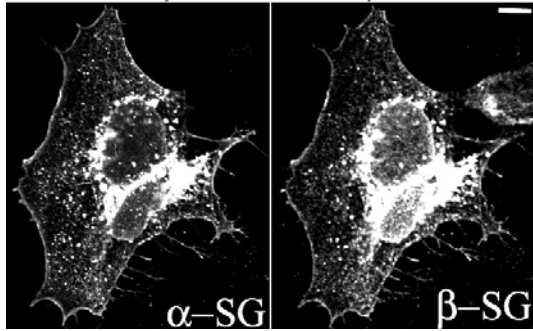
Figure 3-1. **Co-expression of α-, β-, δ- and γ-sarcoglycans in HEK293 cells results in localization at the plasma membrane**. α-sarcoglycan-EGFP is shown on the left and β-sarcoglycan is shown on the right. Bar= approx. 5μm.
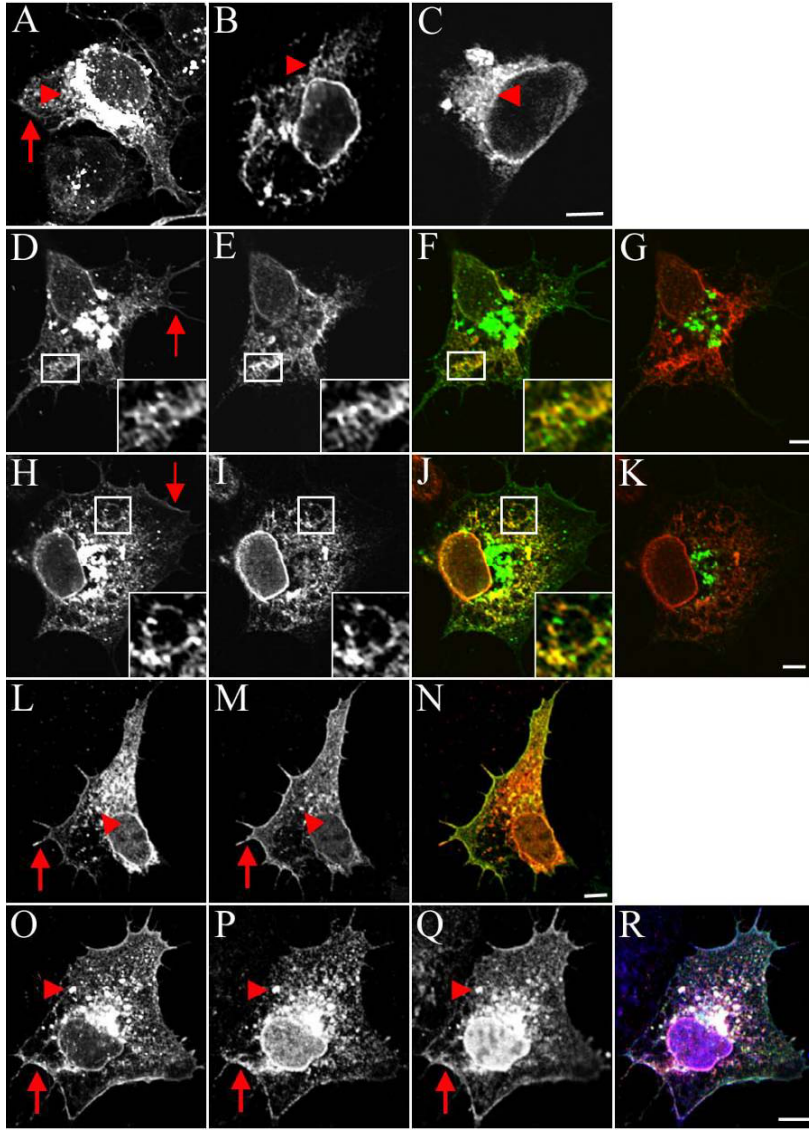
Figure 3-2. Sarcoglycan combinations show specific localization patterns in 293 cells by confocal analysis. (A)
α-sarcoglycan-EGFP. (B) β-sarcoglycan alone. (C) δ-sarcoglycan alone.   (D) α-sarcoglycan-EGFP in cells
expressing α-sarcoglycan-EGFP and β-sarcoglycan. (E) β-sarcoglycan in cell expressing α-sarcoglycan-EGFP and
β-sarcoglycan. (F) Overlay of α-sarcoglycan-EGFP (green) and β-sarcoglycan (red), co-localization in yellow.
Insets show the magnified boxed regions of endoplasmic reticulum-like co-localization. D, E and F are taken at a
high exposure in the green channel to show the endoplasmic reticulum labeling. (G) Regular exposure of α-
sarcoglycan-EGFP demonstrating that the endosomal accumulations do not co-localize with β-sarcoglycan.   (H) α-
sarcoglycan-EGFP in cells expressing α-sarcoglycan-EGFP and δ-sarcoglycan. (I) δ-sarcoglycan in cells expressing
α-sarcoglycan-EGFP and δ-sarcoglycan. (J) Overlay of α-sarcoglycan-EGFP (green) and δ-sarcoglycan (red), co-
localization in yellow, and in insets on endoplasmic reticulum-like structures.   (K) Regular exposure of α-
sarcoglycan-EGFP demonstrating that the endosomal accumulations do not co-localize with δ-sarcoglycan   (L) β-
sarcoglycan in cells expressing β-sarcoglycan and δ-sarcoglycan. (M) δ-sarcoglycan in cells expressing β-
sarcoglycan and δ-sarcoglycan. (N) Overlay of β-sarcoglycan (red) and δ-sarcoglycan (green), co-localization in
yellow. (O) α-sarcoglycan-EGFP in cells expressing α-sarcoglycan-EGFP, β-sarcoglycan, and δ-sarcoglycan. (P) β-
sarcoglycan in cells expressing α-sarcoglycan-EGFP, β-sarcoglycan, and δ-sarcoglycan. (Q) δ-sarcoglycan in cells
expressing α-sarcoglycan-EGFP, β-sarcoglycan, and δ-sarcoglycan. (R) Overlay of α-sarcoglycan-EGFP (green), β-
sarcoglycan (red), and δ-sarcoglycan (blue), co-localization in white.   Arrows show areas of plasma membrane
localization, and arrowheads show areas where the protein is localized intracellularly. Bar=approx. 5µm.
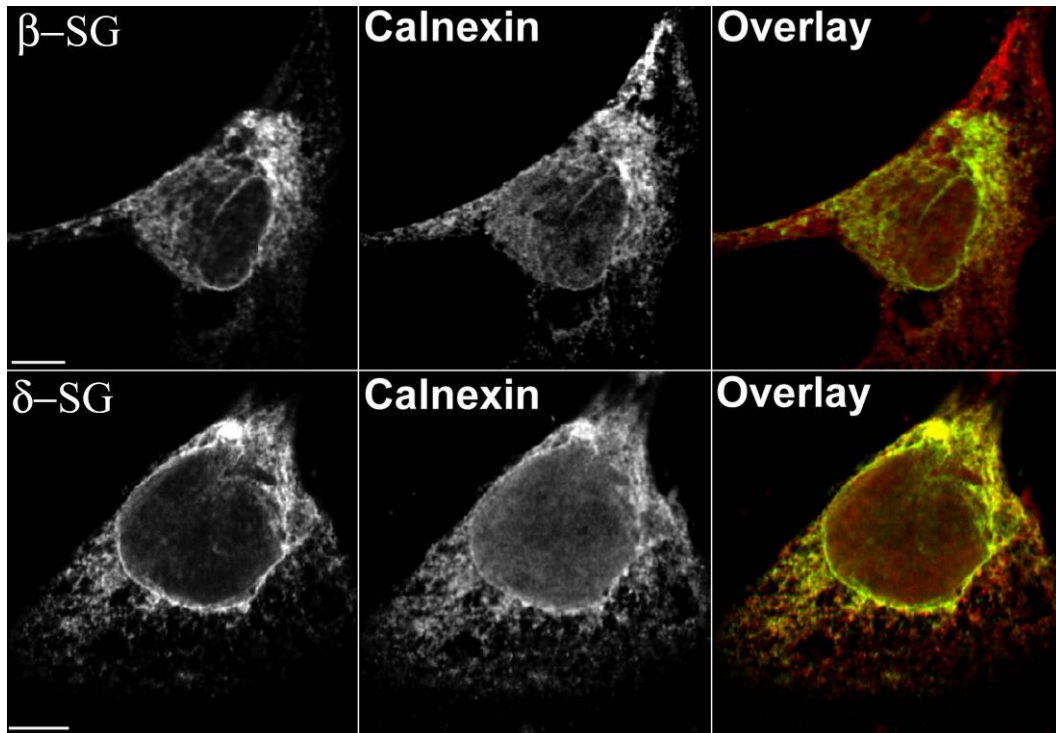
Figure 3-3. β-sarcoglycan and δ-sarcoglycan are localized to the endoplasmic reticulum. β-sarcoglycan and δ-sarcoglycan proteins are shown in red, respectively, and calnexin is shown in green. In yellow are area of co-localization in the overlay image. Bar=approx. 5µm.

β-, δ-sarcoglycan complex formation is not a requirement for α-sarcoglycan–EGFP binding

There have been a number of reports suggesting that β- and δ-sarcoglycan are bound together as a complex (47, 76-78), however conflicting reports exist as to whether in fact β- and δ-sarcoglycan are able to bind α-sarcoglycan independent of each other (76, 77). We use a co-immunoprecipitation assay to determine whether the co-localized α-sarcoglycan–EGFP and β-sarcoglycan or δ-sarcoglycan in the endoplasmic reticulum are interacting directly.

For this experiment, and for the live cell experiments that follow, I used a DsRed version of β-sarcoglycan. This construct produces a protein of the correct size which is recognized by the β-sarcoglycan antibodies (Figure 3-4A). Additionally, this fusion protein localizes appropriately within cells (Figure 3-4B).

A
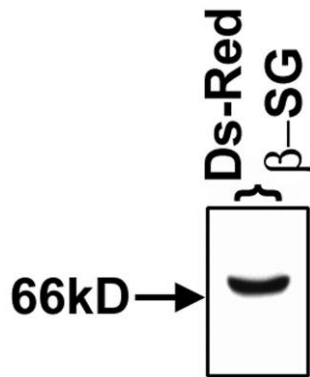
B
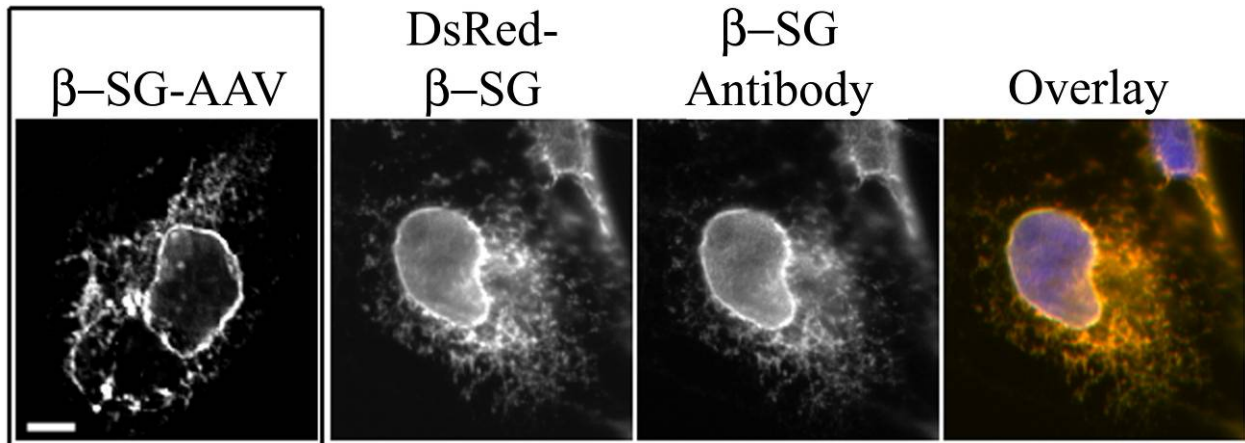
Figure 3-4. Addition of the DsRed tag does not alter the localization of β-sarcoglycan. (A) Western blot of 297 cell lysates transfected with DsRed-β-sarcoglycan, and blotted with an antibody against β-sarcoglycan. A protein that is approximately 70kDa is produced. (B) DsRed-β-sarcoglycan expression pattern in cells compared to the untagged β-sarcoglycan in an AAV vector, show similar localization patterns. DsRed-β-sarcoglycan (red) is recognized with an antibody against β-sarcoglycan (green). Overlay is in yellow, and nuclei are in Blue. Bar=approx. 5μm.
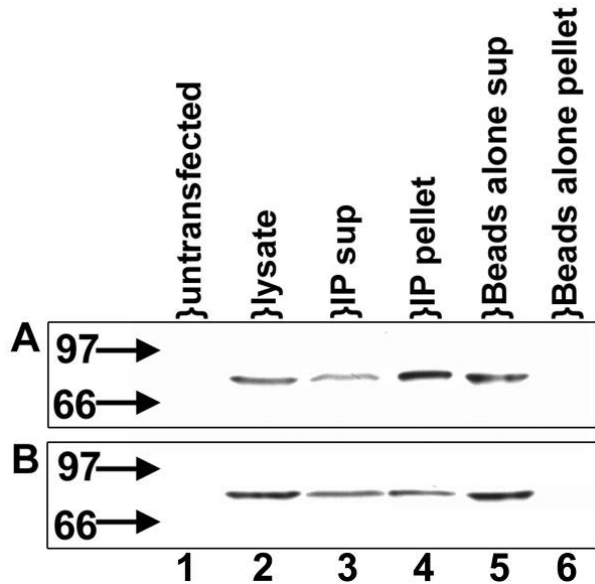
Figure 3-5. α-sarcoglycan-EGFP co-immunoprecipitates with DsRed-β-sarcoglycan and δ-sarcoglycan. Lane 1-untransfected 293 cells labeled with the EGFP antibody. (A) Cells in Panel A were transfected with α-sarcoglycan-EGFP and δ-sarcoglycan. Lane 2- Lysate of HEK293 cells blotted with an EGFP antibody. Lane 3-depleted α-sarcoglycan-EGFP in supernatant of cell lysates immunoprecipitated with a δ-sarcoglycan antibody. Lane 4- Enriched α-sarcoglycan-EGFP in pellets of cell lysates immunoprecipitated with a δ-sarcoglycan antibody. Lane 5- unaltered α-sarcoglycan-EGFP in supernatant of cell lysates immunoprecipitated with Protein G beads alone and no antibody. Lane 6- No α-sarcoglycan-EGFP in pellets of cell lysates immunoprecipitated with Protein G beads alone and no antibody. (B) Cells in Panel B were transfected with α-sarcoglycan-EGFP and DsRed-β-sarcoglycan. Lanes show the same pattern of α-sarcoglycan-EGFP as in A, however all immunoprecipitations were conducted using a β-sarcoglycan antibody.

HEK293 cells were transfected with a combination of α-sarcoglycan–EGFP and DsRed–β-sarcoglycan, or α-sarcoglycan–EGFP and δ-sarcoglycan. Lysates were then immunoprecipitated with antibodies against β-sarcoglycan or δ-sarcoglycan, respectively. The α-sarcoglycan–EGFP co-immunoprecipitated with both lysates (Figure 3-5- lane 4) but not with beads alone (containing no antibody) (Figure 3-5- lane 6). This allows us to conclude that although α-sarcoglycan–EGFP is able to bind individually to both β- and δ-sarcoglycan, the formation of the β-δ-sarcoglycan core complex is necessary for export of the complex out of the endoplasmic reticulum.

Sarcoglycan subcomplexes are detected in post–Golgi apparatus vesicles

To determine if the β-δ-sarcoglycan, and α-β-δ-sarcoglycan subcomplexes are present in post–Golgi apparatus vesicles, I disrupted the Golgi apparatus with 10 μg/ml of Brefeldin-A (BFA). HEK293 cells were transfected with different combinations of α-sarcoglycan–EGFP, Ds-Red–β-sarcoglycan, and δ-sarcoglycan, and then treated for 40 minutes with BFA. The treatment effectively disrupted the Golgi apparatus, evident from Giantin staining (Figure 3-6), but the cells remained intact. These cells were fixed and examined by confocal microscopy. When α-sarcoglycan–EGFP and Ds–Red-β-sarcoglycan are expressed together, the two proteins do not co-localize on discrete post–Golgi apparatus vesicles (Figure 3-7A, B, and C). This was also the case when α-sarcoglycan–EGFP was expressed with δ-sarcoglycan (Figure 3-7D, E, F). When Ds-Red–β-sarcoglycan, and δ-sarcoglycan are expressed together, many discrete vesicles are observed after the BFA treatment, where the two proteins co-localize (Figure 3-7G, H, I-inset). Expression of α-sarcoglycan–EGFP, Ds-Red–β-sarcoglycan, and δ-sarcoglycan together also results in the presence of vesicles containing all three proteins after the BFA treatment (Figure 3-7J, K, L, and M-inset). These data demonstrate that formation of the β-δ-sarcoglycan core is crucial for the movement of vesicles into and through the Golgi apparatus. Additionally, this suggests that the β-δ-sarcoglycan core mediates the movement of the α-β-δ-sarcoglycan subcomplex through the Golgi apparatus.
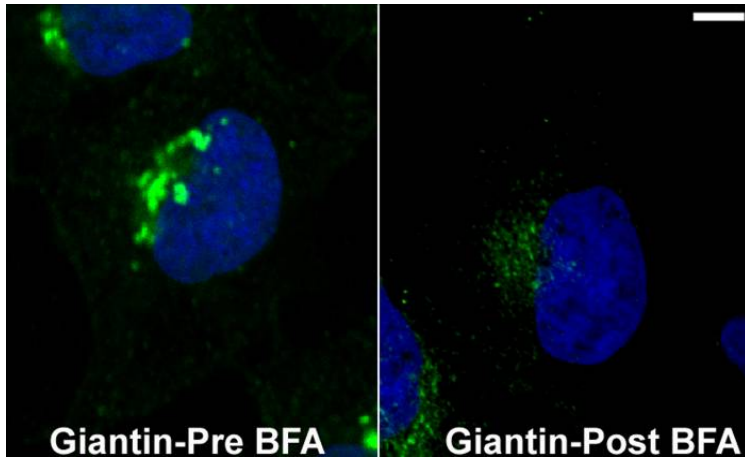
Figure 3-6. The Golgi is disrupted by BFA. The Golgi marker Giantin is seen in green pre, and post BFA treatment. Nuclei are shown in Blue. Bar=approx. 5μm.
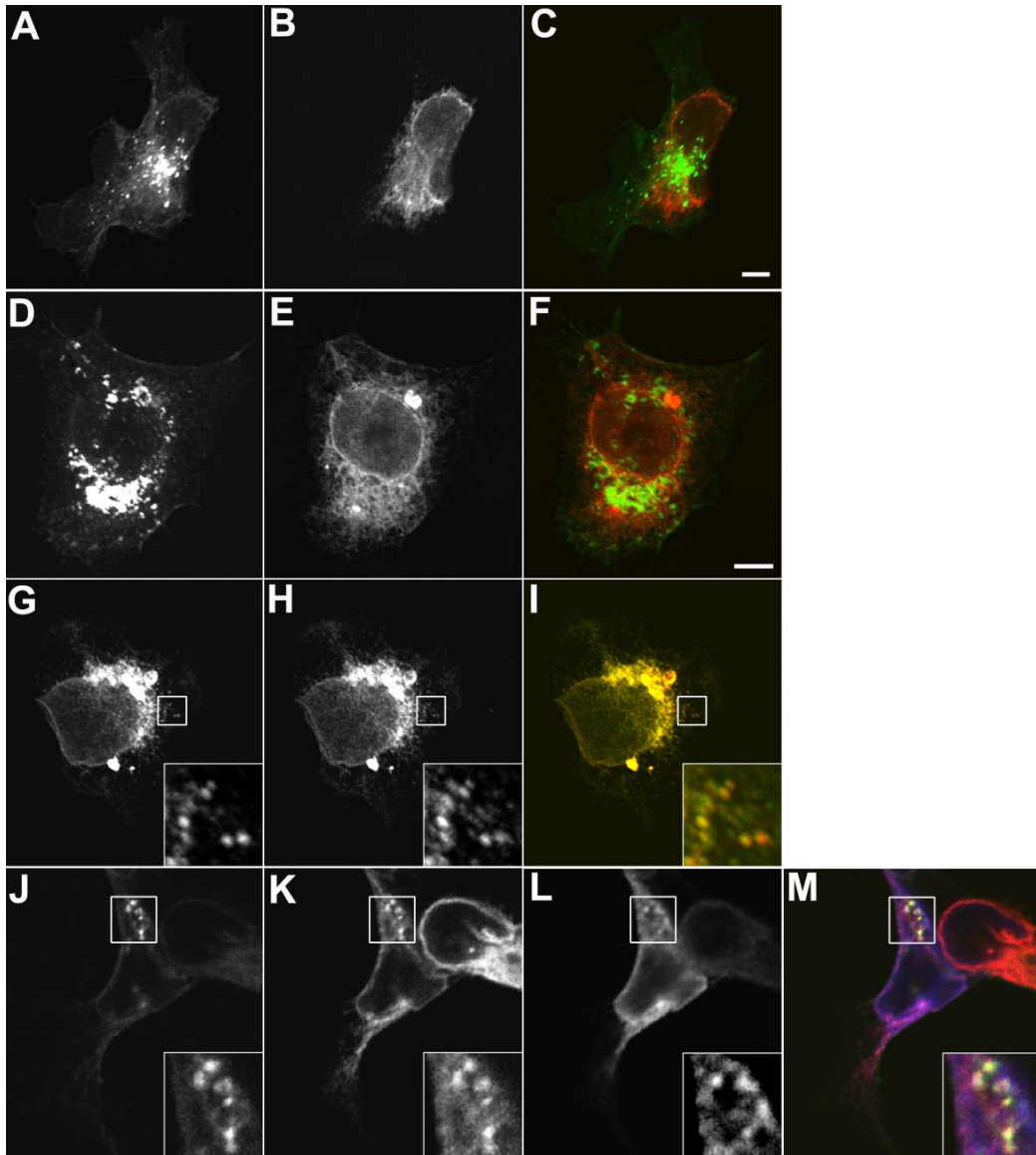
Figure 3-7. Specific sarcoglycan combinations are present together in vesicles when the Golgi complex is disrupted with BFA. (A) α-sarcoglycan-EGFP in cells expressing α-sarcoglycan-EGFP and DsRed-β-sarcoglycan. (B) DsRed-β-sarcoglycan in cell expressing α-sarcoglycan-EGFP and DsRed-β-sarcoglycan. (C) Overlay of α-sarcoglycan-EGFP (green) and DsRed-β-sarcoglycan (red).   (D) α-sarcoglycan-EGFP in cells expressing α-sarcoglycan-EGFP and δ-sarcoglycan.   (E) δ-sarcoglycan in cells expressing α-sarcoglycan-EGFP and δ-sarcoglycan. (F) Overlay of α-sarcoglycan-EGFP (green) and δ-sarcoglycan (red). (G) Ds-Red-β-sarcoglycan in cells expressing DsRed-β-sarcoglycan and δ-sarcoglycan. Inset shows vesicles that co-localize. (H) δ-sarcoglycan in cells expressing DsRed-β-sarcoglycan and δ-sarcoglycan. Inset shows vesicles that co-localize. (I) Overlay of DsRed-β-sarcoglycan (red) and δ-sarcoglycan (green), co-localization in yellow (inset). (J) α-sarcoglycan-EGFP in cells expressing α-sarcoglycan-EGFP, DsRed-β-sarcoglycan, and δ-sarcoglycan. Inset shows vesicles that co-localize.   (K) DsRed-β-sarcoglycan in cells expressing α-sarcoglycan-EGFP, DsRed-β-sarcoglycan, and δ-sarcoglycan. Inset shows vesicles that co-localize. (L) δ-sarcoglycan in cells expressing α-sarcoglycan-EGFP, DsRed-β-sarcoglycan, and δ-sarcoglycan. Inset shows vesicles that co-localize. (M) Overlay of α-sarcoglycan-EGFP (green), DsRed-β-sarcoglycan (red), and δ-sarcoglycan (blue), co-localization in white (inset). Bar=approx. 5μm.

Sarcoglycan subcomplexes are transported in motile vesicles at the cell surface

In order to determine whether specific sarcoglycan-rich vesicles are motile and traffic to or from the cell surface, I transfected combinations of sarcoglycans into HEK293 cells and examined them with total internal reflection fluorescence microscopy (TIR-FM), which detects fluorescence at or close to (150-200nm) the coverslip (169). As I have previously shown, when expressed alone, α-sarcoglycan–EGFP is present on the cell surface (8), and motile vesicles are detected by TIR-FM (Figure 3-8A, a) (8). In contrast when Ds-Red–β-sarcoglycan, and δ-sarcoglycan are expressed in cells alone, there is no detectable labeling at the cell surface (Figure 3-8A, b and c). The minimal signal seen is due to halos of endoplasmic reticulum very close to the plane of the membrane. When α-sarcoglycan–EGFP is expressed with δ-sarcoglycan or Ds-Red–β-sarcoglycan individually, neither the α-δ-sarcoglycan (Figure 3-8A, f) nor the α-β-sarcoglycan (Figure 3-8A, i) are motile at the cell surface. By contrast, when cells are co-transfected with Ds-Red–β-sarcoglycan and δ-sarcoglycan, β-δ-sarcoglycan labeling is detectable at the cell surface (Figure 3-8A, l). Furthermore, Ds-Red–β-sarcoglycan vesicles are now motile at the cell surface (Figure 3-8B-arrowhead). Additionally, expression of the β-δ-sarcoglycan core together with α-sarcoglycan–EGFP results in vesicles containing all three proteins at the cell surface (Figure 3-8A, p). Again in cells containing α-sarcoglycan–EGFP, Ds-Red–β-sarcoglycan, and δ-sarcoglycan, Ds-Red–β-sarcoglycan vesicles are motile and are also positive for α-sarcoglycan–EGFP (Figure 3-8C-arrowhead). These data suggest that the β-δ-sarcoglycan core is crucial for the vesicular transport of not only the β-δ-sarcoglycan core complex, but also subcomplexs involving α-sarcoglycan at the plasma membrane.

A

B

Ds-Red-β–SG

C

α–SG-EGFP

Ds-Red-β–SG

Overlay
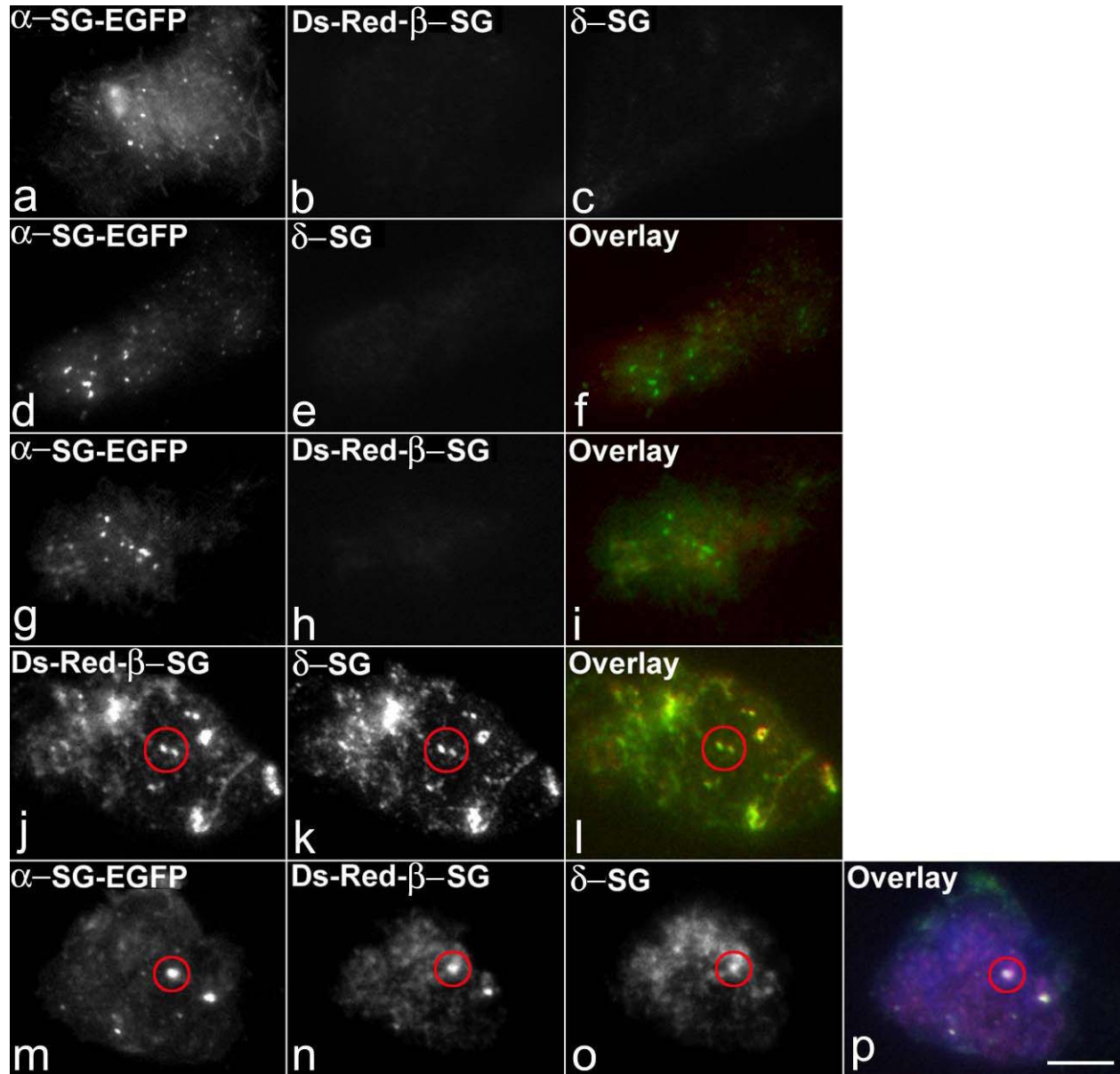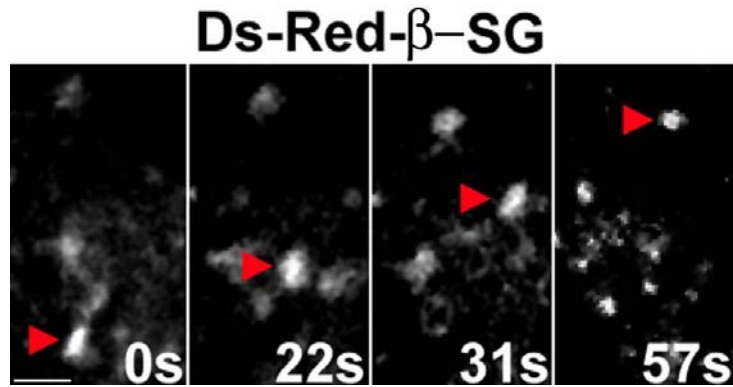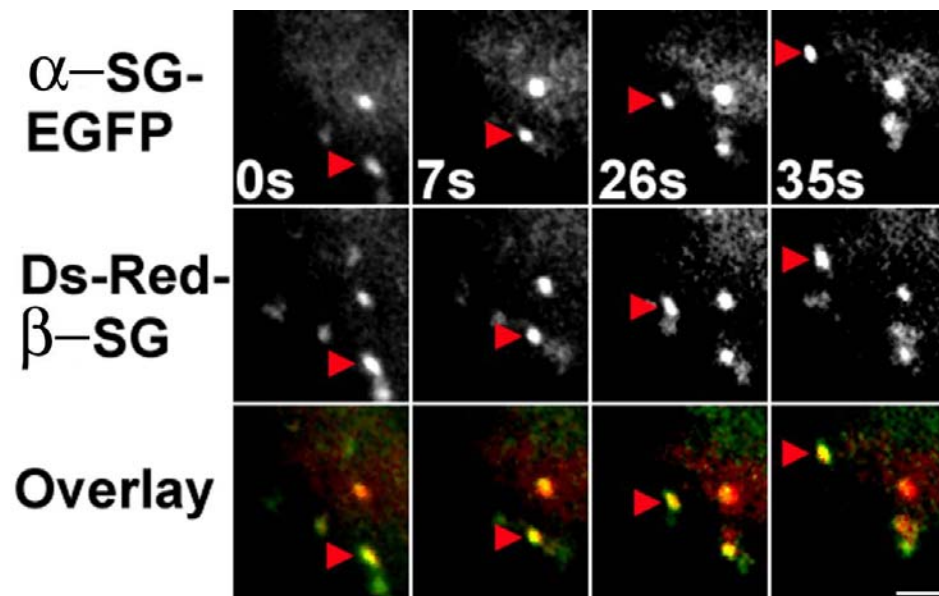
Figure 3-8. Sarcoglycan sub-complexes are motile at the cell surface by TIR-FM. (A) α-sarcoglycan-EGFP vesicles are consistently seen at the cell surface in green (a, d, g, m). DsRed-β-sarcoglycan, and δ-sarcoglycan are not seen at the cell surface when expressed individually (b, c). DsRed-β-sarcoglycan (red), and δ-sarcoglycan (green) positive vesicles are only seen at the cell surface when expressed together and co-localize (j, k, l- red circle, overlay). α-sarcoglycan-EGFP (green), DsRed-β-sarcoglycan (red), and δ-sarcoglycan (blue) positive vesicles are seen at the cell surface when all the proteins are expressed together (m, n, o, p- red circle, overlay). Bar= approx. 5μm. (B) arrowhead shows a motile DsRed-β-sarcoglycan particle at the cell surface when DsRed-β-sarcoglycan and δ-sarcoglycan are expressed together. Consecutive images are taken of live cells over a period of approximately 1 minute. Bar= approx. 1μm. (C) α-sarcoglycan-EGFP (green), DsRed-β-sarcoglycan (red) vesicles are motile together (arrowhead) at the cell surface when α-sarcoglycan-EGFP, DsRed-β-sarcoglycan, and δ-sarcoglycan are co-expressed. Consecutive images were again taken over a period of approximately 35seconds. Bar= approx. 1μm.

101

Deposition of sarcoglycan subcomplexes at the plasma membrane is dependent on the β-δ-sarcoglycan core

In order to determine whether the β-δ-sarcoglycan core promotes the deposition of sarcoglycan subcomplexes at the plasma membrane, combinations of sarcoglycans were transfected into HEK293 cells, and fluorescence at the membrane was quantified. When β-sarcoglycan or δ-sarcoglycan are expressed alone, the fluorescence at the plasma membrane is at baseline levels of 12 and 17 (pixel intensity on a scale of 0-255 (194)), respectively, most of which resulted from endoplasmic reticulum signal close to the membrane, and thus quantified as membrane fluorescence (Figure 3-9). In contrast, when α-sarcoglycan–EGFP is expressed alone, the average fluorescence at the membrane is at about 48 (Figure 3-9). When β-sarcoglycan and δ-sarcoglycan are expressed together, the fluorescence at the membrane increases significantly to approximately 50 for both proteins, representing an approximate 3.4 fold increase (Figure 3-9), and supports previous data (77). Additionally, when the β-δ-sarcoglycan core is expressed together with α-sarcoglycan–EGFP, the fluorescence levels of α-sarcoglycan–EGFP at the plasma membrane increase from 48 to 107, an approximately 2.2-fold increase (Figure 3-9). These data indicate that the β-δ-sarcoglycan core promotes the deposition of sarcoglycan subcomplexes at the plasma membrane of HEK293 cells.
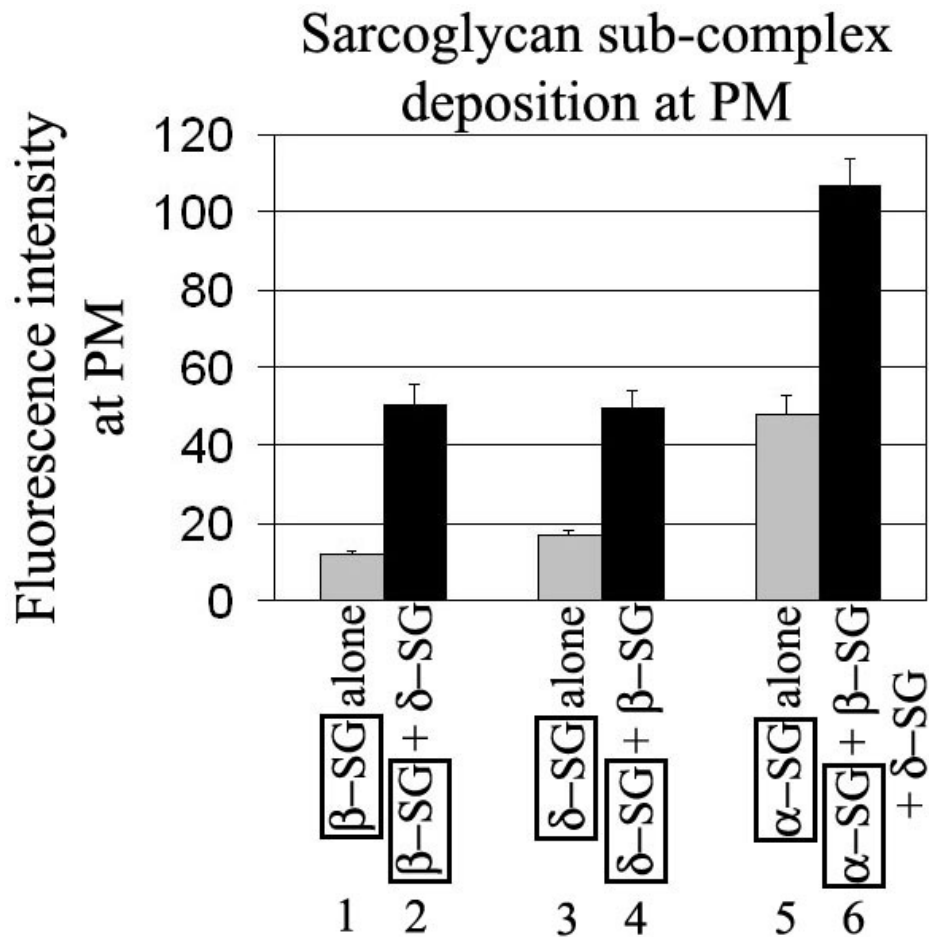
Figure 3-9. α-sarcoglycan-EGFP, β-sarcoglycan and δ-sarcoglycan are more stable at the plasma membrane when both β-sarcoglycan and δ-sarcoglycan are co-expressed. β-sarcoglycan fluorescence intensity at the plasma membrane when expressed alone compared to when co-expressed with δ-sarcoglycan is displayed in bars 1 & 2. δ-sarcoglycan fluorescence intensity at the plasma membrane when expressed alone compared to when co-expressed with β-sarcoglycan is displayed in bars 3 & 4. α-sarcoglycan-EGFP fluorescence intensity at the plasma membrane, when expressed alone compared to when co-expressed with β-sarcoglycan and δ-sarcoglycan is displayed in bars 5 & 6.

Discussion

We have demonstrated that although both β- and δ-sarcoglycans have the ability to bind α-sarcoglycan. Furthermore, formation of the β-δ-sarcoglycan core is essential for the export, delivery, and deposition of both β-δ-sarcoglycan and α-β-δ-sarcoglycan subcomplexes at the plasma membrane of HEK293 cells (Figure 3-10).

103
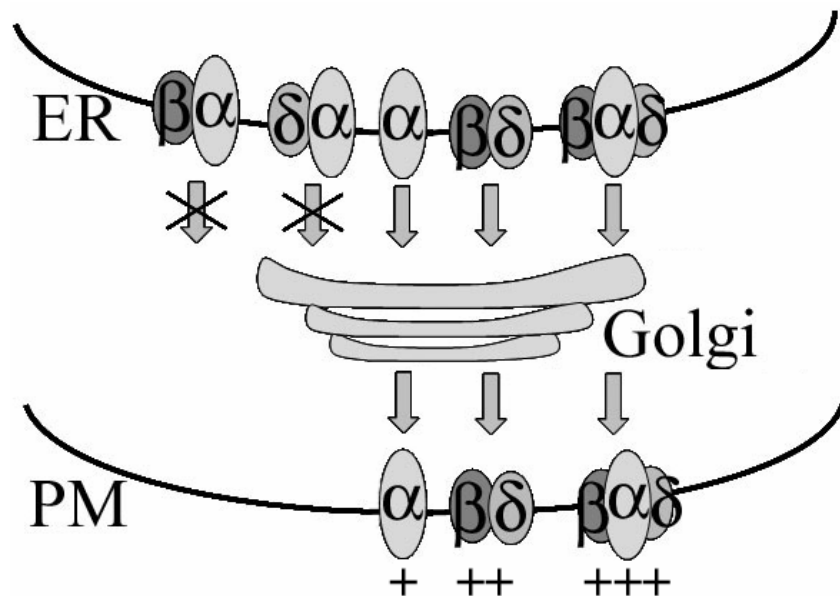
Figure 3-10. **Schematic illustrating formation of the β-δ-sarcoglycan core promotes targeting and deposition of sarcoglycan subcomplexes to the plasma membrane. +'s denote levels of plasma membrane expression.**

The central importance of the β-δ-sarcoglycan core in sarcoglycan complex assembly is well established, but it was previously unclear to what extent this core complex influenced the stability and assembly of residual subcomplexes at the plasma membrane, especially in cases of LGMD-2C. The necessity of the β-δ-sarcoglycan core is exemplified by its ubiquitous nature. Of the four primary sarcoglycan subunits in skeletal muscle, β-, and δ-sarcoglycans are also expressed in smooth muscle, specifically the vascular smooth muscle of coronary arteries. In this case α- and γ-sarcoglycan are replaced by ε- and ζ-sarcoglycan, respectively (34, 195, 196). Additionally the importance of the β-δ-sarcoglycan core at the plasma membrane is reflected in temporal cell culture studies. In these studies, α- and γ-sarcoglycan are located intracellularly until the synchronous expression of β-, and δ-sarcoglycan, which coincides with the translocation and stable expression of α- and γ-sarcoglycan at the plasma membrane (137).

Although biochemical studies in BFA-treated cells support a model for sarcoglycan assembly in the endoplasmic reticulum (78), it was unclear as to whether β- and δ-sarcoglycan are able to bind to α-sarcoglycan in the absence of γ-sarcoglycan. Our data demonstrate that α-sarcoglycan–EGFP in fact binds both β- and δ-sarcoglycan subunits individually. This is in contrast to data presented by Shi et al. in 2004 (77). One possible explanation for this discrepancy is that Shi et al. utilized polyclonal β-sarcoglycan (35) and δ-sarcoglycan (54) antibodies for their co-immunoprecipitation, directed against the extracellular domain of the proteins. In 1998 Chan et al. demonstrated that antibodies directed against the extracellular portion of the sarcoglycans immunoprecipitated fewer sarcoglycans than those against the intracellular portions of the proteins (47). This is presumably due to the interruption of protein–protein interactions mediated by the extracellular portions of the sarcoglycans. The antibodies that I used for our immunoprecipitations were directed against the intracellular portions of β-sarcoglycan and δ-sarcoglycan, and therefore, may explain why they preserve the interaction with α-sarcoglycan whereas the extracellular-directed antibodies did not. Additionally, I used a different cell type and had different experimental procedures. Co-expression of β- and δ-sarcoglycan, however, is a necessity for endoplasmic reticulum export.

Recently Shiga et al. demonstrated that ζ-sarcoglycan acts as a functional homologue of γ-sarcoglycan in the formation of the sarcoglycan complex (197), raising the possibility that ζ-sarcoglycan may be responsible for mediating the interaction and stability of the α-β-δ-sarcoglycan subcomplex at the plasma membrane in LGMD-2C patients. The ζ-sarcoglycan mRNA was highly expressed in brain (197) and is also present in striated muscle and the smooth muscle layer of the coronary artery (198). There have been no reports to date of ζ-sarcoglycan expression in kidney tissue or cells, which do not express endogenous sarcoglycans (168), so I

believe that ζ-sarcoglycan is probably not responsible for deposition of the α-β-δ-sarcoglycan subcomplex in HEK293 cells. However, due to the lack of a commercially available antibody against ζ-sarcoglycan, I could not test this.

In 2000, Crosbie et al. used an antibody directed against the N-terminus of γ-sarcoglycan to demonstrate that truncated versions of γ-sarcoglycan may be responsible for the residual α-β-δ-sarcoglycan at the plasma membrane of LGMD-2C patients expressing a deletion of a nucleotide in position 521 (del521T) (199). In our previous study, I demonstrated that a LGMD-2C patient who did not have the del521T mutation, continued to express robust α-β-δ-sarcoglycan at the plasma membrane (8), and a patient with the del521T mutation had no α-β-δ-sarcoglycan at the plasma membrane (8). Furthermore, Higuchi et al. also demonstrated that a LGMD-2C patient with a deletion in nucleotides 630-702, which conserves the epitope site of the γ-sarcoglycan antibody used (Novocastra Laboratories, Newcastle upon Tyne, UK), had no detectable γ-sarcoglycan yet retained residual α-β-δ-sarcoglycan at the plasma membrane. This evidence supports the hypothesis that the β-δ-sarcoglycan core promotes the deposition of α-β-δ-sarcoglycan at the plasma membrane in some LGMD-2C cases.

The functionality of partial sarcoglycan complexes at the plasma membrane in cases of LGMD-2C is not fully understood. Though it seems to offset the severity of the disease pathology in some cases (8, 56), in others large amounts of residual sarcoglycans are retained at the plasma membrane, yet the patients display severe DMD-like phenotypes (75, 167, 185). Therefore, I believe that it is not possible to draw any reliable clinical correlation between sarcoglycan subcomplex stability and phenotype severity.

We also demonstrated that the co-expression of β- and δ-sarcoglycan promotes the motility of both β-δ-sarcoglycan and α-β-δ-sarcoglycan transport vesicles at the cell surface. Shi

et al. demonstrated that when the sarcoglycans are expressed alone they are not properly glycosylated (77). When proteins are not properly glycosylated, their proper folding is affected (200). Therefore, formation of the β-δ-sarcoglycan core may be essential for the proper glycosylation and thus folding and subsequent export of the core complex out of the endoplasmic reticulum. Alternatively, formation of the β-δ-sarcoglycan core could have an effect on the conformational states of either the β-sarcoglycan or δ-sarcoglycan proteins alone or the β-δ-sarcoglycan core complex (201). This, in turn, may facilitate the export of β-δ-sarcoglycan rich vesicles. Additionally conformational changes may also promote the binding of accessory proteins enabling vesicle motility (202). We previously showed that α-sarcoglycan–EGFP, when expressed alone, is also motile at the cell surface (193); α-sarcoglycan is thought to integrate into the sarcoglycan complex as a later stage (47), so that, unlike β- and δ-sarcoglycan, it is probable that α-sarcoglycan does not require specific sarcoglycan-binding partners at the endoplasmic reticulum, for its exit. Although the increase in α-sarcoglycan membrane labeling may be a result of increased transport due to the formation of the β-δ-sarcoglycan core, our data support a model in which sarcoglycan subcomplex formation is more of a necessity for stability of α-sarcoglycan at the plasma membrane (Figure 3-10).

CONCLUDING SUMMARY AND FUTURE DIRECTIONS

We have come a long way in the last century in understanding the causes and progression of the muscular dystrophies. Today, due to the elucidation of the genetic basis that underlies the pathologies, gene therapy is a realistic option for treatment. Additionally, the advances in microscopic imaging and genetic based probes have facilitated the visualization and analysis of gene behavior in living systems.

In the field of muscular dystrophy, much of the research in the last decade or so has been focused on efficiently delivering genes to muscle tissue with minimal toxicity and long term expression. The intersection of MD research with the imaging world has to date been minimal, and for the most part has been taking a parallel course in advancement. It was my goal in this dissertation to bridge the fields of muscle biology (with respect to the proteins involved in the MDs), and high end optical imaging, allowing us to better understand how these genes, that are considered candidates for therapy in humans behave at the molecular level, in living cells.

The work presented in the last three chapters details the development of a model system to study the efficacy and biology of gene therapy constructs using advanced microscopic imaging procedures. Although microscopic imaging has its limitations when compared to the traditional biochemical approach of scientific research, much of the data presented in this dissertation is the first to visually demonstrate the dynamic trafficking of DPC proteins in vivo. In the future, as in several other cases (186), this may prove to be central to uncovering appropriate targets for therapy.

Efficiency of Mini-Dystrophin

The Mini-Dystrophin transgenes constructed by Wang el al. in 2000 (104), are currently the most promising avenue for treatment of DMD by AAV mediated gene therapy, and are currently being tested in large animal models, such as the golden retriever muscular dystrophy dog (GRMD) (personal communication, Xiao X.). Although previous studies have established that the mini-dystrophin construct reconstitutes components of the DPC, the data presented in chapter 1 are the first to report the integration of the mini-dystrophin protein on a molecular level, in live cells.

One of the most intriguing discoveries made in this chapter was that mutations made within the ZZ β-dystroglycan binding domain, results in a redistribution of the minidystrophin-EGFP protein into the nucleus. Mutagenesis of fluorescently tagged constructs allows quick evaluation of the effect of the mutations on protein traffic, and therefore, is a powerful tool in the rapid assessment of critical domains within proteins that are responsible for their cellular localization. The dramatic redistribution and ablation of β-dystroglycan binding upon ZZ domain mutagenesis illustrates that the minidystrophin construct is integrating into the DPC much the same way as the full length dystrophin molecule. Further research focused on examining the redistribution of the full length dystrophin molecule containing these mutations will provide insight into whether this redistribution is consistent within all dystrophin variants or is specific to the miniature versions, which are more easily able to pass through the nuclear pores.

Additionally the kinetic live cell data demonstrating that minidystropin-EGFP is able to translocate to the plasma membrane relatively rapidly (within 4 hours of expression) clarifies the initial effectiveness studies conducted with the minidystrophin construct (104), illustrating more

clearly that the transgene is rapidly efficient when administered as gene therapy. Since the publication of this report, there have been subsequent studies that have emerged corroborating our data on the functionality of EGFP-minidystrophin fusion genes for cell and gene therapy studies (202), however, these constructs are significantly larger than the ones created and tested in chapter 1, and have not been studied extensively in living cells.

The union of live cell imaging with AAV based gene therapy constructs presented in chapter 1 has proved to be fruitful. Collaborative studies have subsequently been conducted by our group and Dr. Xiao's (University of Pittsburgh) investigating the most effective AAV serotype for delivering minidystrophin transgenes to living muscle. Different AAV serotypes containing EGFP have been used to infect mature C57 myotubes grown in culture and have been imaged live over the course of 5 days (In preparation for publication). Due to the fact that the minidystrophin-EGFP constructs are less than 4.5kb, small enough to fit into an AAV vector cassette, future studies should focus on studying the molecular integration of minidystrophin constructs in whole muscle to ensure that the major deletions within the rod region and C-terminus of the transgene do not affect the long term efficiency and utility of minidystrophin with repeated cycles of contraction and relaxation in vivo.

Sarcoglycan protein traffic

It is now clear that mutations in the sarcoglycans are responsible for the LGMDs; however the true function of the sarcoglycans still remains elusive. In the studies presented in chapter 2 I choose to focus on the most commonly mutated member of the sarcoglycans- α-sarcoglycan. I aimed at using advanced imaging to determine some of the functional properties of α-sarcoglycan. These data add significantly to the field of muscular dystrophy for a number of reasons.

This study is the first to examine the normal and myopathic trafficking of any of the sarcoglycans in living cells, from normal and dystrophic muscle. Furthermore, the data demonstrates that fluorescently tagged α-sarcoglycan is a useful tool to study the dynamic movement of the protein in vivo.

We present the novel finding that α-sarcoglycan utilizes clathrin coats and microtubules during cellular transport. The clathrin constructs utilized in this study were tagged on the light chains of clathrin. The light chain of clathrin is in turn coupled to the clathrin heavy chain; however multiple homologues of this heavy chain are reported to exist. In 2001, Liu et al. reported a novel clathrin homologue, termed clathrin heavy chain 22 (CHC 22), that is predominantly expressed in muscle tissue and is up regulated with myotube differentiation (205). Future work should therefore, be conducted to determine if DPC proteins are trafficked via this novel CHC 22 pathway. The evidence provided in this study is based in large part on live cell microscopy data. Although convincing, one of the limitations to this approach is that the technique cannot confirm a physical interaction between two proteins, merely a co-localization within a sub-cellular domain over time. Further biochemical experimentation should be conducted to confirm a physical association between the specific domains within α-sarcoglycan, and the cellular trafficking machinery, to dissect how the transport is mediated.

This is also the first report demonstrating that any of the members of the DPC recycle from the plasma membrane. The importance of this data is that it not only presents a mechanism by which α-sarcoglycan may control and fine tune the trafficking and expression of the sarcoglycan complex at the membrane, but also presents evidence that α-sarcoglycan behaves like a receptor; an idea which has been discussed in previous studies. Sarcoglycan members other than α-sarcoglycan have been examined for receptor like function (personal

111

communication, Bonnemann C.G.), however there have been no such studies reported for α-sarcoglycan, which should be a focus for future research.

Furthermore, I elucidate how the most commonly occurring R77C mutation affects α-sarcoglycan protein traffic. Due to the fact that the trapping of α-sarcoglycan in the endoplasmic reticulum is in all probability caused by a folding defect, future work should be directed at examining muscle biopsies from patients suffering from this specific mutation to see if the mutated α-sarcoglycan is being trapped in the endoplasmic reticulum of their muscle cells as well. Studies such as crystal structure analysis may elucidate the precise mechanism that prevents its ability to fold correctly, which in turn could serve as an avenue for therapy for patients with this mutation. In these cases, fixing the primary folding defect may be a better mode of therapy than gene replacement, as the mutated gene may still compete for binding of the other sarcoglycans despite the introduction of a normal variant of the gene.

The methodology used in chapter 2 is also unique. I demonstrate that fewer mutations than reported by Patterson and Lippincott-schwartz in 2002, are sufficient to make EGFP photoactivatable. Also, our combination of TIR-FM with photoactivation has not been conducted in any other report. TIR-FM is inherently useful in studying membrane protein complexes; therefore, the approaches utilized in this chapter are specifically applicable when studying the proteins of the DPC. Currently, advanced imaging systems are being manufactured that combine TIR-FM with various other microscopic procedures, such as live-cell confocal microscopy in a single microscope (Olympus, New York). Therefore, future work coupling our approaches to more sophisticated hardware, will provide an unparalleled perspective on the integration of DPC proteins at the membrane of living muscle tissue.

Sarcoglycan sub-complex deposition

The use of TIR-FM is extended to chapter 3, where it is utilized to demonstrate that formation of the β-δ-core of sarcoglycan is crucial for the deposition of sarcoglycan sub-complexes at the plasma membrane.

Previous studies have demonstrated the formation of the β-δ-core, mostly using conventional biochemical methods. However, TIR-FM allows us to visualize the effects of this core formation on vesicle motility at the cell surface. Furthermore, quantification of membrane fluorescence demonstrates that the β-δ-core has a stabilizing effect on sarcoglycans at the plasma membrane. This is a novel finding and has not been demonstrated previously. Quantification of fluorescence however does have significant limitations, as conditions are, for the most part, controlled by the individual that is doing the image acquisition, and is therefore, somewhat subjective. To add to this, each cell expresses different amounts of the transfected transgene, and each antibody has different binding affinities. Although most of these variables can be controlled for, future complementary studies should be conducted using classic biochemical protocols. Additionally, future work should also focus on conclusively determining if a partial re-construction of sarcoglycan sub-complexes does in fact rescue some of the severe phenotypes associated with some forms of LGMD.

DPC assembly

There have been a number of previous reports that have examined DPC assembly from a biochemical standpoint in static systems. The novelty of my wors is that I am able to visualize certain components of DPC assembly in living cells. The findings from Chapters 1, 2, and 3, corroborate the major conclusions drawn from the initial study of patient biopsies in 2001 (8).

The assembly of the DPC can therefore, be broadly separated into dystrophin integration and sarcoglycan integration, which appear to be independent of each other.

The model supported by this thesis is one where dystrophin is able to translocate to the cell surface rapidly after it is produced, and anchor through primary connections to β-dystroglycan. The primary expression of β-dystroglycan is one that has been addressed in literature (137), and the importance of β-dystroglycan in early development is well documented (139). Although dystrophin may use actin as a secondary anchoring scaffold, the live cell studies conducted in the presence of actin disrupting drugs demonstrate that ablation of the actin scaffold doesn't have as deleterious of an effect as the ablation of the β-dystroglycan binding domain. Cote et al. presented data in 2002, where they show that dystrophin is in fact localized to the plasma membrane in some cells that do not express high levels of β-dystroglycan (158). This could be attributed to auto fluorescence, however, future work should focus on clarifying this by conducting studies where mini-dystrophin and full length dystrophin recombinant DNA localization is quantified in dystroglycan null-mice, or primary cell lines derived from these mice.

Evidence is presented in chapters 2 and 3, demonstrating that the sarcoglycans do have different expression profiles when they are expressed alone, which may provide insight into their function. It is clear, however, that, in order to have a stable and complete functioning sarcoglycan complex at the plasma membrane, the synchronous expression of all four members is a necessity. As dystrophin deposition is independent of sarcoglycan expression, so to is sarcoglycan assembly independent of dystrophin expression. Future work should clarify if the sarcoglycans are able to anchor in the absence of β-dystroglycan.

Although the DPC fluorescent constructs in the preceding chapters are some of the first reported, I envision future studies were DPC assembly can be re-created in live cell culture systems, by tagging each of the individual members with different colors. As the spectral separation capabilities of confocal microscopes is continually improving, and the discovery of genetically encoded fluorophores is being reported from many corals and other living creatures, these experiments should not be too far away.

From cells to whole organs

Perhaps one of the greatest limitations to the imaging conducted in this thesis is that it is performed in single cells which are grown on glass coverslips. A major assumption is that this is also how the proteins under investigation are behaving in whole organs, in living animals.

The move from single cells to whole animals requires two major components. One is a vehicle capable of delivering the fluorescently tagged transgenes, so expression is widespread throughout the organ. The constructs reported here are all under 4.5kb, therefore, packaging of these fusion genes into AAV vectors is not only a powerful tool in the evaluation of the success and sustained expression of gene therapy, but also for studying how these genes behave in whole organs. The second component is an imaging system capable of penetrating past the superficial layers of the organ while keeping the animal alive and somewhat homeostatic.

Preliminary efforts I have conducted to fuse these two components and move our imaging models into whole organs were presented at the International Keystone Symposia in 2003. There I described a novel way to evaluate the structure and function of Dystrophin associated proteins (DAP's) in whole skeletal muscle (203). Skeletal muscle is the only organ aside from the placenta that exists as a synciium, therefore, when studying muscle proteins it is advantagous to be able to examine not only large single fiber segments, but also whole fiber

fascicles in their native basement membrane and extracellular matrix. To this end, I employed single photon and multiphoton excitation confocal microscopy techniques to examine the localization of DAP's in whole mount muscle preparations. The z-axis imaging capabilities of both single and multi-photon confocal microscopy, along with the increased depth penetration possible with multiphoton techniques, allow evaluation of protein expression at significant depths in adult mouse skeletal muscle. The distribution of DAP's can therefore, be visualized to an extent not possible using conventional microscopy of thin-sectioned muscle samples (203). While it is possible to access proteins within whole tissue with antibodies using extended staining protocols and harsh membrane permeablization steps, a more rational method for studying proteins in whole muscles is to get the organ to express a tagged version of the protein.

Therefore, future studies should focus on inserting the constructs I have made into the appropriate AAV cassette, and studying their efficacy and behavior in whole adult mouse muscle. As stated earlier, I am a collaborator on studies currently under way evaluating the most effective AAV serotypes for mature muscle infection (In preparation for publication).

Concluding remarks

In conclusion, the data presented in this thesis are aimed at integrating the fields of molecular genetics and cellular biology utilizing advanced microscopic imaging. Through the visualization of molecular behavior in the context of the muscular dystrophies, I demonstrate the fundamental biological properties that underlie the behavior and assembly of the dystrophin associated proteins. Elucidating the basic biology these proteins is paramount in the development of safe and effective therapies for the muscular dystrophies in humans.

APPENDICES

APPENDIX A

MATERIALS AND METHODS

Construction of fusion genes

N- and C- terminus EGFP-minidystrophin constructs

3849 bp mini-dystrophin constructs were made by PCR as described previously by Wang et al. (104). The 3849 minidystrophin contains rods 1, 2, 22, 23, 24 hinge 1, 4, and the CR domain. It was amplified by PCR and ligated to either pEGFP-N1 (clontech, Mountain view, CA) at the Bam H1 site, or pEGFP-C1 (clontech, Mountain view, CA) using Bgl II (Fig. 1*A*). A five or six aa filler was added to EGFP-C1 and N1 respectively to facilitate ligation. Both constructs were verified by automated dideoxy sequencing (U. of Pittsburgh and Genewiz, NJ).

Becker N- and C- halves

N- and C-half constructs were made by PCR from a Becker-minidystrophin template, containing rods 1,2,3,20,21,22,23,24, and detailed by Wang et al. in 2000 (104). The N-half was an amplified region from rod 1-21, and the C-half was an amplified region from rod 22 to the C-terminus. The constructs were then inserted in an AAV vector cassette and CsCl purified.

Alpha-sarcoglycan-EGFP

A-sarcoglycan-EGFP was constructed by cloning α-sarcoglycan from α-sarcoglycan-AAV (graciously provided by E. Hoffman). α-sarcoglycan was amplified using forward primer:

5'-GGATDDCTDAGACACTCTTCTGG- 3',

and reverse primer 5'-GGTGCTGGTCCAGAATGAGGGGC-3'.

The cloned α-sarcoglycan was then ligated at the intracellular C-terminus to EGFP-N1 (clontech, Mountain view, CA). This construct, termed α-sarcoglycan-EGFP was verified by sequencing (Genewiz, North Brunswick, NJ).

DsRed-β-sarcoglycan

DsRed-β-sarcoglycan was constructed by amplifying β-sarcoglycan from β-sarcoglycan-AAV using forward primer:

5'-GGATGGCGGCAGCGGCGGC-3',

and reverse primer 5'- GATGAGTGTTTCCACAGGGCTTG-3'.

The cloned β-sarcoglycan was then ligated at the extracellular C-terminus to pDsRed-express-N1 (Clontech, Mountain view, CA). This construct, termed DsRed-β-sarcoglycan was verified by sequencing (Genewiz, North Brunswick NJ).

Provided constructs

Clathrin light chain (CLC)-DsRed was graciously provided by L. Traub (University of Pittsburgh).

B-sarcoglycan-AAV was graciously provided to us by E. Hoffman (Childrens medical hospital, Washington D.C).

δ-sarcoglycan-AAV was graciously provided to us by X. Xiao (University of Pittsburgh.

Cell lines, transfections and imaging

293 human kidney cells are grown at 37°C in DMEM supplemented with 10%FBS and Penicillin/strepomycin.

C57 control muscle cells were grown at 37ºC in DMEM supplemented with 10%FBS and Penn/Strep, and Bovine Fibroblast growth factor (BD biosciences, San Jose, CA). (Invitrogen). Cells were allowed to differentiate in DMEM+2%FBS+P/S.

C2C12 muscle cell line was grown in the same media as used for the 293 cells, and allowed to differentiate in DMEM with 2% horse serum.

All cells were transfected with lipofectamine 2000 transfection reagent (Invitrogen), in OPTI-MEM media without antibiotics for 6 hrs, after which media was changed back to growth media.

Hela cell line- Cells were grown and transfected in the same conditions as those used for 293 cells.

Injections, tissue extraction and processing

3849-EGFP-N1 and C1, were injected as CsCl purified plasmid DNA into the Tibialis anterior (TA) muscle (50 μg) and Gastocnemius (GAS) (70 μg) of 5 month old male mdx mice with Electroporation at 100v during injection for amplification of plasmid entry. TA and GAS muscles were harvested after 1 week and tissue was fixed in 2% paraformaldahyde for 2 hours. Muscles were then placed in 30% sucrose solution for an additional 24 hours, frozen in isopentane submerged in liquid Nitrogen, and stored and –80ºC. Six micron Sections were cut on a microm cryostat and mounted on superfrost slides. Then sections were stained with Hoecht dye (Watkins lab) for 30 seconds, followed by 3 washes in 1xPBS. Serial sections were also used for immunohistochemistry. Coverslips were mounted onto slides using gelvatol mounting media (Watkins lab). Organ tissues were extracted from a rat and homogenized in TBS containing protease inhibitors (200 mM PMSF & 1 M Benzamide). Extracts were then

centrifuged to remove debris, and cleared supernatants were used for Western blotting and immunoprecipitations.

α-sarcoglycan-EGFP was injected as purified plasmid DNA into the TA (50 μg) and GAS (50 μg), of a 5 month old male C57 black mouse, with electroporation at 100v during injection. TA and GAS muscles were harvested after 1 week and tissue was fixed and prepared as above.

Imaging and Quantification

Confocal imaging was performed on an Olympus FV500 and on a Olympus FV1000 (Melville, NY). Live cell time-lapse imaging was conducted on a Nikon TE 2000 (Melville, NY) inverted microscope. Live cell confocal experiments were performed on the same microscope equipped with a Perkin Elmer spinning disk confocal. TIR-FM experiments were also conducted on the Nikon TE-2000 microscope with a 60x 1.45 NA objective. FRAP and photoactivation experiments were performed on the Olympus FV1000 inverted microscope. Photoactivation and FRAP experiments were conducted with a SIM scanner to acquire images at the 488 nm wavelength while activating or bleaching at 405 nm.

When quantifying β-sarcoglycan and δ-sarcoglycan, in each condition the protein quantified was the first labeled, and the Cy 3 secondary fluorochrome was used in each condition. α-sarcoglycan-EGFP was imaged as is. All imaging conditions, including laser power, photomultiplier tube and offset settings remained constant for each comparison set. Each comparison set was also conducted during the same imaging period on an Olympus FV1000 microscope (Mellville, NY). 12 cells which appeared to have a representative level of protein expression were selected for quantification in each condition. Quantification was conducted using Metamorph software (Molecular devices, Sunnyvale, CA). Membrane regions were

defined by saturating the signal within the cell till the outline of the cell could be clearly

delineated. The defined membrane regions were then applied to the original unaltered

microscope image and the average grey intensity within the region was recorded. Comparisons

were made only within a protein group and not between proteins.

Images were collected and analyzed using Meta Morph (Molecular Devices, Universal imaging

corporation) and simple PCI software (C-Imaging). Quantification was conducted by defining

regions (as stated in figures) and comparing average fluorescence intensities within regions

(MetaMorph, Molecular Devices, Sunnyvale, Ca). In cases where two monoclonal antibodies

were used, only the signal from the monoclonal antibody administered on the cells first was

quantified. All imaging conditions remained constant when comparisons were made. Data

analysis was carried out with Microsoft excel, and averaged results are expressed as mean +/-

SEM (where applicable). Student's t-test was used to compare means.

Immunohistochemistry

All immunohistochemistry was done as follows: Sections and cells were fixed in 2%

paraformaldehyde for 20minutes. Cells were permeablized for 20 minutes using .01% triton X-

100. Sections and cells were then washed 3 times with PBS, followed by 3 times with BSA, and

blocked in 2% BSA or 5% goat serum (diluted in BSA) for at least 45 minutes. They were then

incubated with the appropriate primary antibody for at least 1 hour. The following primary

antibodies were used: Monoclonal α-sarcoglycan (1:100, Nova Castra, Newcastle upon tyne,

UK), m α γ-sarcoglycan (1:100, Nova Castra), m α δ-sarcoglycan (1:50, Nova Castra), m α γ-

sarcoglycan (1:100, Nova Castra), mαBDystro(1:100, Nova Castra labs), Rhodamine/488

Phalloidin (1:250, Molecular Probes, Eugene, OR), rbαEGFP (1:200, Abcam), RbαDys22/23 (Xiao, X. lab, University of Pittsburgh). mαAP-1 (1:250, BD, Franklin lakes, NJ), RbαGiantin (1:400, O. Weisz), mαLAMP-1 (1:25, L. Traub), mαclathrin heavy chain x-22(1:10, L. Traub), mαTf-R (1:25, Cygnus, Southport, NC), mαCalnexin (1:1000, R. Frizzell), mαMHC-1 (1:10, R. Salter). Monoclonal antibodies were used on mouse tissue with a mouse on mouse kit (Vector labs, Burlingame, CA). Two monoclonal were used in succession on the same cells utilizing Fab-1 fragments. In this case appropriate controls were conducted to ensure that our results do not reflect the non-specific binding of the secondary from the second mouse antibody to the first mouse antibody (unpublished data). Sections and cells were then washed 3 times in BSA and incubated with the appropriate Secondary antibodies for 1 hour. Secondaries were Alexa 488, Alexa 564 and Alexa Cy5 (Molecular Probes, Eugene, OR). Sections and cells were then washed 3 times with BSA, followed by 3 times in PBS and stained with a nuclear Hoecht dye (watkins lab). Then they were washed 3 last time in PBS and coverslips were applied using gelvatol mounting media.

Western Blot

293 cells were transfected with the indicated genes and scraped with RIPA buffer 24 hours later. C2C12 cells were scraped at indicated time points. Proteins were resolved by SDS-PAGE on a 8-10% polyacrylamide gel. The proteins were transferred to nitrocellulose membranes (Millipore, Bedford MA) for 1 hour 15 minutes at 110 volts. Membranes were then blocked for overnight (at 4°C) in TTBS containing 5% dehydrated non-fat milk. The blots were then incubated with the indicated primary antibodies (diluted in TTBS containing 1% dehydrated non-fat milk), for at least 1 hour on a shaker. Membranes were then given 3 x 15 minute washes in

123

TTBS and incubated with the appropriate secondary antibody conjugated with HRP (diluted in TTBS with 1% milk), for 1 hour on a shaker. The membranes were given 3 final washes in TTBS (15 minutes each) and visualized with enhanced chemilluminescence, with a 30 second exposure to film (Kodak).

Immunoprecipitations

 Skeletal muscle lysates were incubate with approximately 2 μg of a polyclonal minidystrophin antibody (Xiao lab, University of Pittsburgh). 293 cells were transfected as described and lysates were scraped with RIPA buffer and incubated with 2ug of either a mαβ-dystroglycan antibody (NCL), m α β-sarcoglycan antibody (Nova Castra labs), mαδ- (Nova Castra labs), or RbαDys (Xiao lab). Antibodies were then precipitated using 70μl Protein A (Repligen) and Protein G beads (Sigma), and pellets were subjected to western blotting using antibodies against either mαβ-dystroglycan (NCL), rbαβ-dystroglycan (a generous gift from Mornet lab)(Royuela *et al*., 2003), or rbαEGFP (abcam). Total cell lysate loaded in amounted to approximately 30μg, which was about 4% of the lysate used for the co-immunoprecipitation.

Site directed mutagenesis

All point mutations were conducted on the 3849-EGFP-N1 template using Quick change system (Stratagene). The following mutations were made by PCR:

C433Y-(5'-CCTAAATTCAAGATGGGAATACCTCAGGGTAGCTAGC-3')

C952Y-(5'-ACGAGACTCAAACAACTTACTGGGACCATCCCAAA-3')

C990R-(5'-GCAGAAGGCCCTTCGCTTGGATCTCTTGAGC-3')

C1183F-(5'-CCAAGCATCAGGCCAAATTTAACATCTGCAAAGAGTG-3')

C1207Y-(5'-GCACTTTAATTATGACATCTACCAAAGCTGCTTTTTTTCTGGTCG-3')

C1207S-(5'-GCACTTTAATTATGACATCTCCCAAAGCTGCTTTTTTTCTGGTCG-3')

C1210S-(5'-GACATCTGCCAAAGCTCCTTTTTTTCTGGTCGAGTTGC-3)

C1210Y-(5'- CATCTGCCAAAGCTACTTTTTTTCTGGTCGAGTTG-3')

DNA was sequenced by genewiz (Brunswick, NJ).

The PA-α-sarcoglycan-EGFP was made by conducting quik change mutagenesis (Stratagene, La Jolla, CA) on α-sarcoglycan-EGFP. A T204H mutation was made using forward primer:

5'-CCACTACCTGAGCCACCAGTCCGCCCTGAGC-3',

and reverse primer 5'-GCTCAGGGCGGACTGGTGGCTCAGGTAGTGG-3'.

L64F and a T65S mutations were both made using forward primer:

5'-CCTCGTGACCACCTTCAGCTACGGCGTGCAGTGC-3',

and reverse primer 5'-GCACTGCACGCCGTAGCTGAAGGTGGTCACGAGG-3'.

Mutations were confirmed by sequencing (Genewiz).

The R77C mutant was made by conducting quik change mutagenesis on α-sarcoglycan-EGFP. The mutation was made using forward primer:

5'-GCCCCGGTGGCTCTGCTACACCCAGCG-3',

and reverse primer 5'-CGCTGGGTGTAGCAGAGCCACCGGGGC-3'.

These mutations were also confirmed by sequencing (Genewiz).

DiI experiment

293 cells were transfected with α-sarcoglycan-EGFP. 24 hours after transfection cells were loaded with CM-DiI (ex553/em570 Molecular Probes, Eugene, OR) at 1ug/ml. Cells were

incubated with DiI at 4 $^{\circ}$C for 1hour. Cells were then washed with media and imaged live at 37°C, or fixed and imaged by confocal.

Pressure washing

The pressure washing procedure described here was done by squirting away 293 cells transfected with α-sarcoglycan-EGFP using a pipetter and media. Disattached cells were then aspirated and membrane remains that remained adherent to the coverslip were subjected to immunohistochemistry and imaged.

Uptake assays

For the transferrin uptake assay, Hela cells transfected with α-sarcoglycan-EGFP were serum starved in DMEM without antibiotics or serum for 1hr. Cells were then incubated at 4 $^{\circ}$C with transferrin conjugated to Alexa 568 (Molecular Probes, Eugene, OR) for 1hr at a final concentration of 50ug/ml. Cells were then washed with cold media and warmed to 37 $^{\circ}$C while simultaneously being imaged to capture immediate internalization/endocytic events.

For the α-sarcoglycan Ab internalization assay, 293 cells were transfected with α-sarcoglycan-EGFP. These cells were then incubated with a monoclonal α-sarcoglycan Ab (1:100, Nova castra labs), which recognizes an extracellular domain of the α-sarcoglycan protein. Unpermeablized cells were labeled for 1hr at 4 $^{\circ}$C to selectively label the α-sarcoglycan-EGFP on the membrane. Cells were then transferred to 37 $^{\circ}$C for periods of 20, 40 and 60 minutes, to induce internalization of the antibody. Cells were fixed at these different time points and the α-sarcoglycan ab was visualized using a Cy3 secondary antibody (Molecular Probes).

Drug treatments

Latrunculin A treatment

To determine the appropriate concentration of Latrunculin A (Sigma) to use, dilutions of Latrunculin A ranging from 0.25 μg/ml to 16 μl/ml were tested on 293 and C57 cells at about 80% confluency. Cells were exposed for different time intervals and then fixed and stained for actin. Cell morphology and actin disruption were used as criteria to determine that 0.5 μg/ml is the appropriate concentration to use. This was administered to transfected 293 cells for 5 minutes. Cells were then fixed using 2% paraformaldehyde, and stained for actin (phalloidin, molecular probes).

Nocodazole treatment

To depolymerize microtubules, 293 cells co-transfected with the α-sarcoglycan-EGFP and CLC-DsRed, were incubated with 10μm nocodazole (Sigma, St. Louis, MO) while being imaged live.

Cycloheximide treatment

To inhibit protein synthesis, 293 cells transfected with the α-sarcoglycan-EGFP were incubated 24 hrs after transfection with cycloheximide (Sigma) at a concentration of 50ug/ml, for approximately 2 hrs. Cells were then fixed with 2% paraformaldehyde and imaged.

Brefeldin-A

To disrupt the Golgi, 293 cells co-transfected with the indicated combinations of sarcoglycans were treated with Brefeldin-A at a concentration of 10 mg/ml (O. Weisz). 293 cells were incubated with the Brefeldin-A for approximately 40 minutes after which the cells were fixed for 20 minutes with 2% paraformaldehyde.

APPENDIX B

ABBREVIATIONS

AAV- Adeno-associated virus
AP- Adaptor protein
ATP- Adenosine tri phosphate

BFA- Brefeldin-A
BMD- Becker muscular dystrophy
BSA- Bovine Serum Albumin

CBI- Center for Biologic Imaging
CFTR- Cystic fibrosis transmembrane receptor
CHC- Clathrin heavy chain
CHO- Chinese hamster ovary
CLC- Clathrin light chain
CMV- Cytomegalovirus
CR- Cysteine Rich

DAG- Dystrophin associated glycoprotein
DAP- Dystrophin associated proteins
DIC- Differential interference contrast
DMD- Duchenne Muscular Dystrophy
DMEM- Dulbecco's modified eagle's medium
DPC- Dystrophin protein complex
DsRed- Discosoma red

EGFP- Enhanced green fluorescent protein

FBS- Fetal bovine serum
FRAP- Fluorescence recovery after photobleaching

GAS- Gastrocnemius
GFP- Green fluorescent protein
GRMD- Golden retriever muscular dystrophy

HEK- Human embryonic kidney

LAMP- Lysosomal associated membrane protein
LGMD- Limb Girdle Muscular Dystrophy

MD- Muscular Dystrophy
MHC- Major Histocompatability complex

NA- Numerical appature
NLS- Nuclear localization signal

PA-GFP- Photo activatable GFP
PBS- Phosphate buffered saline
PCR- Polymerase chain reaction
PMSF- Phenylmethylsulphonylfluoride
P/S- Penicillin/Streptomycin

RIPA- Radioimmunoprecipitation

SCARMD- Severe childhood autosomal recessive muscular dystrophy

TA- Tibialis anterior
Tf-R- Transferrin receptor
TIR-FM- Total internal reflectance fluorescence microscopy
TTBS- Tween tris buffer solution

APPENDIX C

MICROSCOPY TECHNIQUES

Live cell microscopy

Static imaging has given us a unique perspective on how proteins behave inside cells. However, in order to truly understand the dynamic nature of protein behavior, it is vital to observe these proteins in real time in living cells. Although, live cell imaging has been conducted in a wide variety of scientific studies through the 1990's, it has not been implemented to study the proteins of the DPC. In order to gain a deeper understanding of the kinetics of dystrophin and sarcoglycan trafficking, live cell imaging is the ideal tool.

There are a few major considerations and limitations to take into account in the development of a live cell imaging model. Firstly, there has to be a signal to image. With the advent of GFP technology, it is possible to track proteins in live cells through the creation of fusion genes. Importantly, one has to ensure that the addition of the GFP tag does not radically alter the normal behavior and localization of the protein of interest. This is the major limitation in the utilization of genetically encoded protein tags. Since the GFP tagged minidystrophin and sarcoglycan constructs used in this dissertation did not show any alteration in function, this was an ideal detection method. The second consideration is the event that is being captured. This goes hand in hand with the third consideration, which is the viability of the sample being imaged. When imaging events that are very dynamic, such as vesicle motility, the sample needs to be exposed to light more frequently. The limitation to this dynamic, rapid imaging is that it in turn may damage or photobleach the sample, or even kill the cell. When the event being imaged is

less dynamic, like the translocation of a protein over the time course of hours, rather than minutes or seconds, the sample can be exposed to light less frequently. This keeps the sample viable for much longer periods of time. However, in turn, all the transition steps that may be taking place are not captured. In order to image the translocation of minidystrophin-EGFP or α-sarcoglycan-EGFP, I was able to image the samples over the time course of several hours, by exposing the cells to low levels of light every few minutes. This in turn allowed the visualization of dystrophin and sarcoglycan translocation kinetics in living cells.

Another consideration in live cell imaging is the focal plane that needs to be imaged. When determining co-localization between two proteins, it is essential that the out of focus planes are eliminated. This is easily done through laser scanning confocal microscopes. The limitation of laser based systems however, is the intense laser light, which rapidly kills the cells. Additionally, the scanning of the laser across the field takes some time, which is not ideal for dynamic live cell events. These issues have been somewhat overcome through the development of light based confocal technologies such as spinning disk confocal systems.

Spinning disk confocal

In spinning disk confocal systems, the excitation light, via a regular bulb source, is split into multiple foci. This is done via a disk with small holes at regulated spaces. The data from the multiple foci are then collected rapidly with a CCD camera (204). Spinning disk systems can achieve speeds of 360 frames a second, however the sensitivity and acquisition depend on a large part on the quality and readout time of the detector (camera) (204).

Although the spinning disk technology is a good solution for live cell imaging of bright specimens, the regular light source is often insufficient for data collection from dimmer signals.

Because the signal in these systems cannot be amplified by either increasing the laser power, or adjusting the photomultiplier tube settings, imaging using spinning disks is limited. For my applications, the signals were generated from bright genetically encoded tags (DsRed and EGFP). Additionally, the event of α-sarcoglycan positive clathrin coated vesicle motility was rapid. For these reasons spinning disk confocal was a suitable live cell imaging method.

Due to the lack of a laser, it is inherently impossible to conduct some laser based imaging applications on microscopes equipped with a spinning disk. Therefore, in some instances live cell imaging had to be done via a regular single photon laser scanning confocal microscope.

Fluorescence recovery after photobleaching (FRAP) and photoactivation

Point scanning laser confocal microscopes have the unique ability to selectively illuminate a defined region of a sample. This, combined with the rapid diffusion and motility of EGFP tagged proteins in live cells, can be exploited to selectively photobleach regions within a cell, and then measure the time it takes for the fluorescence within the region, to recover.

We implemented this technique to determine if the α-sarcoglycan-EGFP fluorescence at the plasma membrane was being replenished. The data presented also demonstrates that intracellular α-sarcoglycan-EGFP vesicles dock at the photobleached regions of the plasma membrane. As FRAP experiment require a laser source, great care must be taken as not to damage the sample being imaged.

GFP variants, containing specific mutations, can also be activated using laser based point scanning systems. These constructs show greatly enhanced fluorescence emission following activation at about 405nm (118). Therefore, selective labeling of subdomains of cells and organelles may be achieved (204). This was especially useful when I aimed at selectively

highlighting specific intracellular regions of α-sarcoglycan-EGFP, and then tracking its movement. For these experiments the photoactivation of α-sarcoglycan-EGFP using a laser point scanning confocal, was combined with total internal reflection fluorescence microscopy.

Total internal reflection fluorescence microscopy (TIR-FM)

This technique has been previously described in the introduction of this dissertation.

Because TIR-FM can be used to monitor events close to the cell surface, it was the ideal method for us to monitor vesicle motility of the DPC proteins.

It should be noted however that the evanescent field created by TIR-FM (approx. 150nm), substantially exceeds the thickness of the actual plasma membrane, which is approximately 7-10nm. Therefore, care and skill is in order to avoid over interpretation of data generated by TIR-FM. Some other drawbacks to TIR-FM systems, is that it is extremely technically demanding, and requires state of the art equipment.

BIBLIOGRAPHY

1. Emery, A., Muntoni F (2003) Duchenne muscular dystrophy. *Oxford University Press, New York*.

2. Meryon, E. (1852) On granular and fatty degeneration of the voluntary muscles. . *Medico-Chirurgical Transactions (London),* **35,** 73-84.

3. Becker, P.E., Kiener F (1955) Eine neu X-chromosomale Muskeldystrophie. *Archiv Fur Psychiatric und Nervenkrankheiten,* **193,** 427-448.

4. Becker, P.E. (1962) Two families of benign sex-linked recessive muscular dystrophy. *Rev Can Biol,* **21,** 551-66.

5. Emery, A.E. (2002) The muscular dystrophies. *Lancet,* **359,** 687-95.

6. Gowers, W.R. (1879) Psuedo-hypertrophic muscular paralysis- a clinical lecture. *J. and A. Churchill, london*.

7. van Ommen, G.J. and Scheuerbrandt, G. (1993) Neonatal screening for muscular dystrophy. Consensus recommendation of the 14th workshop sponsored by the European Neuromuscular Center (ENMC). *Neuromuscul Disord,* **3,** 231-9.

8. Draviam, R., Billington, L., Senchak, A., Hoffman, E.P. and Watkins, S.C. (2001) Confocal analysis of the dystrophin protein complex in muscular dystrophy. *Muscle Nerve,* **24,** 262-72.

9. Emery, A.E. (1991) Population frequencies of inherited neuromuscular diseases--a world survey. *Neuromuscul Disord,* **1,** 19-29.

10. Davies, K.E., Pearson, P.L., Harper, P.S., Murray, J.M., O'Brien, T., Sarfarazi, M. and Williamson, R. (1983) Linkage analysis of two cloned DNA sequences flanking the Duchenne muscular dystrophy locus on the short arm of the human X chromosome. *Nucleic Acids Res,* **11,** 2303-12.

11. Koenig, M., Hoffman, E.P., Bertelson, C.J., Monaco, A.P., Feener, C. and Kunkel, L.M. (1987) Complete cloning of the Duchenne muscular dystrophy (DMD) cDNA and preliminary genomic organization of the DMD gene in normal and affected individuals. *Cell,* **50,** 509-17.

12.   Hoffman, E.P., Monaco, A.P., Feener, C.C. and Kunkel, L.M. (1987) Conservation of the Duchenne muscular dystrophy gene in mice and humans. *Science,* **238,** 347-50.

13.   Hoffman, E.P., Brown, R.H., Jr. and Kunkel, L.M. (1987) Dystrophin: the protein product of the Duchenne muscular dystrophy locus. *Cell,* **51,** 919-28.

14.   Muntoni, F., Torelli, S. and Ferlini, A. (2003) Dystrophin and mutations: one gene, several proteins, multiple phenotypes. *Lancet Neurol,* **2,** 731-40.

15.   Sadoulet-Puccio, H.M. and Kunkel, L.M. (1996) Dystrophin and its isoforms. *Brain Pathol,* **6,** 25-35.

16.   Arahata, K., Ishiura, S., Ishiguro, T., Tsukahara, T., Suhara, Y., Eguchi, C., Ishihara, T., Nonaka, I., Ozawa, E. and Sugita, H. (1988) Immunostaining of skeletal and cardiac muscle surface membrane with antibody against Duchenne muscular dystrophy peptide. *Nature,* **333,** 861-3.

17.   Hoffman, E.P., Fischbeck, K.H., Brown, R.H., Johnson, M., Medori, R., Loike, J.D., Harris, J.B., Waterston, R., Brooke, M., Specht, L. *et al.* (1988) Characterization of dystrophin in muscle-biopsy specimens from patients with Duchenne's or Becker's muscular dystrophy. *N Engl J Med,* **318,** 1363-8.

18.   Watkins, S.C., Hoffman, E.P., Slayter, H.S. and Kunkel, L.M. (1988) Immunoelectron microscopic localization of dystrophin in myofibres. *Nature,* **333,** 863-6.

19.   Zubrzycka-Gaarn, E.E., Bulman, D.E., Karpati, G., Burghes, A.H., Belfall, B., Klamut, H.J., Talbot, J., Hodges, R.S., Ray, P.N. and Worton, R.G. (1988) The Duchenne muscular dystrophy gene product is localized in sarcolemma of human skeletal muscle. *Nature,* **333,** 466-9.

20.   Campbell, K.P. and Kahl, S.D. (1989) Association of dystrophin and an integral membrane glycoprotein. *Nature,* **338,** 259-62.

21.   Kloepfer, H.W. and Talley, C. (1958) Autosomal recessive inheritance of Duchennetype muscular dystrophy. *Ann Hum Genet,* **22,** 138-43.

22.   Buss, O. (1887) Zur Lehre von der Dystrophia muscularis progressive. *Berl Klin Wochnschr*, 49-53.

23.   Ozawa, E., Noguchi, S., Mizuno, Y., Hagiwara, Y. and Yoshida, M. (1998) From dystrophinopathy to sarcoglycanopathy: evolution of a concept of muscular dystrophy. *Muscle Nerve,* **21,** 421-38.

24.   Ben Hamida, M., Fardeau, M. and Attia, N. (1983) Severe childhood muscular dystrophy affecting both sexes and frequent in Tunisia. *Muscle Nerve,* **6,** 469-80.

25. Salih, M.A., Omer, M.I., Bayoumi, R.A., Karrar, O. and Johnson, M. (1983) Severe autosomal recessive muscular dystrophy in an extended Sudanese kindred. *Dev Med Child Neurol,* **25,** 43-52.

26. Somer, H., Voutilainen, A., Knuutila, S., Kaitila, I., Rapola, J. and Leinonen, H. (1985) Duchenne-like muscular dystrophy in two sisters with normal karyotypes: evidence for autosomal recessive inheritance. *Clin Genet,* **28,** 151-6.

27. Minkowski, M., Sidler A (1928) Zur Kenntnis der Dystrophia Musculorum Progresiva und ihrer Verebung. *Schweiz Med Wochenschr,* **9,** 1005-1009.

28. Miyoshi, K. (1944) Erbbiologische und klinische Studien uber die Dystrophia musculorum progressive (text in Japanese with German title). *Jpn J Psychiatry Neurol,* **48,** 116-127, 260-273, 351-385.

29. Dubowitz, V. (1960) Progressive muscular dystrophy of the Duchenne type in females and its mode of inheritance. *Brain,* **83,** 432-9.

30. Jackson, C.E. and Carey, J.H. (1961) Progressive muscular dystrophy: autosomal recessive type. *Pediatrics,* **28,** 77-84.

31. Jackson, C.E. and Strehler, D.A. (1968) Limb-girdle muscular dystrophy: clinical manifestations and detection of preclinical disease. *Pediatrics,* **41,** 495-502.

32. Miyoshi, K. (1967) Hereditary traits in muscular dystrophy (text in Japanese), in Proceedings of the 17th Japan Medical Association. *Japn. Med. Ass. Eds. Toyoko,* **4,** 1070-1081.

33. Miyoshi, K., Tada Y, Nakano M, Kawai H (1974) Malignant Limb-girdle muscular dystrophy (in Japanese), in Official Report of the National Muscular Dystrophy Research Team. *Okinaka, S. ed. Toyoko,* **2,** 39-49.

34. Laval, S.H. and Bushby, K.M. (2004) Limb-girdle muscular dystrophies--from genetics to molecular pathology. *Neuropathol Appl Neurobiol,* **30,** 91-105.

35. Bonnemann, C.G., Modi, R., Noguchi, S., Mizuno, Y., Yoshida, M., Gussoni, E., McNally, E.M., Duggan, D.J., Angelini, C. and Hoffman, E.P. (1995) Beta-sarcoglycan (A3b) mutations cause autosomal recessive muscular dystrophy with loss of the sarcoglycan complex. *Nat Genet,* **11,** 266-73.

36. Nigro, V., de Sa Moreira, E., Piluso, G., Vainzof, M., Belsito, A., Politano, L., Puca, A.A., Passos-Bueno, M.R. and Zatz, M. (1996) Autosomal recessive limb-girdle muscular dystrophy, LGMD2F, is caused by a mutation in the delta-sarcoglycan gene. *Nat Genet,* **14,** 195-8.

37. Noguchi, S., McNally, E.M., Ben Othmane, K., Hagiwara, Y., Mizuno, Y., Yoshida, M., Yamamoto, H., Bonnemann, C.G., Gussoni, E., Denton, P.H. *et al.* (1995) Mutations in the dystrophin-associated protein gamma-sarcoglycan in chromosome 13 muscular dystrophy. *Science,* **270,** 819-22.

38. Roberds, S.L., Leturcq, F., Allamand, V., Piccolo, F., Jeanpierre, M., Anderson, R.D., Lim, L.E., Lee, J.C., Tome, F.M., Romero, N.B. *et al.* (1994) Missense mutations in the adhalin gene linked to autosomal recessive muscular dystrophy. *Cell,* **78,** 625-33.

39. Bushby, K.M. (1999) The limb-girdle muscular dystrophies-multiple genes, multiple mechanisms. *Hum Mol Genet,* **8,** 1875-82.

40. Ervasti, J.M. and Campbell, K.P. (1991) Membrane organization of the dystrophin-glycoprotein complex. *Cell,* **66,** 1121-31.

41. Hack, A.A., Groh, M.E. and McNally, E.M. (2000) Sarcoglycans in muscular dystrophy. *Microsc Res Tech,* **48,** 167-80.

42. Yoshida, M. and Ozawa, E. (1990) Glycoprotein complex anchoring dystrophin to sarcolemma. *J Biochem (Tokyo),* **108,** 748-52.

43. Yoshida, M., Suzuki, A., Yamamoto, H., Noguchi, S., Mizuno, Y. and Ozawa, E. (1994) Dissociation of the complex of dystrophin and its associated proteins into several unique groups by n-octyl beta-D-glucoside. *Eur J Biochem,* **222,** 1055-61.

44. Mizuno, Y., Yoshida, M., Yamamoto, H., Hirai, S. and Ozawa, E. (1993) Distribution of dystrophin isoforms and dystrophin-associated proteins 43DAG (A3a) and 50DAG (A2) in various monkey tissues. *J Biochem (Tokyo),* **114,** 936-41.

45. Yamamoto, H., Mizuno, Y., Hayashi, K., Nonaka, I., Yoshida, M. and Ozawa, E. (1994) Expression of dystrophin-associated protein 35DAG (A4) and 50DAG (A2) is confined to striated muscles. *J Biochem (Tokyo),* **115,** 162-7.

46. Holt, K.H. and Campbell, K.P. (1998) Assembly of the sarcoglycan complex. Insights for muscular dystrophy. *J Biol Chem,* **273,** 34667-70.

47. Chan, Y.M., Bonnemann, C.G., Lidov, H.G. and Kunkel, L.M. (1998) Molecular organization of sarcoglycan complex in mouse myotubes in culture. *J Cell Biol,* **143,** 2033-44.

48. Beckmann, J.S. (1996) Genetic studies and molecular structures: the dystrophin associated complex. *Hum Mol Genet,* **5,** 865-7.

49. Mizuno, Y., Noguchi, S., Yamamoto, H., Yoshida, M., Nonaka, I., Hirai, S. and Ozawa, E. (1995) Sarcoglycan complex is selectively lost in dystrophic hamster muscle. *Am J Pathol,* **146,** 530-6.

50. Mizuno, Y., Noguchi, S., Yamamoto, H., Yoshida, M., Suzuki, A., Hagiwara, Y., Hayashi, Y.K., Arahata, K., Nonaka, I., Hirai, S. *et al.* (1994) Selective defect of sarcoglycan complex in severe childhood autosomal recessive muscular dystrophy muscle. *Biochem Biophys Res Commun,* **203,** 979-83.

51. Roberds, S.L., Anderson, R.D., Ibraghimov-Beskrovnaya, O. and Campbell, K.P. (1993) Primary structure and muscle-specific expression of the 50-kDa dystrophin-associated glycoprotein (adhalin). *J Biol Chem,* **268,** 23739-42.

52. Dickens, N.J., Beatson, S. and Ponting, C.P. (2002) Cadherin-like domains in alpha-dystroglycan, alpha/epsilon-sarcoglycan and yeast and bacterial proteins. *Curr Biol,* **12,** R197-9.

53. Ozawa, E., Mizuno, Y., Hagiwara, Y., Sasaoka, T. and Yoshida, M. (2005) Molecular and cell biology of the sarcoglycan complex. *Muscle Nerve,* **32,** 563-76.

54. McNally, E.M., Yoshida, M., Mizuno, Y., Ozawa, E. and Kunkel, L.M. (1994) Human adhalin is alternatively spliced and the gene is located on chromosome 17q21. *Proc Natl Acad Sci U S A,* **91,** 9690-4.

55. Fanin, M., Duggan, D.J., Mostacciuolo, M.L., Martinello, F., Freda, M.P., Soraru, G., Trevisan, C.P., Hoffman, E.P. and Angelini, C. (1997) Genetic epidemiology of muscular dystrophies resulting from sarcoglycan gene mutations. *J Med Genet,* **34,** 973-7.

56. Vainzof, M., Passos-Bueno, M.R., Pavanello, R.C., Marie, S.K., Oliveira, A.S. and Zatz, M. (1999) Sarcoglycanopathies are responsible for 68% of severe autosomal recessive limb-girdle muscular dystrophy in the Brazilian population. *J Neurol Sci,* **164,** 44-9.

57. Carrie, A., Piccolo, F., Leturcq, F., de Toma, C., Azibi, K., Beldjord, C., Vallat, J.M., Merlini, L., Voit, T., Sewry, C. *et al.* (1997) Mutational diversity and hot spots in the alpha-sarcoglycan gene in autosomal recessive muscular dystrophy (LGMD2D). *J Med Genet,* **34,** 470-5.

58. Duggan, D.J., Gorospe, J.R., Fanin, M., Hoffman, E.P. and Angelini, C. (1997) Mutations in the sarcoglycan genes in patients with myopathy. *N Engl J Med,* **336,** 618-24.

59. Eymard, B., Romero, N.B., Leturcq, F., Piccolo, F., Carrie, A., Jeanpierre, M., Collin, H., Deburgrave, N., Azibi, K., Chaouch, M. *et al.* (1997) Primary adhalinopathy (alpha-sarcoglycanopathy): clinical, pathologic, and genetic correlation in 20 patients with autosomal recessive muscular dystrophy. *Neurology,* **48,** 1227-34.

60. Kawai, H., Akaike, M., Endo, T., Adachi, K., Inui, T., Mitsui, T., Kashiwagi, S., Fujiwara, T., Okuno, S., Shin, S. *et al.* (1995) Adhalin gene mutations in patients with autosomal recessive childhood onset muscular dystrophy with adhalin deficiency. *J Clin Invest,* **96,** 1202-7.

61. Piccolo, F., Roberds, S.L., Jeanpierre, M., Leturcq, F., Azibi, K., Beldjord, C., Carrie, A., Recan, D., Chaouch, M., Reghis, A. *et al.* (1995) Primary adhalinopathy: a common cause of autosomal recessive muscular dystrophy of variable severity. *Nat Genet,* **10,** 243-5.

62. Hackman, P., Juvonen, V., Sarparanta, J., Penttinen, M., Aarimaa, T., Uusitalo, M., Auranen, M., Pihko, H., Alen, R., Junes, M. *et al.* (2005) Enrichment of the R77C alpha-sarcoglycan gene mutation in Finnish LGMD2D patients. *Muscle Nerve,* **31,** 199-204.

63. Betto, R., Senter, L., Ceoldo, S., Tarricone, E., Biral, D. and Salviati, G. (1999) Ecto-ATPase activity of alpha-sarcoglycan (adhalin). *J Biol Chem,* **274,** 7907-12.

64. Sandona, D., Gastaldello, S., Martinello, T. and Betto, R. (2004) Characterization of the ATP-hydrolysing activity of alpha-sarcoglycan. *Biochem J,* **381,** 105-12.

65. Lim, L.E., Duclos, F., Broux, O., Bourg, N., Sunada, Y., Allamand, V., Meyer, J., Richard, I., Moomaw, C., Slaughter, C. *et al.* (1995) Beta-sarcoglycan: characterization and role in limb-girdle muscular dystrophy linked to 4q12. *Nat Genet,* **11,** 257-65.

66. Fougerousse, F., Durand, M., Suel, L., Pourquie, O., Delezoide, A.L., Romero, N.B., Abitbol, M. and Beckmann, J.S. (1998) Expression of genes (CAPN3, SGCA, SGCB, and TTN) involved in progressive muscular dystrophies during early human development. *Genomics,* **48,** 145-56.

67. Bonnemann, C.G., Wong, J., Ben Hamida, C., Hamida, M.B., Hentati, F. and Kunkel, L.M. (1998) LGMD 2E in Tunisia is caused by a homozygous missense mutation in beta-sarcoglycan exon 3. *Neuromuscul Disord,* **8,** 193-7.

68. Noguchi, S., Wakabayashi-Takai, E., Sasaoka, T. and Ozawa, E. (2001) Analysis of the spatial, temporal and tissue-specific transcription of gamma-sarcoglycan gene using a transgenic mouse. *FEBS Lett,* **495,** 77-81.

69. Thompson, T.G., Chan, Y.M., Hack, A.A., Brosius, M., Rajala, M., Lidov, H.G., McNally, E.M., Watkins, S. and Kunkel, L.M. (2000) Filamin 2 (FLN2): A muscle-specific sarcoglycan interacting protein. *J Cell Biol,* **148,** 115-26.

70. Nigro, V., Piluso, G., Belsito, A., Politano, L., Puca, A.A., Papparella, S., Rossi, E., Viglietto, G., Esposito, M.G., Abbondanza, C. *et al.* (1996) Identification of a novel sarcoglycan gene at 5q33 encoding a sarcolemmal 35 kDa glycoprotein. *Hum Mol Genet,* **5,** 1179-86.

71. Higuchi, I., Kawai, H., Umaki, Y., Kawajiri, M., Adachi, K., Fukunaga, H., Nakagawa, M., Arimura, K. and Osame, M. (1998) Different manners of sarcoglycan expression in genetically proven alpha-sarcoglycan deficiency and gamma-sarcoglycan deficiency. *Acta Neuropathol (Berl),* **96,** 202-6.

72. Liu, L.A. and Engvall, E. (1999) Sarcoglycan isoforms in skeletal muscle. *J Biol Chem,* **274,** 38171-6.

73. Vainzof, M., Moreira, E.S., Canovas, M., Anderson, L.V., Pavanello, R.C., Passos-Bueno, M.R. and Zatz, M. (2000) Partial alpha-sarcoglycan deficiency with retention of the dystrophin-glycoprotein complex in a LGMD2D family. *Muscle Nerve,* **23,** 984-8.

74. Takano, A., Bonnemann, C.G., Honda, H., Sakai, M., Feener, C.A., Kunkel, L.M. and Sobue, G. (2000) Intrafamilial phenotypic variation in limb-girdle muscular dystrophy type 2C with compound heterozygous mutations. *Muscle Nerve,* **23,** 807-10.

75. Vorgerd, M., Gencik, M., Mortier, J., Epplen, J.T., Malin, J.P. and Mortier, W. (2001) Isolated loss of gamma-sarcoglycan: diagnostic implications in autosomal recessive limb-girdle muscular dystrophies. *Muscle Nerve,* **24,** 421-4.

76. Sakamoto, A., Ono, K., Abe, M., Jasmin, G., Eki, T., Murakami, Y., Masaki, T., Toyo-oka, T. and Hanaoka, F. (1997) Both hypertrophic and dilated cardiomyopathies are caused by mutation of the same gene, delta-sarcoglycan, in hamster: an animal model of disrupted dystrophin-associated glycoprotein complex. *Proc Natl Acad Sci U S A,* **94,** 13873-8.

77. Shi, W., Chen, Z., Schottenfeld, J., Stahl, R.C., Kunkel, L.M. and Chan, Y.M. (2004) Specific assembly pathway of sarcoglycans is dependent on beta- and delta-sarcoglycan. *Muscle Nerve,* **29,** 409-19.

78. Noguchi, S., Wakabayashi, E., Imamura, M., Yoshida, M. and Ozawa, E. (2000) Formation of sarcoglycan complex with differentiation in cultured myocytes. *Eur J Biochem,* **267,** 640-8.

79. Ervasti, J.M., Ohlendieck, K., Kahl, S.D., Gaver, M.G. and Campbell, K.P. (1990) Deficiency of a glycoprotein component of the dystrophin complex in dystrophic muscle. *Nature,* **345,** 315-9.

80. Cullen, M.J., Walsh, J., Roberds, S.L. and Campbell, K.P. (1996) Ultrastructural localization of adhalin, alpha-dystroglycan and merosin in normal and dystrophic muscle. *Neuropathol Appl Neurobiol,* **22,** 30-7.

81. Ervasti, J.M. and Campbell, K.P. (1993) A role for the dystrophin-glycoprotein complex as a transmembrane linker between laminin and actin. *J Cell Biol,* **122,** 809-23.

82. Ibraghimov-Beskrovnaya, O., Ervasti, J.M., Leveille, C.J., Slaughter, C.A., Sernett, S.W. and Campbell, K.P. (1992) Primary structure of dystrophin-associated glycoproteins linking dystrophin to the extracellular matrix. *Nature,* **355,** 696-702.

83.   Jung, D., Yang, B., Meyer, J., Chamberlain, J.S. and Campbell, K.P. (1995) Identification and characterization of the dystrophin anchoring site on beta-dystroglycan. *J Biol Chem,* **270,** 27305-10.

84.   Lakonishok, M., Muschler, J. and Horwitz, A.F. (1992) The alpha 5 beta 1 integrin associates with a dystrophin-containing lattice during muscle development. *Dev Biol,* **152,** 209-20.

85.   Ahn, A.H. and Kunkel, L.M. (1995) Syntrophin binds to an alternatively spliced exon of dystrophin. *J Cell Biol,* **128,** 363-71.

86.   Madhavan, R. and Jarrett, H.W. (1995) Interactions between dystrophin glycoprotein complex proteins. *Biochemistry,* **34,** 12204-9.

87.   Yang, B., Jung, D., Rafael, J.A., Chamberlain, J.S. and Campbell, K.P. (1995) Identification of alpha-syntrophin binding to syntrophin triplet, dystrophin, and utrophin. *J Biol Chem,* **270,** 4975-8.

88.   Henry, M.D. and Campbell, K.P. (1996) Dystroglycan: an extracellular matrix receptor linked to the cytoskeleton. *Curr Opin Cell Biol,* **8,** 625-31.

89.   Henry, M.D. and Campbell, K.P. (1999) Dystroglycan inside and out. *Curr Opin Cell Biol,* **11,** 602-7.

90.   Rentschler, S., Linn, H., Deininger, K., Bedford, M.T., Espanel, X. and Sudol, M. (1999) The WW domain of dystrophin requires EF-hands region to interact with beta-dystroglycan. *Biol Chem,* **380,** 431-42.

91.   Ishikawa-Sakurai, M., Yoshida, M., Imamura, M., Davies, K.E. and Ozawa, E. (2004) ZZ domain is essentially required for the physiological binding of dystrophin and utrophin to beta-dystroglycan. *Hum Mol Genet,* **13,** 693-702.

92.   Roses, A.D. (1990) Duchenne muscular dystrophy. In: Current Therapy in Neurologic Disease. *R.T. Johnson, Ed., B.C. Decker (Philadelphia)***,** 399-402.

93.   Snyder, R.O. and Flotte, T.R. (2002) Production of clinical-grade recombinant adeno-associated virus vectors. *Curr Opin Biotechnol,* **13,** 418-23.

94.   Flotte, T.R. (2005) Adeno-associated virus-based gene therapy for inherited disorders. *Pediatr Res,* **58,** 1143-7.

95.   Xiao, X., Li, J. and Samulski, R.J. (1996) Efficient long-term gene transfer into muscle tissue of immunocompetent mice by adeno-associated virus vector. *J Virol,* **70,** 8098-108.

96.   Kessler, P.D., Podsakoff, G.M., Chen, X., McQuiston, S.A., Colosi, P.C., Matelis, L.A., Kurtzman, G.J. and Byrne, B.J. (1996) Gene delivery to skeletal muscle results in

sustained expression and systemic delivery of a therapeutic protein. *Proc Natl Acad Sci US A,* **93,** 14082-7.

97.   Pruchnic, R., Cao, B., Peterson, Z.Q., Xiao, X., Li, J., Samulski, R.J., Epperly, M. and Huard, J. (2000) The use of adeno-associated virus to circumvent the maturation-dependent viral transduction of muscle fibers. *Hum Gene Ther,* **11,** 521-36.

98.   Greelish, J.P., Su, L.T., Lankford, E.B., Burkman, J.M., Chen, H., Konig, S.K., Mercier, I.M., Desjardins, P.R., Mitchell, M.A., Zheng, X.G. *et al.* (1999) Stable restoration of the sarcoglycan complex in dystrophic muscle perfused with histamine and a recombinant adeno-associated viral vector. *Nat Med,* **5,** 439-43.

99.   Xiao, X., Li, J., Tsao, Y.P., Dressman, D., Hoffman, E.P. and Watchko, J.F. (2000) Full functional rescue of a complete muscle (TA) in dystrophic hamsters by adeno-associated virus vector-directed gene therapy. *J Virol,* **74,** 1436-42.

100.   Cordier, L., Hack, A.A., Scott, M.O., Barton-Davis, E.R., Gao, G., Wilson, J.M., McNally, E.M. and Sweeney, H.L. (2000) Rescue of skeletal muscles of gamma-sarcoglycan-deficient mice with adeno-associated virus-mediated gene transfer. *Mol Ther,* **1,** 119-29.

101.   Dong, J.Y., Fan, P.D. and Frizzell, R.A. (1996) Quantitative analysis of the packaging capacity of recombinant adeno-associated virus. *Hum Gene Ther,* **7,** 2101-12.

102.   Sun, L., Li, J. and Xiao, X. (2000) Overcoming adeno-associated virus vector size limitation through viral DNA heterodimerization. *Nat Med,* **6,** 599-602.

103.   Duan, D., Yue, Y., Yan, Z. and Engelhardt, J.F. (2000) A new dual-vector approach to enhance recombinant adeno-associated virus-mediated gene expression through intermolecular cis activation. *Nat Med,* **6,** 595-8.

104.   Wang, B., Li, J. and Xiao, X. (2000) Adeno-associated virus vector carrying human minidystrophin genes effectively ameliorates muscular dystrophy in mdx mouse model. *Proc Natl Acad Sci U S A,* **97,** 13714-9.

105.   Coulton, G.R., Morgan, J.E., Partridge, T.A. and Sloper, J.C. (1988) The mdx mouse skeletal muscle myopathy: I. A histological, morphometric and biochemical investigation. *Neuropathol Appl Neurobiol,* **14,** 53-70.

106.   Tanabe, Y., Esaki, K. and Nomura, T. (1986) Skeletal muscle pathology in X chromosome-linked muscular dystrophy (mdx) mouse. *Acta Neuropathol (Berl),* **69,** 91-5.

107.   Angelini, C., Beggs, A.H., Hoffman, E.P., Fanin, M. and Kunkel, L.M. (1990) Enormous dystrophin in a patient with Becker muscular dystrophy. *Neurology,* **40,** 808-12.

108. England, S.B., Nicholson, L.V., Johnson, M.A., Forrest, S.M., Love, D.R., Zubrzycka-Gaarn, E.E., Bulman, D.E., Harris, J.B. and Davies, K.E. (1990) Very mild muscular dystrophy associated with the deletion of 46% of dystrophin. *Nature,* **343,** 180-2.

109. Deconinck, N., Ragot, T., Marechal, G., Perricaudet, M. and Gillis, J.M. (1996) Functional protection of dystrophic mouse (mdx) muscles after adenovirus-mediated transfer of a dystrophin minigene. *Proc Natl Acad Sci U S A,* **93,** 3570-4.

110. Prasher, D.C., Eckenrode, V.K., Ward, W.W., Prendergast, F.G. and Cormier, M.J. (1992) Primary structure of the Aequorea victoria green-fluorescent protein. *Gene,* **111,** 229-33.

111. Shimomura, O., Johnson, F.H. and Saiga, Y. (1962) Extraction, purification and properties of aequorin, a bioluminescent protein from the luminous hydromedusan, Aequorea. *J Cell Comp Physiol,* **59,** 223-39.

112. Chalfie, M., Tu, Y., Euskirchen, G., Ward, W.W. and Prasher, D.C. (1994) Green fluorescent protein as a marker for gene expression. *Science,* **263,** 802-5.

113. Zimmer, M. (2002) Green fluorescent protein (GFP): applications, structure, and related photophysical behavior. *Chem Rev,* **102,** 759-81.

114. Tsien, R.Y. (1998) The green fluorescent protein. *Annu Rev Biochem,* **67,** 509-44.

115. March, J.C., Rao, G. and Bentley, W.E. (2003) Biotechnological applications of green fluorescent protein. *Appl Microbiol Biotechnol,* **62,** 303-15.

116. Wahlfors, J., Loimas, S., Pasanen, T. and Hakkarainen, T. (2001) Green fluorescent protein (GFP) fusion constructs in gene therapy research. *Histochem Cell Biol,* **115,** 59-65.

117. Matz, M.V., Fradkov, A.F., Labas, Y.A., Savitsky, A.P., Zaraisky, A.G., Markelov, M.L. and Lukyanov, S.A. (1999) Fluorescent proteins from nonbioluminescent Anthozoa species. *Nat Biotechnol,* **17,** 969-73.

118. Patterson, G.H. and Lippincott-Schwartz, J. (2002) A photoactivatable GFP for selective photolabeling of proteins and cells. *Science,* **297,** 1873-7.

119. Chapdelaine, P., Moisset, P.A., Campeau, P., Asselin, I., Vilquin, J.T. and Tremblay, J.P. (2000) Functional EGFP-dystrophin fusion proteins for gene therapy vector development. *Protein Eng,* **13,** 611-5.

120. Axelrod, D. (1981) Cell-substrate contacts illuminated by total internal reflection fluorescence. *J Cell Biol,* **89,** 141-5.

121. Schneckenburger, H. (2005) Total internal reflection fluorescence microscopy: technical innovations and novel applications. *Curr Opin Biotechnol,* **16,** 13-8.

122. Betz, W.J., Mao, F. and Smith, C.B. (1996) Imaging exocytosis and endocytosis. *Curr Opin Neurobiol,* **6,** 365-71.

123. Oheim, M., Loerke, D., Stuhmer, W. and Chow, R.H. (1998) The last few milliseconds in the life of a secretory granule. Docking, dynamics and fusion visualized by total internal reflection fluorescence microscopy (TIRFM). *Eur Biophys J,* **27,** 83-98.

124. Kunkel, L.M., Hejtmancik, J.F., Caskey, C.T., Speer, A., Monaco, A.P., Middlesworth, W., Colletti, C.A., Bertelson, C., Muller, U., Bresnan, M. *et al.* (1986) Analysis of deletions in DNA from patients with Becker and Duchenne muscular dystrophy. *Nature,* **322,** 73-7.

125. Tuffery-Giraud, S., Chambert, S., Demaille, J. and Claustres, M. (1999) Point mutations in the dystrophin gene: evidence for frequent use of cryptic splice sites as a result of splicing defects. *Hum Mutat,* **14,** 359-68.

126. Kapsa, R., Kornberg, A.J. and Byrne, E. (2003) Novel therapies for Duchenne muscular dystrophy. *Lancet Neurol,* **2,** 299-310.

127. Andre, B. and Springael, J.Y. (1994) WWP, a new amino acid motif present in single or multiple copies in various proteins including dystrophin and the SH3-binding Yes-associated protein YAP65. *Biochem Biophys Res Commun,* **205,** 1201-5.

128. Bork, P. and Sudol, M. (1994) The WW domain: a signalling site in dystrophin? *Trends Biochem Sci,* **19,** 531-3.

129. Koenig, M., Monaco, A.P. and Kunkel, L.M. (1988) The complete sequence of dystrophin predicts a rod-shaped cytoskeletal protein. *Cell,* **53,** 219-26.

130. Ponting, C.P., Blake, D.J., Davies, K.E., Kendrick-Jones, J. and Winder, S.J. (1996) ZZ and TAZ: new putative zinc fingers in dystrophin and other proteins. *Trends Biochem Sci,* **21,** 11-13.

131. Kaplitt, M.G., Leone, P., Samulski, R.J., Xiao, X., Pfaff, D.W., O'Malley, K.L. and During, M.J. (1994) Long-term gene expression and phenotypic correction using adeno-associated virus vectors in the mammalian brain. *Nat Genet,* **8,** 148-54.

132. Muzyczka, N. (1992) Use of adeno-associated virus as a general transduction vector for mammalian cells. *Curr Top Microbiol Immunol,* **158,** 97-129.

133. Kay, M.A., Manno, C.S., Ragni, M.V., Larson, P.J., Couto, L.B., McClelland, A., Glader, B., Chew, A.J., Tai, S.J., Herzog, R.W. *et al.* (2000) Evidence for gene transfer and

expression of factor IX in haemophilia B patients treated with an AAV vector. *Nat Genet,* **24,** 257-61.

134.   Campeau, P., Chapdelaine, P., Seigneurin-Venin, S., Massie, B. and Tremblay, J.P. (2001) Transfection of large plasmids in primary human myoblasts. *Gene Ther,* **8,** 1387-94.

135.   Royuela, M., Chazalette, D., Hugon, G., Paniagua, R., Guerlavais, V., Fehrentz, J.A., Martinez, J., Labbe, J.P., Rivier, F. and Mornet, D. (2003) Formation of multiple complexes between beta-dystroglycan and dystrophin family products. *J Muscle Res Cell Motil,* **24,** 387-97.

136.   Brennan, P.A., Jing, J., Ethunandan, M. and Gorecki, D. (2004) Dystroglycan complex in cancer. *Eur J Surg Oncol,* **30,** 589-92.

137.   Radojevic, V., Lin, S. and Burgunder, J.M. (2000) Differential expression of dystrophin, utrophin, and dystrophin-associated proteins in human muscle culture. *Cell Tissue Res,* **300,** 447-57.

138.   Sgambato, A. and Brancaccio, A. (2005) The dystroglycan complex: from biology to cancer. *J Cell Physiol,* **205,** 163-9.

139.   Williamson, R.A., Henry, M.D., Daniels, K.J., Hrstka, R.F., Lee, J.C., Sunada, Y., Ibraghimov-Beskrovnaya, O. and Campbell, K.P. (1997) Dystroglycan is essential for early embryonic development: disruption of Reichert's membrane in Dag1-null mice. *Hum Mol Genet,* **6,** 831-41.

140.   Chen, Y.J., Spence, H.J., Cameron, J.M., Jess, T., Ilsley, J.L. and Winder, S.J. (2003) Direct interaction of beta-dystroglycan with F-actin. *Biochem J,* **375,** 329-37.

141.   Dunckley, M.G., Wells, K.E., Piper, T.A., Wells, D.J. and Dickson, G. (1994) Independent localization of dystrophin N- and C-terminal regions to the sarcolemma of mdx mouse myofibres in vivo. *J Cell Sci,* **107 (Pt 6),** 1469-75.

142.   Spector, I., Shochet, N.R., Kashman, Y. and Groweiss, A. (1983) Latrunculins: novel marine toxins that disrupt microfilament organization in cultured cells. *Science,* **219,** 493-5.

143.   Hoffman, E.P. and Kunkel, L.M. (1989) Dystrophin abnormalities in Duchenne/Becker muscular dystrophy. *Neuron,* **2,** 1019-29.

144.   Nicholson, L.V., Johnson, M.A., Gardner-Medwin, D., Bhattacharya, S. and Harris, J.B. (1990) Heterogeneity of dystrophin expression in patients with Duchenne and Becker muscular dystrophy. *Acta Neuropathol (Berl),* **80,** 239-50.

145. den Dunnen, J.T. (2004) Leiden muscular dystrophy pages. *Leiden university medical center*.

146. Fabb, S.A., Wells, D.J., Serpente, P. and Dickson, G. (2002) Adeno-associated virus vector gene transfer and sarcolemmal expression of a 144 kDa micro-dystrophin effectively restores the dystrophin-associated protein complex and inhibits myofibre degeneration in nude/mdx mice. *Hum Mol Genet,* **11,** 733-41.

147. Sakamoto, M., Yuasa, K., Yoshimura, M., Yokota, T., Ikemoto, T., Suzuki, M., Dickson, G., Miyagoe-Suzuki, Y. and Takeda, S. (2002) Micro-dystrophin cDNA ameliorates dystrophic phenotypes when introduced into mdx mice as a transgene. *Biochem Biophys Res Commun,* **293,** 1265-72.

148. Watchko, J., O'Day, T., Wang, B., Zhou, L., Tang, Y., Li, J. and Xiao, X. (2002) Adeno-associated virus vector-mediated minidystrophin gene therapy improves dystrophic muscle contractile function in mdx mice. *Hum Gene Ther,* **13,** 1451-60.

149. Cox, G.A., Sunada, Y., Campbell, K.P. and Chamberlain, J.S. (1994) Dp71 can restore the dystrophin-associated glycoprotein complex in muscle but fails to prevent dystrophy. *Nat Genet,* **8,** 333-9.

150. Decrouy, A., Renaud, J.M., Lunde, J.A., Dickson, G. and Jasmin, B.J. (1998) Mini- and full-length dystrophin gene transfer induces the recovery of nitric oxide synthase at the sarcolemma of mdx4cv skeletal muscle fibers. *Gene Ther,* **5,** 59-64.

151. Corrado, K., Rafael, J.A., Mills, P.L., Cole, N.M., Faulkner, J.A., Wang, K. and Chamberlain, J.S. (1996) Transgenic mdx mice expressing dystrophin with a deletion in the actin-binding domain display a "mild Becker" phenotype. *J Cell Biol,* **134,** 873-84.

152. Rafael, J.A., Cox, G.A., Corrado, K., Jung, D., Campbell, K.P. and Chamberlain, J.S. (1996) Forced expression of dystrophin deletion constructs reveals structure-function correlations. *J Cell Biol,* **134,** 93-102.

153. Norwood, F.L., Sutherland-Smith, A.J., Keep, N.H. and Kendrick-Jones, J. (2000) The structure of the N-terminal actin-binding domain of human dystrophin and how mutations in this domain may cause Duchenne or Becker muscular dystrophy. *Structure,* **8,** 481-91.

154. Rybakova, I.N., Amann, K.J. and Ervasti, J.M. (1996) A new model for the interaction of dystrophin with F-actin. *J Cell Biol,* **135,** 661-72.

155. Malhotra, S.B., Hart, K.A., Klamut, H.J., Thomas, N.S., Bodrug, S.E., Burghes, A.H., Bobrow, M., Harper, P.S., Thompson, M.W., Ray, P.N. *et al.* (1988) Frame-shift deletions in patients with Duchenne and Becker muscular dystrophy. *Science,* **242,** 755-9.

156. Wessel, H.B. (1990) Dystrophin: a clinical perspective. *Pediatr Neurol,* **6,** 3-12.

157. Cohn, R.D., Henry, M.D., Michele, D.E., Barresi, R., Saito, F., Moore, S.A., Flanagan, J.D., Skwarchuk, M.W., Robbins, M.E., Mendell, J.R. *et al.* (2002) Disruption of DAG1 in differentiated skeletal muscle reveals a role for dystroglycan in muscle regeneration. *Cell,* **110,** 639-48.

158. Cote, P.D., Moukhles, H. and Carbonetto, S. (2002) Dystroglycan is not required for localization of dystrophin, syntrophin, and neuronal nitric-oxide synthase at the sarcolemma but regulates integrin alpha 7B expression and caveolin-3 distribution. *J Biol Chem,* **277,** 4672-9.

159. Lenk, U., Oexle, K., Voit, T., Ancker, U., Hellner, K.A., Speer, A. and Hubner, C. (1996) A cysteine 3340 substitution in the dystroglycan-binding domain of dystrophin associated with Duchenne muscular dystrophy, mental retardation and absence of the ERG b-wave. *Hum Mol Genet,* **5,** 973-5.

160. Lesage, B., Beullens, M., Nuytten, M., Van Eynde, A., Keppens, S., Himpens, B. and Bollen, M. (2004) Interactor-mediated nuclear translocation and retention of protein phosphatase-1. *J Biol Chem,* **279,** 55978-84.

161. Sastri, M., Barraclough, D.M., Carmichael, P.T. and Taylor, S.S. (2005) A-kinase-interacting protein localizes protein kinase A in the nucleus. *Proc Natl Acad Sci U S A,* **102,** 349-54.

162. Matsumura, K., Tome, F.M., Collin, H., Azibi, K., Chaouch, M., Kaplan, J.C., Fardeau, M. and Campbell, K.P. (1992) Deficiency of the 50K dystrophin-associated glycoprotein in severe childhood autosomal recessive muscular dystrophy. *Nature,* **359,** 320-2.

163. Jones, K.J., Kim, S.S. and North, K.N. (1998) Abnormalities of dystrophin, the sarcoglycans, and laminin alpha2 in the muscular dystrophies. *J Med Genet,* **35,** 379-86.

164. Vainzof, M., Passos-Bueno, M.R., Canovas, M., Moreira, E.S., Pavanello, R.C., Marie, S.K., Anderson, L.V., Bonnemann, C.G., McNally, E.M., Nigro, V. *et al.* (1996) The sarcoglycan complex in the six autosomal recessive limb-girdle muscular dystrophies. *Hum Mol Genet,* **5,** 1963-9.

165. Anastasi, G., Cutroneo, G., Trimarchi, F., Santoro, G., Bruschetta, D., Bramanti, P., Pisani, A. and Favaloro, A. (2004) Evaluation of sarcoglycans, vinculin-talin-integrin system and filamin2 in alpha- and gamma-sarcoglycanopathy: an immunohistochemical study. *Int J Mol Med,* **14,** 989-99.

166. Bonnemann, C.G., Wong, J., Jones, K.J., Lidov, H.G., Feener, C.A., Shapiro, F., Darras, B.T., Kunkel, L.M. and North, K.N. (2002) Primary gamma-sarcoglycanopathy (LGMD 2C): broadening of the mutational spectrum guided by the immunohistochemical profile. *Neuromuscul Disord,* **12,** 273-80.

167. Hack, A.A., Lam, M.Y., Cordier, L., Shoturma, D.I., Ly, C.T., Hadhazy, M.A., Hadhazy, M.R., Sweeney, H.L. and McNally, E.M. (2000) Differential requirement for individual sarcoglycans and dystrophin in the assembly and function of the dystrophin-glycoprotein complex. *J Cell Sci,* **113 (Pt 14),** 2535-44.

168. Draviam, R.A., Wang, B., Li, J., Xiao, X. and Watkins, S.C. (2006) Mini-dystrophin efficiently incorporates into the dystrophin protein complex in living cells. *J Muscle Res Cell Motil*, **27**, 53-67.

169. Axelrod, D. (1989) Total internal reflection fluorescence microscopy. *Methods Cell Biol,* **30,** 245-70.

170. Brodsky, F.M., Chen, C.Y., Knuehl, C., Towler, M.C. and Wakeham, D.E. (2001) Biological basket weaving: formation and function of clathrin-coated vesicles. *Annu Rev Cell Dev Biol,* **17,** 517-68.

171. Pearse, B.M. (1976) Clathrin: a unique protein associated with intracellular transfer of membrane by coated vesicles. *Proc Natl Acad Sci U S A,* **73,** 1255-9.

172. Daro, E., van der Sluijs, P., Galli, T. and Mellman, I. (1996) Rab4 and cellubrevin define different early endosome populations on the pathway of transferrin receptor recycling. *Proc Natl Acad Sci U S A,* **93,** 9559-64.

173. Harding, C., Heuser, J. and Stahl, P. (1983) Receptor-mediated endocytosis of transferrin and recycling of the transferrin receptor in rat reticulocytes. *J Cell Biol,* **97,** 329-39.

174. Mellman, I. (2000) Quo vadis: polarized membrane recycling in motility and phagocytosis. *J Cell Biol,* **149,** 529-30.

175. Schmid, S.L., Fuchs, R., Male, P. and Mellman, I. (1988) Two distinct subpopulations of endosomes involved in membrane recycling and transport to lysosomes. *Cell,* **52,** 73-83.

176. Jin, M. and Snider, M.D. (1993) Role of microtubules in transferrin receptor transport from the cell surface to endosomes and the Golgi complex. *J Biol Chem,* **268,** 18390-7.

177. Wilbur, J.D., Hwang, P.K. and Brodsky, F.M. (2005) New faces of the familiar clathrin lattice. *Traffic,* **6,** 346-50.

178. Hanover, J.A., Willingham, M.C. and Pastan, I. (1984) Kinetics of transit of transferrin and epidermal growth factor through clathrin-coated membranes. *Cell,* **39,** 283-93.

179. Kelly, R.B. (1990) Microtubules, membrane traffic, and cell organization. *Cell,* **61,** 5-7.

180. Thyberg, J. and Moskalewski, S. (1985) Microtubules and the organization of the Golgi complex. *Exp Cell Res,* **159,** 1-16.

181. De Brabander, M.J., Van de Veire, R.M., Aerts, F.E., Borgers, M. and Janssen, P.A. (1976) The effects of methyl (5-(2-thienylcarbonyl)-1H-benzimidazol-2-yl) carbamate, (R 17934; NSC 238159), a new synthetic antitumoral drug interfering with microtubules, on mammalian cells cultured in vitro. *Cancer Res,* **36,** 905-16.

182. Haase-Pettingell, C.A. and King, J. (1988) Formation of aggregates from a thermolabile in vivo folding intermediate in P22 tailspike maturation. A model for inclusion body formation. *J Biol Chem,* **263,** 4977-83.

183. Kopito, R.R. (2000) Aggresomes, inclusion bodies and protein aggregation. *Trends Cell Biol,* **10,** 524-30.

184. Wetzel, R. (1994) Mutations and off-pathway aggregation of proteins. *Trends Biotechnol,* **12,** 193-8.

185. Hack, A.A., Ly, C.T., Jiang, F., Clendenin, C.J., Sigrist, K.S., Wollmann, R.L. and McNally, E.M. (1998) Gamma-sarcoglycan deficiency leads to muscle membrane defects and apoptosis independent of dystrophin. *J Cell Biol,* **142,** 1279-87.

186. Kleizen, B., Braakman, I. and de Jonge, H.R. (2000) Regulated trafficking of the CFTR chloride channel. *Eur J Cell Biol,* **79,** 544-56.

187. Ang, A.L., Taguchi, T., Francis, S., Folsch, H., Murrells, L.J., Pypaert, M., Warren, G. and Mellman, I. (2004) Recycling endosomes can serve as intermediates during transport from the Golgi to the plasma membrane of MDCK cells. *J Cell Biol,* **167,** 531-43.

188. Pagny, S., Lerouge P, faye L, gomord V. (1999) Signals and mechanisms for protein retention in the endoplasmic reticulum. *J of Exp botany,* **50,** 157-164.

189. Johnston, J.A., Ward, C.L. and Kopito, R.R. (1998) Aggresomes: a cellular response to misfolded proteins. *J Cell Biol,* **143,** 1883-98.

190. Notterpek, L., Ryan, M.C., Tobler, A.R. and Shooter, E.M. (1999) PMP22 accumulation in aggresomes: implications for CMT1A pathology. *Neurobiol Dis,* **6,** 450-60.

191. Tran, P.B. and Miller, R.J. (1999) Aggregates in neurodegenerative disease: crowds and power? *Trends Neurosci,* **22,** 194-7.

192. Draviam, R., Shand, S, Simon, SW (2006) The Beta-Delta core of sarcoglycan is essential for deposition at the plasma membrane. *Muscle Nerve,* **In Press**.

193. Draviam, R., Wang B, Shand S, Xiao X, Watkins SC (2006) Alpha-Sarcoglycan is recycled from the plasma membrane in the absence of sarcoglycan complex assembly. *Traffic,* **7,** 793-810.

194.	Feili-Hariri, M., Dong, X., Alber, S.M., Watkins, S.C., Salter, R.D. and Morel, P.A. (1999) Immunotherapy of NOD mice with bone marrow-derived dendritic cells. *Diabetes,* **48,** 2300-8.

195.	Durbeej, M. and Campbell, K.P. (1999) Biochemical characterization of the epithelial dystroglycan complex. *J Biol Chem,* **274,** 26609-16.

196.	Wheeler, M.T. and McNally, E.M. (2003) Sarcoglycans in vascular smooth and striated muscle. *Trends Cardiovasc Med,* **13,** 238-43.

197.	Shiga, K., Yoshioka, H., Matsumiya, T., Kimura, I., Takeda, S. and Imamura, M. (2006) zeta-Sarcoglycan is a functional homologue of gamma-sarcoglycan in the formation of the sarcoglycan complex. *Exp Cell Res*.

198.	Wheeler, M.T., Zarnegar, S. and McNally, E.M. (2002) Zeta-sarcoglycan, a novel component of the sarcoglycan complex, is reduced in muscular dystrophy. *Hum Mol Genet,* **11,** 2147-54.

199.	Crosbie, R.H., Lim, L.E., Moore, S.A., Hirano, M., Hays, A.P., Maybaum, S.W., Collin, H., Dovico, S.A., Stolle, C.A., Fardeau, M. *et al.* (2000) Molecular and genetic characterization of sarcospan: insights into sarcoglycan-sarcospan interactions. *Hum Mol Genet,* **9,** 2019-27.

200.	Ermonval, M., Duvet, S., Zonneveld, D., Cacan, R., Buttin, G. and Braakman, I. (2000) Truncated N-glycans affect protein folding in the ER of CHO-derived mutant cell lines without preventing calnexin binding. *Glycobiology,* **10,** 77-87.

201.	Goh, C.S., Milburn, D. and Gerstein, M. (2004) Conformational changes associated with protein-protein interactions. *Curr Opin Struct Biol,* **14,** 104-9.

202.	Laporte, S.A., Oakley, R.H., Holt, J.A., Barak, L.S. and Caron, M.G. (2000) The interaction of beta-arrestin with the AP-2 adaptor is required for the clustering of beta 2-adrenergic receptor into clathrin-coated pits. *J Biol Chem,* **275,** 23120-6.

203.	Draviam, R., Papworth G, Watkins SC (2003) Analysis of dystrophin associated proteins in whole adult mouse muscle using single photon and multiphoton confocal microscopy. *Keystone symposia-Optical imaging: Applications to biology and medicine*.

204.	Stephens, D.J. and Allan, V.J. (2003) Light microscopy techniques for live cell imaging. *Science,* **300,** 82-6.